Dissertation

Mechanisms of heart failure with preserved ejection fraction

submitted by

Dott.

Alessio Alogna

for the academic degree of

Doctor of Philosophy (PhD)

at the

Medical University of Graz

Department of Cardiology

under the supervision of

PD Dr. Heiner Post

Assoz. Prof. Priv.Doz. Dr. Gunther Marsche

2016

Declaration

I hereby declare that this dissertation is my own original work and that I have fully acknowledged by name all of those individuals and organisations that have contributed to the research for this dissertation. Due acknowledgement has been made in the text to all other material used. Throughout this dissertation and in all related publications I followed the guidelines of "Good Scientific Practice".

Acknowledgement

I firstly would like to acknowledge Dr. Heiner Post, my supervisor and mentor. From the very beginning of my experience in Graz, I deeply enjoyed his excellent supervision. He was able to guide me through the acquisition of a solid scientific methodology, from the formulation of an original hypothesis to the final editing of a manuscript. He has a unique enthusiasm for science, and I´m looking forward to working together in the next stage of my career.

I would also like to thank my co-supervisor Prof. Gunther Marsche for his intellectual support and critical comments.

Next, I would like to thank Prof. Burkert Pieske for giving me the unique chance to develop my career in the cardiovascular research field and for having supervised my work.

I consider a privilege to have worked with Dr. Michael Schwarzl. He is a brilliant scientist and a good friend.

My biggest gratitude goes to all the people that worked in the pig-lab, Martin, Birgit, Jochen, David, Vladimir, Aida, Reinhard and Manfred.

Thanks to Prof. Mächler for his support. Thanks to Dr. Ursula and Gert Reiter for the cooperation and the fun experimental work together.

Thanks to Prof. Simon Sedej for his generous mentoring and support.

Many thanks to the faculty members of the fantastic DK-MOLIN PhD program, and in particular to Prof. Akos Heinemann and Dr. Miriam Sedej. The extraordinary support to students, the desire to improve and the excellent scientific environment are just a brief description of three excellent years. Thanks to all my fellow colleagues for the stimulating scientific discussions within courses, journal clubs, meetings and retreats.

Thanks to all the researchers of the Vascular Dept. at Bayer Healthcare Research Centre in Wuppertal for their support and the good work together.

My gratitude goes to Prof. Nazha Hamdani, Prof. Wolfgang Linke, Prof. Paul Steendijk and Prof. Mühlfeld for the collaborations.

Thanks to the people from the Dept. of Cardiology for the time spent together: Daniel, Gudrun, Frank, Paulina, Eva, Viktoria, Snjezana, Senka, Uwe, Patrick, Markus, Felix, Ewald, Dirk, Tina and Doris.

Special thanks to Andreas Lueger. He deserves my deepest esteem and gratitude.

Thanks to my Austrian family from “Good village”, without their support my experience in Graz would have never been possible.

Thanks to Elena for her unconditional support throughout the past years.

Thanks to my family. They are my light and no words can express the importance of their constant presence in every phase of my life.

Thanks to all my friends, especially the Austrian-German-Hungarian-Italian-Swiss Crew.

Finally, I would like to thank the one and only person who makes my world better every day, Kaja.

This thesis is dedicated to the memory of HH Shri Mataji Nirmala Devi.

Table of Content

Abbreviations and Definitions

Abbreviations

A	late diastolic mitral peak blood flow velocity
ACE-I	angiotensin converting enzyme inhibitors
AF	atrial fibrillation
ANP	atrial natriuretic peptide
ARB	angiotensin receptor blocker
AT	acceleration time
BB	beta-blocker
BNP	B-type natriuretic peptide
BSA	body surface area
CaMK	Ca2+/calmodulin-dependent kinase
CC	circumferential strain
cGMP	cyclic guanylate monophosphate
CMR	cardiac magnetic resonance
D	early diastolic pulmonary venous peak velocity
DOCA	deoxycorticosteroneacetate
DT	deceleration time
E	early diastolic mitral peak blood flow velocity
E’	early diastolic myocardial tissue velocity
ECG	electrocardiography
EDPVR	end-diastolic pressure-volume relationship
ESC	European Society of Cardiology
ESPVR	end-systolic pressure-volume relationship
FiO2	fraction of inspired oxygen
FLASH	fast low angle shot
HEPES	4-(2-hydroxyethyl)-1-piperazineethanesulfonic acid
HF	heart failure
HFpEF	heart failure with preserved ejection fraction

HFrEF	heart failure with reduced ejection fraction
HT	hyperthermia
i. m.	intramuscular
i. v.	intravenous
If	pacemaker funny current
IVRT	isovolumetric relaxation time
LA	left atrial / left atrium
LL	longitudinal strain
LV	left ventricular / left ventricle
LVMM	left ventricular muscle mass
LZ	leucine zipper
MAPSE	mitral annular plane systolic excursion
MH	mild hypothermia
MOLLI	modified Look-Locker inversion recovery
MRA	mineralocorticoid receptor antagonist
NADPH	nicotinamide-adenine dinucleotide phosphate
NCX	sodium calcium exchanger
NEP	neprylisin
NO	nitric oxide
NP	natriuretic peptides
NT	normothermia
NT-proBNP	N-terminal end of pro-B-type-natriuretic-peptide
NYHA	New York Heart Association
PDE	phosphodiesterase
pGC	particulate guanylate cyclase
PH	pulmonary hypertension
PKA	protein kinase A
PKG	protein kinase G
RAAS	Renin-Angiotensin-Aldosterone System

ROS reactive oxygen species

RR radial strain

RV right ventricular / right ventricle

S systolic pulmonary venous peak blood flow velocity

SDS-PAGE sodium dodecyl sulfate polyacrylamide gel electrophoresis

SERCA sarcoplasmic/endoplasmic reticulum calcium ATPase

sGC soluble guanylate cyclase

TGF transforming growth factor

US United States

V(coll,lv) total myocardial collagen content

V(myo,lv) total myocardial myocyte content

V(ves,lv) total myocardial blood vessel content

vs versus

VV(coll/int) volume fraction of collagen fibrils related to the interstitium

VV(coll/lv) volume fraction of collagen fibrils related to the left ventricle

VV(int/lv) volume fraction of the interstitium related to the left ventricle

VV(myo,lv) volume fraction of cardiomyocytes related to the left ventricle

VV(ves/lv) volume fraction of blood vessels related to the left ventricle

List of Figures

List of Tables

Abstract

Heart failure with preserved ejection fraction (HFpEF) is a highly prevalent clinical syndrome that is reaching epidemic proportions in western societies. The hemodynamic and molecular mechanisms behind this disease are still incompletely understood, and no treatment so far has shown to impact on its natural history. The classical hallmark of the disease is left ventricular (LV) diastolic dysfunction, deriving from a combination of impaired isovolumic active relaxation, reduced mid-diastolic suction and decreased end-diastolic capacitance, i.e. passive elastic proprieties of the myocardium. Temperature is a major determinant of cardiac function, and we have previously shown that mild hypothermia (33 °C, MH) induces acute LV diastolic dysfunction by incomplete relaxation, while substantially increasing LV contractility. However, a direct comparison with hyperthermia (40.5°C, HT) has never been performed in vivo. We therefore set up a first study to investigate the effect of temperature on myocardial function in healthy closed-chest pigs by pressure-volume analysis. At each temperature step, we further characterized the effect of temperature on myocardial function by comparison with a standard inotropic drug, i.e. dobutamine. While cooling from HT to normothermia (38°C, NT) and from NT to MH increased LV contractility to the same magnitude as a clinically relevant dose of dobutamine, the end-diastolic pressure-volume relationship (EDPVR) was progressively shifted leftwards, indicating opposite effects of HT and MH on LV compliance. This shift was reversed by dobutamine infusion during MH. These findings address the effect of high and low temperatures on cardiac function, and underline the possible synergistic role of β-adrenergic stimulation and cooling in a condition of impaired contractile function, i.e. cardiogenic shock.

As mentioned above, an increased LV stiffness at rest is characteristic of the disease. However, most patients become symptomatic preferably during exercise, and a limited myocardial perfusion and contractility reserve may play a role. We therefore set up a cardiac magnetic resonance (CMR) imaging study to investigate LV function and perfusion during dobutamine stress in a previously established porcine model of early-stage HFpEF, induced by deoxycorticosteroneacetate (DOCA) pellets, combined with high-salt and high-sugar diet. The protocol consisted of two CMR imaging sessions, one at rest and one during stress. Aside numerous functional alterations at rest, such as altered myocardial muscle mechanics and left ventricular filling characteristics, an impaired increase of cardiac index during dobutamine stress was paralleled by a reduced myocardial perfusion reserve. Exercise induced myocardial ischemia may therefore be a contributor to LV dysfunction in HFpEF.

HFpEF evolves from the accumulation of a multitude of cardiovascular comorbidities, leading to increased systemic inflammation, oxidative stress and coronary microvascular endothelial inflammation. Nitric oxide (NO) bioavailability is therefore reduced, and the NO-cyclic GMP (cGMP)-protein kinase G (PKG) pathway is affected, leading to a stiffer LV through its impact on the phosphorylation state and on the function of the major myofilament protein titin. Enhancement of PKG activity has emerged in the past years as a possible therapeutic approach. In our study, enhancing PKG activity via acute pharmacological stimulation of the soluble guanylate cyclase (sGC) in healthy pigs did not exert any beneficial effect on LV compliance, as confirmed by the unchanged phosphorylation state of titin, but rather exerted a slightly negative inotropic effect. In a series using the previously established porcine model of early stage HFpEF, only phosphodiesterase V inhibition via sildenafil, but not sGC stimulation or their combination, increased LV compliance, while both treatments clearly decreased LV contractility. These data argue against the concept that acute potentiation of cGMP-dependent signaling via a direct sGC stimulator can recruit a preload reserve, neither in healthy nor in hypertrophied LV myocardium. In final experiments, we tested the differential impact of NO-mediated (via nitroglycerin infusion, acting on sGC) versus NO-independent stimulation (via atrial natriuretic peptide infusion, acting on pGC) of the cGMP-PKG-titin pathway. Acute bicoronary infusion of these substances, at doses not affecting systemic vascular resistance, induced a rightward shift of the EDPVR in a dose-dependent manner. These data address the need of new strategies to directly impact on the hypertrophied LV myocardium, avoiding the well-known clinical limitation of an exaggerated effect on vasculature in patients sensitive to load changes. The molecular mechanisms underlying the observed increase of LV compliance in response to atrial natriuretic peptide remain to be investigated.

Zusammenfassung

Herzinsuffizienz mit erhaltener linksventrikulärer Ejektionsfraktion (HFpEF, heart failure with preserved ejection fraction) ist ein klinisches Syndrom, welches ein epidemisches Ausmaß in der westlichen Welt angenommen hat. Die hämodynamischen und molekularen Mechanismen hinter dieser Erkrankung sind immer noch unzureichend verstanden, und bisher konnte keine Therapie einen Einfluss auf den natürlichen Krankheitsverlauf nehmen. Das klassische Merkmal des HFpEF ist die linksventrikuläre (LV) diastolische Dysfunktion, die aus der Kombination einer beeinträchtigten isovolumetrischen aktiven Relaxation, reduzierter früh-diastolischer Sogwirkung und einer verminderten enddiastolischen Dehnbarkeit besteht. Die Temperatur ist eine wesentliche Determinante der kardialen Funktion. So konnten wir kürzlich zeigen, dass eine milde Hypothermie (33° C, MH) eine akute linksventrikuläre diastolische Dysfunktion durch eine inkomplette Relaxation induziert, während die LV-Kontraktilität ansteigt. Allerdings wurden bisher keine direkten Vergleiche mit einer induzierten Hyperthermie (40,5°C, HT) in vivo durchgeführt. Wir untersuchten daher den Einfluss der Temperatur auf die myokardiale Funktion bei gesunden anästhesierten Schweinen mit der Druck-Volumen Analyse. Bei jeder Temperaturstufe führten wir eine inotrope Stimulation mit Dobutamin durch. Während die Temperatursenkung von HT zu Normothermie (38°C, NT) ebenso wie die von NT zu MH die linksventrikuläre Kontraktilität im gleichen Ausmaß erhöhte wie Dobutamin, wurde die end-diastolische Druck-Volumen Beziehung (end-diastolic pressure-volume relationship, EDPVR) zunehmend nach links verschoben, eine Senkung der Temperatur vermindert also die linksventrikuläre Dehnbarkeit. Diese Linksverschiebung wurde durch eine Dobutamin-Infusion während MH aufgehoben. Dies impliziert einen synergistischen Effekt der beta-adrenergen Stimulation und Kühlung bei eingeschränkter Kontraktilität im kardiogenen Schock hin.

Die erhöhte linksventrikuläre Steifigkeit in Ruhe ist ein Charakteristikum des HFpEF. Die meisten Patienten werden aber erst bei Belastung symptomatisch. Wir haben daher eine MRT-Studie in einem kürzlich etablierten Schweinemodell eines Frühstadiums des HFpEF (DOCA-pellets in Kombination mit stark salz- und zuckerhaltiger Ernährung) zur Überprüfung der LV-Funktion und –perfusion während Dobutamin-induziertem Stress durchgeführt. Wir beobachteten einen reduzierten Anstieg des Herzindex während des Dobutamin-induzierten Stresses, der von einem verminderten Anstieg der Myokardperfusion begleitet wurde, Eine belastungsinduzierte Myokardischämie könnte somit zur LV-Dysfunktion bei HFpEF beitragen.

HFpEF entsteht durch die Akkumulation kardiovaskulärer Risikofaktoren, die wiederum zu einer systemischen Entzündung, oxidativem Stress und koronarer mikrovaskulärer Inflammation führen. Die Bioverfügbarkeit von Stickstoffmonoxid (nitric oxide, NO) ist reduziert, wodurch der NO-cGMP-Protein kinase-G (PKG)-pathway betroffen ist. Dies wiederum führt in vitro durch geänderte Phosphorylierung und Funktion des Myofilament-Proteins Titin zu einer erhöhten Steifigkeit des LV. Die Erhöhung der PGK-Aktivität ist in den letzten Jahren daher als möglicher therapeutischer Ansatz diskutiert worden. In unserer Studie zeigen wir, dass die akute systemische pharmakologische Stimulation der löslichen Guanylatcyclase (soluble guanylate cyclase, sGC) bei gesunden Schweinen keinen Effekt auf die LV-Compliance hat (bestätigt durch den unveränderten Phosphorylisationsstatus des Titins), hingegen aber einen leichten negativ inotropen Effekt ausübt. In einer Serie im bereits etablierten Schweinemodell des HFpEF konnte nur die Phosphodiesterase-V-Inhibition durch Sildenafil, nicht aber die sGC-Stimulation oder deren beider Kombination die LV-compliance erhöhen, während aber beide Behandlungen die LV-Kontraktilität reduzierten. Schließlich testeten wir den Effekt einer NO-abhängigen (via intrakoronarer Nitroglycerin-Infusion mit Wirkung auf sGC) versus NO-unabhängigen Stimulation (via intrakoronarer atrialer natriuretischer Peptid-Infusion mit Wirkung auf pGC) des cGMP-PKG-Titin-pathway. Beide Substanzen induzierten eine dosis-abhängige Rechtsverschiebung der EDPVR ohne Effekt auf den systemischen Widerstand. Diese Daten illustrieren den Bedarf einer zielgerichteteren Therapie des Myokards bei HFpEF ohne systemische Nebenwirkungen. Der der Wirkung des atrialen natriuretischen Peptids zugrundeliegende molekulare Mechanismus ist Gegenstand zukünftiger Forschung.

Chapter 1:

Introduction

1.1 Definition of heart failure

In the latest available guidelines of the European Society of Cardiology (ESC), heart failure is defined as "an abnormality of cardiac structure or function leading to failure of the heart to deliver oxygen at a rate commensurate with the requirements of the metabolizing tissues, despite normal filling pressures (or only at the expense of increased filling pressures)" (1). Clinically, this abnormality is manifesting with a syndrome characterized by typical signs, such as pulmonary crackles, elevated jugular venous pressure and third heart sound (gallop rhythm), and symptoms such as breathlessness, fatigue and ankle swelling (1). However, the signs are mostly related to sodium and volume retention and easily modified by diuretic treatment, and they therefore may not be present in patients already under diuretics for other comorbidities. In addition, the abovementioned symptoms may be non-specific, may occur in non-cardiac disease as well, and they have a limited diagnostic value. In this regard, circulating plasma natriuretic peptides levels are increased when a heart is diseased or the load on the heart chambers is increased, and they have been shown to increase the diagnostic accuracy, being therefore recommended in the international guidelines on heart failure (HF) management (1, 2). B-type natriuretic peptide (BNP) and N-terminal pro B-type natriuretic peptide (NT-proBNP) are the two most commonly used in the clinical setting. An important step in the heart failure diagnostic algorithm is to identify the underlying etiology. Myocardial disease, including coronary artery disease, hypertensive heart disease and familial or acquired cardiomyopathies, is the most common cause of heart failure (1). Valvular, pericardial, endocardial and arrhythmic disease are other important causes of heart failure, and their identification is of paramount importance, given the direct therapeutic implications.

1.1.1 Heart failure with reduced vs preserved ejection fraction

Ejection fraction (EF) is defined as the fraction of blood ejected by the ventricle relative to its end-diastolic volume, and it is mathematically calculated as stroke volume (difference between end-diastolic and end-systolic volume) divided by end-diastolic volume. EF can be easily measured by means of echocardiography, and it is often used in the clinical arena to assess the inotropic status of the left ventricle (LV). EF is not only a mere parameter of LV contractile function, but it is an important prognostic marker, with lower EF indicating poorer survival (1, 3), and most clinical trials select patients upon ejection fraction.

According to the guidelines, heart failure patients should be differentiated between two major clinical phenotypes, with reduced (HFrEF) and with preserved ejection fraction (HFpEF). An EF ≤35% has been used to enroll patients in most of the HFrEF trials, and this is the population of heart failure patients that has shown more therapeutic advances in the past decades (4-9). On the other hand, current ESC guidelines define HFpEF patients as having an EF>50%. Patients with an EF in the range 35-50% are therefore representing a grey area, have mild systolic dysfunction and no clinical trials showed a benefit in this subgroup of HF patients (10-12). HFpEF diagnosis is indeed more complicated, consisting of several steps, and it is largely based on exclusion of potential non-cardiac causes of patients' symptoms (1, 13, 14), such as anaemia or chronic lung disease. Current international guidelines on HF suggest the following criteria for the diagnosis of HFpEF: i) signs and symptoms consistent with a diagnosis of HF; ii) preserved ejection fraction (LV EF≥50%); iii) relevant structural heart disease (LV hypertrophy/LA enlargement) and/or objective measures showing an impaired LV diastolic function (1, 2). As mentioned above, BNP and NT-proBNP are playing an important role in the diagnostic algorithm of HF, being used as a rule-out test. The exclusion cut-off point differs between acute and chronic HF (1, 2). Of note, high levels of BNP and NT-proBNP are associated with a poor prognosis. After debating for many years (15, 16), it is now widely accepted that HFrEF and HFpEF are two distinct clinical entities with differing demographic characteristics. The major evidence of the existence of two different entities in the heart failure syndrome is related to the different etiologies and risk factors among them, with HFrEF being mostly associated with coronary artery disease and male gender, while HFpEF occurs mainly in obese and hypertensive post-menopausal women. The terminology HFpEF and HFrEF is preferred over the traditional one, "systolic" and "diastolic" heart failure, because it is now clear that HFrEF patients have diastolic dysfunction as well, and that HFpEF patients have at least a slightly reduced systolic function, when measured by more sensitive approaches, such as myocardial strain imaging (17).

1.1.2 Terminology of heart failure time course

Another important distinction within the syndromic spectrum of HF is between "acute" and "chronic" HF. According to the ESC definition, "Chronic HF" patients are the ones who have been experiencing symptoms and have HF signs for some time (1). A treated patient with symptoms and signs, stable for at least a month, is defined as "stable". The deterioration

of this condition, often leading to hospitalization, is defined as “acute HF” or “decompensated HF”. New or “de novo” HF is the acute presentation of HF as a consequence of an acute myocardial infarction or an acute viral myopericarditis. In the latter situation, the acute cause of HF usually solves completely, while in the former remains and carries a future risk of decompensation. Future prognostic admissions are considered important prognostic indicators in the natural history of HF (1). In fact, in patients with chronic HF, the risk of death is greatest in the early period after discharge after a hospitalization for HF and is directly related to the duration and frequency of HF hospitalizations (18). The “chronic HF” treatment is targeting the underlying pathophysiological mechanisms leading to LV remodeling, while the “acute HF” treatment aims to improve symptoms and stabilize the hemodynamic condition of the patients, presenting usually with pulmonary edema or cardiogenic shock. Rates of adverse outcomes in patients admitted for “acute HF” remain high, either in-hospital or after discharge, and a recent large prospective observational study has shown a relatively lower mortality rate of patients with “chronic HF”, compared to the “acute HF” patients (19).

1.2 Epidemiology of heart failure

Approximately 15 million Europeans and 6 million Americans suffer from HF, with annual direct and indirect costs in the billions (20). The prevalence of HF is about 1-2% in the adult population in western countries, and it is high as 10% in persons above 70 years old (21). Given the ageing of population, epidemiologists already in the early 90s predicted an exponential increase of HF incidence and prevalence in the upcoming decades (22). However, recent epidemiology data from Olmstead County, Minnesota, collected between 2000 and 2010, show an important reduction of HF incidence. This reduction was greater for HFrEF than for HFpEF, and contrasted with no apparent change in mortality (23), once again addressing the heavy public-health burden of this disease. Indeed, In spite of all medical efforts, the 5-year mortality of heart failure has decreased significantly less than that of malignant diseases (24), and the median survival of patients after the initial diagnosis is still only of less than 3 years (25, 26). The reported mortality rates in different populations of HF patients at 1 year vary between 24 and 41% (25-32), and at 5 year between 65 and 75% (23-26, 30, 31).

1.2.1 Risk factors of heart failure with preserved ejection fraction

HFpEF accounts for nearly half of clinical heart failure cases, and over 90% of these patients are aged ≥60 years at the time of diagnosis, meaning that this enormous public-health problem will continue to grow along with the increased longevity in western societies (33). Although the incidence of HFpEF does not seem to be increased, its prevalence have increased in the past decades, with a total prevalence of 1.0-2.9% (23, 34, 35). This is also related to an increased awareness of the disease, and a higher burden of lifestyle-related risk factors, such as obesity and diabetes (36). However, the contribution of risk factors to the overall burden of the disease is certainly difficult to evaluate, given the heterogeneity of HFpEF individuals enrolled in clinical trials, and given the synergistic interaction of risk factors (37). The difficult stratification of these patients is tightly linked to the complex pathophysiology of the disease, involving multiple risk factors and comorbidities. The concept of phenotypization (38) and phenomapping (39) of HFpEF patients is therefore emerging as a possible approach to target patients' subgroups rather than the whole population, as performed in many inconclusive clinical trials in the past years.

Most important risk factors for HFpEF are hypertension (40), older age and female gender (41, 42), and the prevalence of HFpEF was shown in a recent Portuguese survey to be as high as 10% in the subgroup of women aged 80 years or more (43). In addition, depending on the characteristics of the population studied, hypertension is present in 50 to 90 % of HFpEF patients, clearly higher than in both the general population and in the HFrEF patients (3, 11, 12, 44, 45). Interestingly, despite this strong causal relation with HFpEF, hypertension is associated with a neutral of better survival after the onset of heart failure (46). Atrial fibrillation (47), obesity (48), diabetes (49, 50) and coronary artery disease are other important comorbidities often present in the HFpEF population. In addition, there is a number of non-cardiac conditions associated with an increased risk of HFpEF, such as sleep apnea (51), chronic obstructive pulmonary disease (52), chronic kidney disease (53) and systemic inflammatory diseases (54), making the diagnosis and the prospective investigation of HFpEF mechanisms even more complicated (36). In the past years, as an attempt to connect and explain this complex spectrum of comorbidities, several studies are addressing microvascular dysfunction deriving from the low-grade inflammation induced by the abovementioned comorbidities as a possible pathogenetic mechanism (55). High risk of HFpEF within the aged and female population could be therefore related to the relatively frequent occurrence of microvascular heart disease in those demographic subsets (36, 56).

1.3 Current treatment options for heart failure

The international HF guidelines define the objectives in the management of this condition as based on three pillars: i) relieve symptoms and signs ii) prevent hospital admission and iii) improve survival (1, 2). However, only the latter two have been used as primary outcome measures for the most clinical trials, in part because they document an impact on the natural history of HF, and in part because it is more difficult to measure objectively the effect of a treatment on signs and symptoms, especially in large and randomized multicenter studies (57). In the past decades, there have been many advances in the field of HF treatment, with clear reduction of hospitalization and mortality of these patients. However, in this regard, there is a striking difference between the two forms of HF, with several pharmacological and device therapies now recommended for HFrEF, but not for HFpEF. Below, while summarizing current evidences in this field, we will briefly touch upon issues relevant to our experimental work.

1.3.1 Therapies of HFrEF

Several advances in the abovementioned "hard" endpoints have characterized the past decades of HFrEF clinical research. This is not surprising, when considering that, in contrast to HFpEF, the pathophysiology of HFrEF is somehow clearer, and there are several small and large animal models available to test new compounds for a solid proof-of-concept translation towards the clinical arena. For many years now, the main focus of the clinical approach to HFrEF has been based on targeting the Renin-Angiotensin-Aldosterone System (RAAS) and the neurohormonal system overdrive, and angiotensin converting enzyme inhibitors (ACE-I), Angiotensin receptor blockers (ARB), beta-blockers (BB), mineralcorticoid receptor antagonists (MRA) are now part of a clinician daily routine. In addition, in the past years has emerged a role in the treatment of chronic HF for a selective inhibitor of the I_f current in the sinoatrial node, ivabradine (58). However, the counter-regulatory hormonal pathways, namely the natriuretic peptide (NP) system, are also enhanced in HF, and the endopeptidase responsible for NP degradation, neprilysin (NEP), has gained attention as a possible pharmacological target. A recent clinical trial (59) has shown that impacting on this pathway through pharmacological NEP inhibition in combination with ARB, via the new compound LCZ 696, markedly improves survival of

chronic HFrEF patients in comparison to standard therapy with ACE-Is, opening a whole new field of investigation for the upcoming years.

1.3.2 Therapies of HFpEF

In the current ESC HF guidelines, the brief paragraph on HFpEF therapeutic recommendations goes straight to the heart of the problem in a laconic way: "No treatment has yet been shown, convincingly, to reduce morbidity and mortality in patients with HFpEF."(1). And indeed, the trials conducted to assess the efficacy of ACE-Is (11), ARBs (10, 12) and BBs (60) have failed to show any improvement in HFpEF patients' survival. Another unsuccessful clinical trial has recently tested the effect of phosphodiesterase (PDE) -5A inhibition via sildenafil (45) on clinical status and exercise capacity. We will further discuss the implications behind these neutral results in the paragraphs below. The MRA spironolactone, after showing promising results in the Aldosterone Receptor Blockade in Diastolic HF (Aldo-DHF) trial, failed to show any beneficial effect in a large international multicenter study, the so-called Treatment of Preserved Cardiac Function HF with an Aldosterone Antagonist (TOPCAT) trial (61). In this case, geographical differences between clusters of patients enrolled in different parts of the world may be partly explain the neutral results, and further trials are warranted (62). Some promising results are coming from the abovementioned combined ARB and NEP inhibitor, LCZ-696. This compound was tested in a phase II trial, showing a greater reduction of NT-proBNP at 12 weeks compared to Valsartan (63). In addition, the follow up at 36 weeks of these patients showed a greater reduction of left atrial (LA) volume index, an improvement of NYHA functional class and estimated glomerular filtration rate. Of note, all these changes were independent of reduction in systolic blood pressure (64). A Phase III clinical trial in HFPEF patients is currently under way and it will clarify if these preliminary findings will translate in an improved outcome. Another important dose-finding phase II study is investigating the effect of a soluble guanlylate cyclase (sGC) stimulator, vericiguat, in both preserved and reduced ejection fraction patients. In the HFrEF arm of the study, vericiguat was well tolerated but did not impact on the primary end-point, NT-pro BNP change from baseline to 12 weeks (65). The results from the preserved ejection fraction arm should be available in the upcoming months. The experimental background of this study will be discussed in the next paragraphs.

Finally, it is worth mentioning that a non-pharmacological approach, such as exercise training in HFpEF patients, has shown the most promising results in terms of improved exercise capacity and diastolic function (66). This underpins once again the importance of considering the broad phenotypic spectrum of HFpEF patients in its complexity. A better understanding of HFpEF pathophysiology is essential to help the development of targeted treatments for this condition. In this regard, it has been proposed that a better baseline characterization of patients with a selective phenotyping would allow a better tailoring of the treatment (39, 67). The most recent and ongoing clinical studies in HFpEF are summarized in Table 1.1.

Study	Design	Drug/intervention	Number of patients	Primary endpoint	Results
EX-DHF(66)	RCT-PoC	Exercise training	67	Peak VO2	+2.6 mL/kg/min (p<0.001)
PARAMOUNT (63)	RCT-PoC	LCZ696 vs valsartan	266/71	Change NT-proBNP	Ratio LCZ696/valsartan = 0.77 (p=0.005)
ALDO DHF (68)	RCT-PoC	Spironolactone vs placebo	422/67	(A) E/E′ (B) Peak VO2	(A) 12.1 vs 13.6 (p<0.001) (B) 16.8 versus 16.9 (p=NS)
RELAX (45)	RCT-PoC	Sildenafil vs placebo	216/69	Peak VO2	-0.2 vs −0.2 mL/kg/min (p=NS)
TOP-CAT (61)	RCT-Outcome	Spironolactone vs placebo	3445/69	CV death, HF hospitalization and aborted cardiac arrest	Follow up 3.3 years, 18 vs 20 (p=NS)
SOCRATES-preserved (69)	RCT-PoC	Vericiguat	Enrollment closed	Change NT-proBNP	Results in 2016
PARAGON HF	RCT-Outcome	LCZ696 vs valsartan	Enrolling	CV death and HF hospitalization	Results in 2019

Table 1.1: Recent and ongoing studies in HFpEF. RCT: randomized clinical trial, PoC: proof-of-concept, CV: cardiovascular, HF: heart failure, VO_2: oxygen consumption.

1.4 Pathophysiology of HFpEF - Hemodynamic mechanisms

HFpEF was historically first named “diastolic heart failure”, with an increased left ventricular stiffness at rest being the hemodynamic hallmark of the disease (70). However, in the past years several groups have shown that HFpEF is not solely caused by left ventricular diastolic dysfunction, but that it is rather a mosaic of multiple components, ranging from impairment of systolic reserve function to atrial dysfunction, endothelial dysfunction, vascular stiffening, pulmonary hypertension and right ventricular dysfunction (33). These components play a little role at rest and, indeed, most patients become symptomatic during a stress-induced increase of venous return, typically during exercise (71). All the major HFpEF pathophysiology mechanisms seem therefore to reflect a cardiac reserve limitation (33).

1.4.1 LV structural remodeling

Early studies have shown that the majority of HFpEF patients have a characteristic concentric LV hypertrophy and markedly differ from HFrEF patients for the absence of chamber dilatation (72, 73). Structural remodeling is defined via quantification of LV geometry, mass and volume. The degree of LV remodeling is therefore characterized by these three dimensions, and it is now clear that even when LV hypertrophy is not present, cellular hypertrophy can be present (74) and detectable as an increased LV mass compared to patient´s baseline values or in relation to LV volume. This concept is supported by further population-based studies showing that concentric remodeling without hypertrophy and even normal geometry are as well present in this heterogeneous population (75, 76). Major differences in common patterns of LV remodeling between HFpEF and HFrEF patients are summarized in Table 1.2.

Parameters	HFpEF	HFrEF
End-systolic volume	= or ↓	↑
End-diastolic volume	=	↑
LV mass	↑	↑
LV mass/end-diastolic volume	↑	= or ↓
Wall thickness	↑	↓
LV geometry and shape	Concentric / normal	Eccentric / spherical

Table 1.2: Common patterns of LV remodeling in HFpEF and HFrEF. ↓: decreased, ↑: increased, =: unchanged.

1.4.2 Impaired LV diastolic function

The loss of LV end-diastolic capacitance observed in HFpEF patients can result from a functional impairment occurring in one of the 3 phases of diastole: "slowed" LV active relaxation in early diastole, poor mid-diastolic suction and elevated end-diastolic stiffness, i.e. change of myocardial passive properties per se (77).

The active relaxation is the energy-consuming phenomenon of pressure decay in the LV during early diastole, with a molecular counterpart of calcium reuptake in the sarcoplasmic/endoplasmic reticulum calcium ATPase (SERCA) stores and myofilament dissociation. The pressure decay rate is measured as the isovolumic relaxation constant τ (tau). The time necessary to allow the LV to relax completely, or in other words to allow the pressure to drop back to baseline values at the end of diastole, is mathematically defined as 3.5 times τ. The diastolic time is normally much longer than 3.5 times τ, and it therefore allows LV complete relaxation. When heart rate is increased, during physical exercise for example, a healthy LV enhances relaxation, τ is shorter and atrial and LV filling pressure are not increased. However, τ was shown to be prolonged already at rest in most of the invasive studies on HFpEF patients (70, 78). In addition, the relaxation enhancement during exercise is lost, resulting in incomplete relaxation and therefore increased atrial and LV end-diastolic pressures (71, 79, 80).

A second mechanism of diastolic dysfunction is a reduced mid-diastolic suction. In healthy subjects, an intraventricular pressure gradient is generated in the LV, leading to the generation of a vacuum in the LV that literally sucks blood from the atrium. This

phenomenon is accentuated during increased venous return, and has the finalistic aim to avoid an increase of atrial pressure. The extent of LV suction is determined mainly by the mitral annulus longitudinal motion, by the mechanical LV untwisting, and by the end-systolic volume from the previous contractile cycle, to be imagined as the extent of compression of a spring (the more compressed, the stronger is the subsequent uncoil). An impairment of these components leads to a reduced suction, and the LV filling can happen only at the expense of an increased LA pressure and consequent pronounced LA kick (81). In addition, LA functional reserve was shown to be eroded in HFpEF patients, further contributing to exercise intolerance (82).

A third mechanism of diastolic dysfunction is an increased LV passive stiffness. The viscoelastic properties of the LV are determined by the sum of extracellular matrix, cardiomyocytes and sarcomeric proteins, chamber and pericardium mechanical changes. (5,64). LV passive stiffness is an important determinant of LV filling pressure in HFpEF, and the gold standard to assess LV passive stiffness consists in deriving invasively the slope and the position of the end-diastolic pressure-volume relationship. This concept plays a central role in our work, and we will further discuss its implications in the next paragraphs.

1.4.3 LV systolic function and cardiovascular reserve

For many years, systolic function was believed to be preserved in the HFpEF population. This conceptual mistake was deriving from the misleading identification of the ejection fraction with the LV systolic function. The common knowledge was that HFpEF patients would decompensate in late stages of the disease, and only then have a reduced systolic function. Many studies have now demonstrated that this is not always the case, and slight abnormalities of systolic function are present already in early stages of the disease. These changes become more pronounced during physiological stress, and systolic abnormalities were shown via both load-independent measurements and strain-speckle tracking imaging of regional wall motion (83-87). Interestingly, the severity of systolic dysfunction correlates with the severity of prognosis in HFpEF patients (85).

1.4.4 RV function and pulmonary hypertension

Pulmonary hypertension (PH) is highly prevalent and often severe in HFpEF patients (88), particularly during physical exercise (80). PH and right ventricular (RV) dysfunction have

emerged in the past years as prognostic markers for adverse events (89-91). Both pulmonary venous and arterial hypertension, i.e. a precapillary component, are contributing to PH (88). On the same line, RV dysfunction is caused not only by contractile dysfunction but it is also the consequence of the vascular-ventricular mismatch derived from PH (90). Elevated pulmonary arterial systolic pressure (PASP) was shown to be a strong predictor of mortality in HFpEF, and each 10 mmHg increase in PASP is associated with a 28% increase in 3-year mortality (88). RV contractile dysfunction and PH are therefore now considered a possible therapeutic target in this population (92). In this regard, the RELAX trial, testing the impact of the vasodilator sildenafil on HFpEF patients, has failed to improve exercise capacity, quality of life and clinical biomarkers (45). One explanation of this failure may be related to the mild estimated PASP in the enrolled population, suggesting the need to focus on HFpEF patients with a more pronounced PH.

1.4.5 Vascular stiffening and dysfunction

HFpEF patients are further characterized by an impaired vasodilation response. In fact, not only they have a higher end-systolic elastance (Ees), meaning a higher LV end-systolic stiffness, but they also have a higher arterial stiffness (Ea), calculated as the ratio between LV end-systolic pressure and stroke volume (93). In other words, the ventricular-arterial coupling, represented by the ratio of these two parameters, is compromised in those patients, especially during exercise (80, 94). This leads to the well-known phenomenon of pronounced fluctuations in blood pressure for any given change in preload, afterload or stroke volume, adding a challenge in the pharmacological management of these patients.

1.4.6 Chronotropic incompetence

Chronotropic incompetence is another peculiar feature of HFpEF patients, manifesting itself with a blunted heart rate response during exercise in most of the studies (95-98). This seems to be related to an autonomic impairment. Chronotropic incompetence becomes apparent as a lack of early (99) and exercise-peak (71) heart rate increase, mainly driven by parasympathetic tone withdrawal, but also as an impaired heart rate recovery after exercise (96), pointing towards both an overexcited sympathetic tone and blunted parasympathetic one. This phenomenon is independently associated with adverse outcome (100).

1.4.7 Transmural gradient of dyssynchrony

Echocardiographic studies demonstrated that in HFPEF global LV function suffers from a loss of longitudinal shortening that is compensated by radial and circumferential shortening (84), along with a loss of LV twist and untwist during systole and diastole. This indicates a damage primarily of subendocardial muscle fibers. These fibers have a helical orientation and are most responsible for the rotatory component LV contraction (101). It therefore appears to exist a certain transmural gradient of LV dysfunction, evolving over time and progressively impairing LV torsion and rotation. Chapter 4 of this work investigates these mechanisms in a CMR imaging study of our porcine model of early-stage HFpEF.

1.5 Pathophysiology of HFpEF - molecular and cellular mechanisms

The pathophysiology of HFpEF has been investigated extensively in the past years, yet many characteristic features of the disease need to be elucidated. One of the major issues is related to the fact that patients develop diastolic dysfunction way before becoming symptomatic (102). The mechanisms leading patients into the symptomatic phase are unknown. However, it is clear that aging is an important contributor to this process, and some authors have therefore defined HFpEF as an ultimate form of cardiac aging or "presbycardia" (33). We will now briefly touch upon the major components of this phenomenon.

1.5.1 Myocardial interstitial fibrosis

Myocardial stiffening is the result of both processes involving extracellular matrix and the cardiomyocyte per se. An increased total collagen volume has been shown in endocardial biopsie tissue from HFpEF patients (74, 103). Type I and III collagen are both elevated, and this is associated with a reduced activity of the major collagenase systems, responsible for their turnover. Another important feature of the extracellular matrix in HFpEF patients, beside the reduced collagen turnover, is the increase of cross-linking within the collagen structure that renders the myocardium more rigid (104, 105). These structural changes seem to promote fibrosis, being the extracellular matrix not only a passive scaffold, but regulating the interaction of several cellular signalling pathways. The mechanisms behind these matrix alterations have been linked to increased inflammatory markers, commonly related to conditions such as diabetes and neurohumoral activation of the renin-angiotensin-aldosterone system (106).

1.5.2 Oxidative stress

Cardiovascular comorbidities such as aging, hypertension, diabetes, obesity and physical inactivity lead to increased systemic inflammation (55, 107). High levels of circulating inflammatory cytokines, such as interleukin 6, tumor necrosis factor α, soluble ST2 and pentraxin 3 were reported in HFpEF patients (55, 108). These factors play a role in the induction of endothelial dysfunction, mediated by an increased intracellular reactive oxygen species (ROS) production by higher NADPH oxidase-2 expression in macrophages and

endothelial cells, and , at the same time, by a higher expression of adhesion molecules such as vascular cell adhesion molecule-1, intercellular adhesion molecule-1 and E-selectin (109, 110). The increased oxidative stress lowers nitric oxide (NO) bioavailability and NO dependent signaling from endothelial cells to cardiomyocytes is affected. In fact, a lower cyclic GMP (cGMP) concentration and protein kinase G (PKG) activity have been shown in LV biopsies of these patients and have been mechanistically linked to the classical hallmark of the disease, LV stiffness and diastolic dysfunction, through its impact on the function of the major myofilamental protein titin (111). High level of inflammatory cells secreting transforming growth factor β (TGF-β) were also shown in HFpEF patients. In the same study, primary human fibroblasts isolated from endomyocardial biopsies and exposed to transforming growth factor β (TGF-β), transdifferentiated to myofibroblasts, producing more collagen and decreasing the levels of matrix metalloproteinase-1, the major system of matrix degradation (109).

1.5.3 Titin and myocyte stiffness

Titin is a giant protein (≈ 3800kDa) that spans from the Z-disk to the M-band of the half sarcomere (112). In vitro studies have previously shown that titin plays a major role in regulating passive tension of cardiomyocytes in the physiological range of sarcomere lengths (113). In mammalian hearts two major isoforms of titin are expressed, N2B and N2BA, the former being stiffer and shorter, the latter longer and more compliant (112). Titin-based passive myofilament stiffness is largely determined by the ratio of these isoforms (114). In addition, on a shorter time scale titin stiffness is modulated via posttranslational modification of the elastic I-band and regions N2Bus and PEVK(112), involving processes such as phosphorylation, carbonylation, oxidation and formation of disulphide bridges. In particular, phosphorylation of the two isoforms by incubation with PKG and protein kinase A (PKA) is known to reduce skinned myofibers‘ and isolated myofibrils‘ passive stiffness in human and canine left ventricles (115). In the past years, more than 28 phosphorylation sites involved in the posttranslational modulation of titin have been identified within the N2Bus and PEVK regions by in vitro kinase assays or mass spectrometry (112). Phosphorylation of the abovementioned N2Bus residues via PKG, PKA (113, 116) and calcium/calmodulin-dependent protein kinase (CaMK) II δ (117) decreased titin-based passive myofilament stiffness in human failing and non-failing myocardial tissue. Vice versa, phosphorylation of the PEVK residues increased titin-based passive myofilament stiffness in murine and canine

LV skinned myocardium (118). Chapter 5 of this work will provide data on the experimental pharmacological targeting of the abovementioned titin's residues.

1.5.4 Calcium signaling and active relaxation

Impairment of active relaxation is related to alterations in calcium signalling. The process of cardiomyocyte relaxation follows Ca^{2+} reuptake into the sarcoplasmic reticulum through SERCA. The intracellular Ca^{2+} is additionally extruded via the Na^{+}/Ca^{2+} exchanger (NCX). The activity of SERCA is regulated by phosphorylation of the regulatory protein phospholamban. Phosphorylation of phospholamban via PKA and CaMK release the inhibitory interaction of this protein with SERCA, increasing its Ca^{2+} affinity. Dyssynchronous intracellular Ca^{2+} delay leading to prolonged action potential and increased diastolic Ca^{2+} levels has been described in diastolic dysfunction (119, 120). In addition, studies have demonstrated a correlation between expression of Ca^{2+} handling protein and diastolic dysfunction. Experimental data indicate that the ratio SERCA/phospholamban is decreased with age-related diastolic dysfunction (121-123). A consistent amount of data on post-translational modifications of other Ca^{2+} channels and Ca^{2+} handling proteins as a substrate for diastolic dysfunction are present in literature.

1.6 Temperature modulation of LV function

The induction of Mild hypothermia (MH) has been for many years an established therapeutic option to improve neurological outcome and survival in patients after resuscitation from out-of-hospital cardiac arrest (124). However, the recent Targeted Temperature Management (TTM) trial (125) failed to demonstrate any difference between MH and low normothermia (NT) in resuscitated patients, raising the question whether cooling or merely the avoidance of fever mediates neuroprotection and better patient outcome. To better understand the mechanisms behind the effect of different temperatures on biological systems in vivo is therefore of paramount importance, and additionally holds clinical implications.

Langendorff described the role of temperature in modulating cardiac function already more than a century ago. Cooling was shown to increase contractility in isolated rodent and human cardiac muscle strips (126, 127), isolated rat and rabbit hearts (128, 129), and in dogs (130) and pigs in vivo (131). Vice versa, hyperthermia (HT) decreased LV contractility in isolated cardiac muscle strips from rats (126) and in isolated dog hearts (132). In line with that, two small-scale clinical studies in patients with cardiogenic shock demonstrated an increase of cardiac index during intravascular cooling (133, 134).

On the other hand, MH has been known to induce pronounced diastolic dysfunction, as evidenced by slowed active relaxation and reduced LV end-diastolic capacitance at decreased spontaneous heart rates (130, 131). In our lab, we therefore use MH as a model of acute LV diastolic dysfunction, and we previously suggested that the prolongation of relaxation during MH is so profound that it limits LV filling and compliance and thereby induces a leftward shift of the EDPVR despite spontaneous bradycardia (135). Vice versa seminal studies indicate that HT induces a higher end-diastolic capacitance as compared to NT (77), but the mechanisms behind that have not been investigated. In Chapter 3, we therefore compared the effects of HT and MH on myocardial function in detail by pressure-volume analysis.

1.7 The nitric oxide-cyclic GMP- protein kinase G signaling pathway

As an attempt to connect the clinical evidences on HFpEF patients to the single cardiomyocyte level, a paradigm was proposed by Paulus and Tschöpe (55). The accumulation of multiple cardiovascular comorbidities is causing increased inflammation, oxidative stress and coronary microvascular endothelial inflammation. NO bioavailability is reduced by microvascular inflammation, and the NO-cGMP-PKG pathway is affected, ultimately leading to a stiffer titin (111). In the past years, cGMP-enhancing drugs have therefore emerged as possible therapeutic approach. Following solid preclinical findings on the anti-remodelling effect of PKG activation, several pharmacological therapies to enhance cGMP have been developed in the past years. The earlier clinical trials of PDE5 inhibitors, NO donors, GC activators and neprilysin inhibitors have focused on the acute vasodilatory effects. The focus is now shifting towards their potential direct myocardial effects independent of afterload reduction (136).

1.7.1 cGMP signaling in the cardiomyocyte

Cyclic GMP is an important signaling molecule in the cardiomyocyte. It is produced either via the cytosolic soluble guanylate cyclase (sGC) activated by nitric oxide or by the transmembrane particulate guanylate cyclase (pGC), activated by the natriuretic peptides. The best-characterized downstream signaling effector of cGMP is the cGMP-dependent Protein Kinase, also called PKG. Mammals have two genes that encode PKG I and II, but only PGK I is expressed and plays a relevant role in the cardiovascular system (137). PKG I is expressed in various cardiovascular cell types such as vascular smooth muscle cells, fibroblasts, endothelial cells and cardiomyocytes (137). PKG enzymes are homodimers with a rod-like structure, activated already at submicromolar concentrations of cGMP. PKG I has two splice variants, PKG Iα and Iβ, that differ in the length of the N-terminal leucine zipper (LZ) within the regulatory domain (137). The LZ is not only a passive element allowing a high affinity homodimerization, but it is responsible for the interaction with particular kinase substrates and for the subcellular localization of different isoforms (138). PKG Iα has a higher affinity to cGMP than the Iβ isoform, meaning that it can be activated at lower cGMP concentrations and works in other subcellular compartments depending on a gradient of

cGMP (138). The role of PKG I in cardiovascular disease has been elucidated in the past years, via in-vitro analyses of phosphorylated substrates and via genetic engineering in mice. Mice with whole body PKGI deletion show a decreased life-span and are difficult to study, but clearly show an impaired vascular relaxation (139). Several studies have investigated the role of PKG I upstream activation in single cardiomyocytes subjected to neurohormonal stimulation. In rat neonatal cardiomyocytes both exogenous NO and NPs inhibit norepinephrine (140, 141) and angiotensin II-induced (141) hypertrophy. This anti-hypertrophic effect was also shown in rat adult cardiomyocytes (142), indicating that this is driven by the enhancement of cGMP in the cell. Gene transfer of PKGI in neonatal cardiomyocytes confirmed that the downstream effector of this effect is indeed PKGI (143). Interestingly, whole body PKGIα LZ mutants develop hypertension and earlier systolic and diastolic dysfunction post transverse aortic constriction compared to wild type (144). These mice do not respond to cGMP enhancement by the phosphodiesterase type 5 (PDE5) inhibitor sildenafil, showing that LZ binding partners mediate the cGMP-PKG mediated anti-hypertrophic effects (145). In summary, there is strong preclinical evidence that PKGI is an important mediator of the anti-remodeling effects of cGMP enhancing therapies. The downstream substrates of PKG still need to be identified in vivo, but evidence points towards myofilament proteins known to be modulated by PKG, such as titin (146).

1.7.2 PKG activators and strategies to enhance cGMP

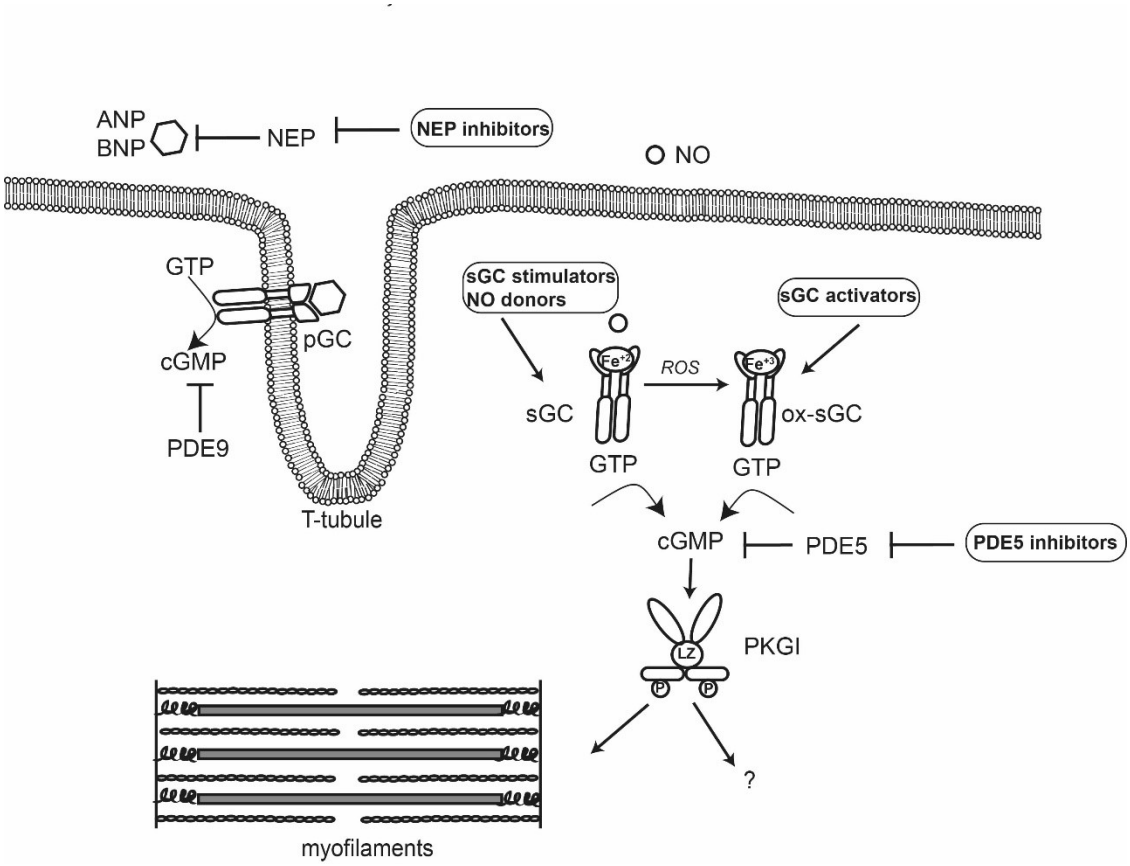

Figure 1.1: Classes of drugs modulating the cyclic GMP-protein kinase G pathway within the cardiomyocyte. Cyclic GMP is produced either via the cytosolic soluble guanylate cyclase (sGC) activated by nitric oxide or by the transmembrane particulate guanylate cyclase (pGC), activated by the natriuretic peptides. PDE5 is responsible for the breakdown of cGMP produced by sGC, while PDE9 of the one by pGC. The downstream substrates of protein kinase G (PKG) still need to be identified in vivo, but evidence points towards myofilament proteins. Soluble GC stimulators target only non-oxidized sGC (Fe^{2+}), vice versa sGC activators target oxidized sGC (Fe^{3+}). LZ: leucine zipper.

1.7.2.1 Nitric oxide donors

Nitric oxide activates sGC, which, in turns, increases cGMP concentration and activates PKG. The effects of NO donors on LV function have been well characterized. In vitro studies showed that exogenous NO exerts a negative inotropic effect mediated by downstream PKG (147), in part by reduced myofilament Ca^{2+}-sensitivity via Troponin I-phosphorylation (148) and by reduced Ca^{2+}-transients via L-type Ca^{2+}-channel phosphorylation (149). On the other hand, the NO donor sodium nitroprusside (SNP) increases diastolic cell length, inducing earlier LV relaxation (150) in vitro. In line with that, in patients with chest pain but no evidence of coronary lesions, intracoronary infusion of SNP resulted in a slightly decreased

LV peak systolic pressure and an acute increase of LV end-diastolic capacitance (151). In theory, the described effects on LV compliance would make NO donors ideal to tackle LV stiffness in HFpEF patients. However, several issues are limiting the use of these drugs in the clinical arena. Firstly, heart failure patients chronically treated with NO donors develop a vascular tolerance. Nitrate tolerance impairs the vasodilation response of these patients, partly due to an increased vascular oxidative stress (152). Secondly, chronic administration of the NO donor isosorbide mononitrate was shown to increase vascular oxidative stress and induce endothelial dysfunction by increasing the expression of endothelin (153). Finally, HFpEF patients are sensitive to preload reduction and they are therefore more susceptible to hemodynamic instability and stroke volume reduction from vasodilation than HFrEF patients (154). NO donors remain important options for vascular unloading and to decrease filling pressures in acutely decompensated patients, rather than in chronic heart failure.

1.7.2.2 Posphodiesterase 5 inhibitors

There are 11 PDE families in mammals, and at least 9 PDEs are recognized to play a role in the cardiovascular system (138). These enzymes are responsible for the specific breakdown either of cAMP or of cGMP or both. PDE5 acts specifically on cGMP. The role of PDE5 in LV remodeling has been proposed in the groundbreaking study of Takimoto on PDE5 knock-out mice (155). Pharmacological inhibition of PDE5 has therefore been extensively studied in the past years. As mentioned above, the administration of the PDE5 inhibitor sildenafil increased LV compliance in a canine model of LV concentric hypertrophy (146), supporting the possible translation of these findings in patients. In fact, sildenafil increased LV capacitance in HF-PEF patients with pulmonary hypertension, as evidenced by lower pulmonary capillary wedge pressures at higher LV end-diastolic diameters (156). However, the first randomized clinical phase IIb trial on HFpEF patients (RELAX) was completely negative, failing to improve exercise capacity and clinical status of patients (45). There are several reasons for that. First, PDE5 was shown to be upregulated in the LV of end-stage HFrEF patients, but never in HFpEF patients. PDE 5 inhibitors seem to be more effective in reducing right ventricular load in pulmonary hypertension, rather than in HFpEF patients. Another reason for the clinical failure of these class of drugs may be related to the subcellular microdomains of cGMP recruited by inhibition of PDE5, which is NO-dependent and therefore not effective in recruiting a preload reserve in a condition of reduced NO bioavailability. A recent study has shifted now the attention towards the PDE 9 isoform

(157), which seems to be responsible for a pool of cGMP located at the T-tubular invagination of the plasma membrane, produced by the atrial natriuretic peptide (ANP)-pGC pathway and independent from NO.

1.7.2.3 sGC stimulators and activators

The sGC stimulators and activators are two recently discovered classes of compounds that are able to modulate sGC. The mode of action differs between sGC stimulating and sGC activating compounds. A sGC stimulator targets only non-oxidized sGC (Fe^{2+}) and acts by increasing its basal cGMP production in a NO-independent way and, at the same time, rendering the enzyme more sensitive to endogenous NO. Thus, NO-mediated effects are more pronounced in the presence of sGC-stimulators (i.e. synergistic effect) (158, 159). In contrast, a sGC activator targets only oxidized sGC-molecules (Fe^{3+}) and enables them to produce cGMP in the absence of NO. In contrast to sGC-stimulators, NO-mediated effects are thus not influenced by sGC-activators (i.e. additive effect) (159, 160). Soluble GC activators are therefore ideal drugs to substitute NO in a condition of endothelial dysfunction, with increased oxidative stress and potentially oxidized or heme-free sGC. So far, this class of drugs has been tested only in HFrEF patients. The sGC activator Cinaciguat was shown to potently unload the heart, increase cardiac output and renal flow without any further neurohormonal activation in canine model of congestive heart failure (161). The first clinical data in acute decompensated heart failure showed reduction of filling pressure and an increased cardiac ouput. However, a phase 2b clinical trial in a similar population was terminated early because of excessive hypotension in the Cinaciguat arm (162).

The sGC stimulators reduced renal and cardiac organ damage in experimental high- and low-renin models (163). Recently, in a phase IIb clinical study in patients with pulmonary hypertension caused by systolic LV dysfunction, the sGC stimulator riociguat failed in reducing pulmonary artery pressure, but increased cardiac index, stroke volume and improved systemic and pulmonary resistance (164). An oral sGC stimulator, BAY 1021189 or vericiguat, is now under investigation in a phase II clinical trial, recruiting both HFpEF and HFrEF patients (SOCRATES) (69). The results of the HFrEF arm of the study have been recently published, showing that vericiguat was well tolerated but did not impact on the primary end-point, NT-pro BNP change from baseline to 12 weeks (65). The results of the HFpEF arm are expected in the upcoming months.

1.7.2.4 Neprilysin inhibitors

The effect of natriuretic peptides is mediated by 3 different receptors, 2 of which are membrane-bound receptors (also termed NP receptors) and cGMP-coupled. ANP and BNP are mainly secreted from the heart and act via NPR-A, inducing cGMP synthesis on the inner plasma membrane. C-type NP is directly released from endothelial cells and acts via NPR-B. ANP and BNP induce both vasodilation and natriuresis, while CNP does not induce natriuresis at physiological concentrations (165). The vasopeptidase enzyme neprilysin is responsible for the breakdown of NPs. Inhibitors of neprilysin have been developed in the past years. Omapatrilat, a combination of an angiotensin-converting enzyme and neprilysin inhibitor showed promising results in HFrEF (166), but excessive angioedema in a subsequent phase III clinical trial hindered further investigation on this compound (167). A new compound, LCZ696, combining an angiotensin receptor and neprilysin inhibitor has been developed, and we already mentioned above the promising results of this compound in a phase II trial (63).

1.8 Aims of the thesis

The objectives of this project are:

(i) to study mechanisms of temperature-dependent modulation of LV myocardial function (Chapter 3)

(ii) to characterize LV mechanics and myocardial perfusion during stress in a large animal model of early-stage HFPEF - a Cardiac Magnetic Resonance (CMR) imaging study (Chapter 4)

(iii) to evaluate the impact of pharmacological targeting of the cGMP-PKG-titin pathway on myocardial function in our early-stage HFPEF model (Chapter 5).

Chapter 3 summarizes content that has been recently published in a peer-reviewed journal. The introductive paragraphs on cGMP enhancing therapies have been recently published as an invited review in a peer-reviewed journal. Chapter 4 presents magnetic resonance imaging data obtained from Dr. Ursula Reiter, Department of Radiology, Medical University of Graz, within a cooperation between our departments. All the data presented in Chapter 5 are part of a manuscript under preparation for submission.

Chapter 2:

General Material and Methods

2.1 In-vivo experiments

The experiments reported in the current work were performed between 2012 and 2015. The experimental protocols were approved by the local bioethics committee of Vienna, Austria (BMWF-66.010/0127-II/3b/2011, BMWF-66.010/0055-II/3b/2012, BMWF-66.010/0128-II/3b/2012, BMWF-66.010/0091-II/3b/2013), and conform to the "European Convention for the Protection of Vertebrate Animals used for Experimental and other Scientific Purposes" (Council of Europe No 123, Strasbourg 1985). Landrace pigs were ordered from Heinz Stelzl, Großklein, Austria, and were delivered at the Institute for Biomedical Research of the Medical University of Graz (Roseggerweg 48, 8036 Graz, Austria). The pigs had at least one-week acclimatization time in the stables, in order to reduce as much as possible the impact of environmental stressors on the experimental results. The animals were fasted overnight with free access to water, and the experiments were performed either at the Section for Surgical Research, Dept. of Experimental Surgery (Auenbruggerplatz 15, 8036 Graz, Austria) or at the abovementioned Institute for Biomedical Research. After sedation, animals were intubated and mechanically ventilated. The regimen of anaesthesia was a combination of inhalational and intravenous anaesthetics, aiming at reducing single drug doses and therefore encountering the least side effects. The choice of the intravenous anaesthetics followed the principle of avoiding accumulation in the blood circulation, especially in the experiments with hypothermia-induced low metabolism, and avoiding as much as possible drugs heavily impacting on LV contractile function, such as barbiturates. A general overview of the drugs is given in Table 2.1, and a more detailed discussion will be provided in the method section of the respective experimental protocols.

Table 2.1: General list of compounds used in the in-vivo part of this experimental work. i.m.: intramuscular, i.v.: intravenous.

Compound	Brand name	Company	Administration route
Atrial natriuretic factor (1-28, human)	na	Bachem AG, Bubendorf, CH	i.v.
Azaperone	Stresnil 40 mg/ml	aniMedica GmbH, Senden-Bösensell, Germany	i.m.
BAY 41-8543	na	Bayer Healthcare, Wuppertal, Germany	i.v.
Butorphanol	Butomidor 10 mg/ml Ampullen	Richter Pharma, Wels, Austria	i.v.
Dobutamine	Dobutamin "ERWO" 12,5 mg/ml Ampullen	ERWO Pharma GmbH Brunn am Gebirge, Austria	i.v.
Fentanyl	Fentanyl-Janssen 0.1 mg Ampullen	Janssen-Cilag Pharma, Vienna, Austria	i.v.
Heparin Natrium	Heparin Natrium 25000 25000 E/5ml flaschen	Ratiopharm GmbH, Ulm, Germany	i.v.
Ketamine	Ketasol Injektionslösung für Tiere, 100 mg/ml	aniMedica GmbH, Senden-Bösensell, Germany	i.m. and i.v.
Midazolam	Midazolam "ERWO" 5 mg/ml Ampullen	ERWO Pharma GmbH, Brunn am Gebirge, Austria	i.m and i.v.
Nitroglycerin	NITRO POHL 1 mg/ml Ampullen	G. Pohl-Boskamp, Vienna, Austria	i.v.
Pancouronium	Pancouronium bromid 2 mg/ml Ampullen	ratiopharm GmbH, Ulm, Germany	i.v.
Propofol	Propofol "Fresenius" 1% Emulsion	Fresenius Kabi, Graz, Austria	i.v.
Sevoflurane	Sevorane	Abbott GmbH, Vienna, Austria	inhalation
Sildenafil citrate	n.a.	Molekula GmbH, Munich, Germany	i.v.

2.1.1 Invasive hemodynamic measurements

2.1.1.1 Experimental setup for invasive hemodynamic measurements

The experimental setup has been established in previous works from our group, and its stability shown in several publications (131, 135, 168-170). On the day of the experiment, Landrace pigs were sedated with midazolam and ketamine. After administration of propofol, the animals were intubated, mechanically ventilated and anaesthesia was continued with sevoflurane, fentanyl, midazolam, pancuronium and ketamine. The animals were ventilated (Julian, Draeger, Vienna, Austria) with an FiO2 of 0.5, an I:E-ratio of 1:1.5, a positive end-expiratory pressure of 5 mmHg and a tidal volume of 10 ml/kg. The respiratory rate was adjusted continuously to maintain an end-tidal carbon dioxide partial pressure between 35 and 40 mmHg.

Sheaths were introduced into both carotid arteries and internal jugular veins. Under fluoroscopic guidance, a Swan-Ganz catheter (Edwards Lifesciences CCO connected to Vigilance I, Edwards Lifesciences, Irvine, CA, USA), a quadripolar stimulation catheter in the high right atrium (Response 6F, St. Jude Medical, USA), a LV conductance catheter along LV long-axis (5F, 12 electrodes, 7 mm spacing, MPVS Ultra, Millar Instruments, Houston, Texas, USA) and a valvuloplasty catheter (24 ml, Osypka, Rheinfelden, Germany) in the descending aorta were introduced. In the experiments investigating the effect of different temperatures on cardiac function, an additional 14-F sheath was introduced into the left femoral vein, and an intravascular cooling catheter connected to a cooling device (Accutrol™ Catheter 14F and InnerCool RTx Endovascular System, Philips Healthcare, Vienna, Austria) was positioned in the inferior caval vein. The body core temperature was measured at the tip of the Swan-Ganz-catheter. A patient warming system (Bair Hugger, Warmtouch Series 500/OR, 3M, Germany) with warming cover was used to maintain the body temperature at 38.0°C, or, when included in the protocol, to raise body temperature and maintain it at 40.5°C. A balanced crystalloid infusion (Elo-Mel Isoton, Fresenius, Austria) was continuously administered at a fixed rate of 10 ml/kg/h. Urine outflow was enabled by a suprapubic catheter. Given the invasive instrumentation with multiple catheters, a 100 IU/kg heparin bolus followed by a 75 IU/kg/h continuous infusion was administered to prevent venous thrombosis. After instrumentation, the animals were allowed to stabilize for 45 min.

Figure 2.1: Standard experimental setup, Section for Surgical Research, Dept. of Experimental Surgery, Medical University of Graz. Courtesy of Dr. M. Manninger.

2.1.1.2 Devices and technical equipment

Recordings were performed at 1kHz sampling rate using Labchart 7, a commercially available software (ADInstruments, Colorado Springs, CO, USA) provided by purchase of the control unit for the pressure-conductance catheter from Millar Instruments (MPVS Ultra, Millar Instruments, Houston, TX, USA). This catheter allows the simultaneous recording of LV pressure and up to seven conductance segments. Cardiac output and temperature were continuously monitored and recorded via a Swan-Ganz catheter, connected to the main laptop via an external monitor (Vigilance I, Edwards Lifesciences, Irvine, CA, USA). Right atrial pacing (twice-diastolic threshold, 1 ms pulse duration) was performed using an external stimulator (UHS20, Biotronik, Germany).

Aortic, central venous and pulmonary arterial pressure signals were recorded connecting respectively an arterial sheath, the central venous and pulmonary arterial port of the Swan-Ganz catheter to a bridge amplifier (custom built by Prof. A. Lueger, Medical University of Graz). Calibration before any experiment followed the manufacturer's instructions.

2.1.1.3 Experimental protocol and raw data acquistion

In each of the experiments of this work, steady-state hemodynamics were acquired and averaged over three respiratory cycles. To generate pressure-volume relationships, afterload was increased briefly three times by inflating the intraaortic balloon catheter. During these recordings, the tidal volume was set to the respirator's minimum of 50 ml in order to

minimize the effect of respirator-induced alterations of intrathoracic pressure. At each protocol step, conductance catheter measurements were calibrated by hypertonic saline (3 boluses of 3 ml at 10%) and cardiac output continuously derived from the Swan-Ganz catheter. More details on the calibration method are given in the paragraph on principles of conductance technique.

In most of the experimental protocols, after measurements at spontaneous heart rate, we increased heart rate to multiples of 20bpm up to the maximum rate followed by steady contractions. At each pacing step, steady-state measurements and aortic occlusions were repeated. We hence aimed to obtain a complete characterization of LV function over a wide range of heart rates.

2.1.1.4 Principles of conductance technique for pressure-volume analysis

Generating pressure-volume loops in real time, under steady-state conditions and during changes in loading conditions allows to assess cardiac performance independent, as much as possible, from loading conditions. The conductance catheter, established by Baan et colleagues (171), consists of multiple electrodes generating an electric field via a low-amplitude, high-frequency constant current. In brief, the local electric field generates a voltage potential difference between adjacent electrodes, and passes through blood and surrounding tissues, translating into changes in electrical conductance (G) of the blood pool and chamber structures. These changes can then be correlated to changes in chamber volume. However, this signal is not calibrated, having the physical unit of electric conductance, i.e. siemens. In our experiments, the conductance catheter was positioned in LV long-axis and the signal acquired over 4 up to 7 electrodes, depending on LV anatomy of the animal. LV volume signal was then calibrated to absolute volume [V(t)] was calibrated using the equation $V(t)= (1/\alpha)(L^2/\sigma_b)[G(t)-G^p]$ (171, 172), where α is a dimensionless constant, L is the electrode spacing, σ_b is blood conductivity, G(t) is the total conductance measured and G^p indicates the so called parallel conductance. G^p represents the conductance of chamber structures surrounding the blood, and, in our study, it was estimated via intravenous hypertonic saline boli (172). Subtracting G^p from G(t) gives us the mere conductance of the intracavitary blood. This difference is then directly proportional to the absolute LV volume by $(1/\alpha)(L^2/\sigma_b)$, and this latter factor can then be calculated by dividing $[G(t)-G^p]$ by the stroke volume obtained, in our study, by a Swan-Ganz continuous cardiac output monitoring.

The pressure signal is generated via a piezo-membrane located at the tip of the catheter, converting the mechanical strain into an electric resistance.

2.1.1.5 Data processing

Pressure-volume data and time intervals were analysed off-line by CircLab Software (custom made by P. Steendijk) (135). This software allows a beat-to-beat analysis of the acquired signals. End-diastole was defined as the time-point of zero crossing of dP/dt before its rapid upstroke. End-systole was defined as the time point of maximum pressure/volume ratio. The end-diastolic pressure-volume relationship (EDPVR) was derived from an exponential fit of end-diastolic pressure and volume data points during aortic occlusion following the formula $LVP_{ed} = \alpha \bullet e^{\beta \bullet LVVed}$. The end-systolic pressure-volume relationship (ESPVR) was derived using a linear fit of end-systolic pressure and volume data points, characterized by the slope (end-systolic elastance, Ees) and volume axis intercept (V_0). The slope Ees is a load-dependent measure of contractility (173), and to compare ESPVRs, it is therefore important to compare changes of both Ees and V_0 (174). In addition, to obtain single-point measures of pressure-volume relationships, we calculated LV volumes at an end-diastolic pressure of 10 mmHg (LV VPed10) and at an end-systolic pressure of 100 mmHg (LV VPes100). LV VPed10 is a measure of LV capacitance and reflects how the size of the LV is altered by interventions (174). The second index, LV VPes100, is derived applying the same approach to the ESPVR and integrates slope and x-axis intercept of the ESPVR at a representative end-systolic pressure (135, 175).
The isovolumic relaxation constant τ (ms) was calculated based on the method of Glantz (176, 177). Cardiac power output (CPO) was calculated as the product of cardiac output and the difference between mean aortic pressure and central venous pressure, divided by a constant (451) and expressed in Watt (W) (178).

2.1.2 Blood samples

When of interest for the study, at each step of the experimental protocol one set of arterial and pulmonary arterial blood samples was processed immediately after withdrawal using a blood gas analyser (ABL 600; Radiometer, Copenhagen, Denmark) equipped for the temperature-corrected measurement of oxygen saturation, partial oxygen and carbon dioxide pressures, pH, acid-base status, haemoglobin and lactate.

2.1.3 Cardiac tissue harvesting – sequential myocardial biopsies

At the end of our invasive hemodynamic measurements, catheters were removed and the cardiac explant procedure was started with invasive arterial pressure and pulse oximetry monitoring. A median thoracotomy was performed, pericardium opened and positive end-expiratory pressure reduced to 0 mmHg, reducing interaction of lung with the operative field. Beating-heart LV transmural biopsies (kai Europe GbmH, Solingen, Germany) were taken from the lateral free wall, as far as possible from the left arterial descending coronary artery, in order to preserve the chance of a cardiomyocyte isolation procedure through perfusion of this vessel. All biopsies were carefully rinsed, immediately frozen into liquid nitrogen and stored at -80°C. Large vessels were then clamped, a bolus of 100 mmol potassium was given to sacrifice the animals. Further biopsies were taken, rinsed carefully and placed in 10 % formaldehyde for histological analyses.

In case of sequential LV transmural biopsies, a lateral thoracotomy was performed and the LV was exposed in a pericardial cradle. After stabilisation for 30 min, a pouch suture was prepared on the LV lateral wall, 2-3 transmural LV biopsies were taken from the beating heart and the pouch suture was immediately closed. Next, the drug of interest was infused according to the protocol, and further biopsies were taken, frozen and stored as described above.

2.1.4 Cardiac Magnetic Resonance Imaging

On the day of the CMR investigation, animals were brought to the Section for Surgical Research, Dept. of Experimental Surgery, where they were sedated, intubated, mechanically ventilated and anaesthetized as described above. Sheaths were introduced in an internal carotid artery and in a jugular vein, in order to monitor arterial blood pressure and infuse volume, respectively. Pigs were then quickly transported to the Cardiac magnetic resonance imaging Department, while continuously ventilated by a regular emergency transport ventilator (Oxylog 1000, Draeger, Vienna, Austria). In the CMR scanner, respiratory gases (PM 8050 MRI, Dräger Medical, Germany), heart rate and arterial blood pressure (Precess 3160, InVivo, FL, USA) were continuously monitored. Oral temperature was assessed by a sublingual thermometer, and temperature was kept constant at 38°C via cold saline infusion and adjustment of the MR scanner ventilation system.

2.1.4.1 Image aquisition

CMR imaging was performed on a 3T MR scanner (Magnetom Trio, Siemens Healthcare, Germany) using a phased-array 6-channel body matrix coil together with a spine matrix coil. Subjects were investigated in a single session during free breathing in the supine position with electrodes for electrocardiographical (ECG) gating positioned on the chest. After assessment of cardiac and myocardial function, blood flow and LV T1 times at rest, measurements were repeated during β-adrenergic stress, which was induced by intravenous infusion of dobutamine (ERWO Pharma, Austria) at rates of 2-8 µg/kg/min, targeting a heart rate increase of approximately 25%.

For assessment of ventricular function, retrospectively ECG-gated, 2D segmented fast low-angle shot (FLASH) cine images (temporal resolution, 27 ms interpolated to 40 cardiac phases; echo time, 2.7 ms; flip angle, 15°-20°; voxel size, 1.9×1.6×6.0-8.0 mm3) were obtained in the LV two-chamber, three- and four-chamber views (Figure 2.2), and in contiguous short-axis slices covering the entire LV in 12-14 slices. Two-fold averaging was used to suppress breathing artefacts.

Time-resolved three-directional phase-contrast imaging (4D flow) data were acquired to measure mitral annular tissue velocity and blood flow in the left heart, the pulmonary veins and the coronary sinus; the structures were covered by gapless slices with a retrospectively ECG-gated, two-dimensional spoiled gradient-echo-based three-directional velocity-

encoded cine phase-contrast sequence (velocity encoding in all directions, 110 cm·s-1; measured temporal resolution, 46 ms interpolated to 25 cardiac phases per cardiac cycle; echo time, 2.9 ms; flip angle, 15°; voxel size, 2.5×1.8×4.0 mm3; 3-fold averaging).

To study myocardial strain, tagged cine images were acquired with a retrospectively ECG-gated FLASH with spatial modulation of magnetization (SPAMM) in the short axis (basal, mid-ventricular and apical) and in the 4-chamber orientation (grid spacing, 6mm; temporal resolution, 20 ms interpolated to 50 cardiac phases; echo time, 3.3 ms; flip angle, 12°; voxel size, 1.8×1.3×6.0-8.0 mm3; 3-fold averaging).

An ECG-gated modified Look-Locker inversion recovery (MOLLI) prototype sequence with single-shot balanced steady-state free precession (bSSFP) readout, motion correction and automatic T1 map generation (MOLLI protocol 5(5)5(5)5; echo spacing, 2.6 ms; echo time, 1.1 ms; flip angle, 35°; voxel size, 2.1×1.4×8.0 mm3) was used to acquire myocardial T1 maps at end-diastole.

2.1.4.2 Left ventricular and myocardial function

Short-axis cine images were analyzed by syngo.via software (MR Cardiac Function, Siemens Healthcare, Erlangen, Germany). Analyses were performed by Dr. U. Reiter and collaborators, Dept. of Radiology, Medical University of Graz, Austria.

To assess LV volume vs. time curves, LV epicardial and endocardial borders, excluding papillary muscles from myocardium, were traced manually in end-diastole and end-systole and semi-automatically adjusted to all cardiac phases (Figure 2.2). To define the basal plane, the position of the mitral valve was evaluated from the cine four-chamber view.

Normalized end-diastolic volume (EDV), end-systolic volume (ESV), stroke volume, cardiac output, and LV ejection fraction were evaluated from end-diastolic and end-systolic cardiac phases with the body surface area estimated according to BSA (m2) = 0.0734×weight0.656 (179).

Papillary muscles were included when measuring normalized left ventricular mass (LVMM), but they were excluded in determining normalized mean end-diastolic and end-systolic wall thickness and thickening at the basal, mid-myocardial and apical levels; 16 myocardial segments were evaluated, according to the American Heart Association (AHA) segmentation scheme (180). Global normalized end-diastolic (WTED) and end-systolic (WTES) wall thickness, as well as LV wall thickening, were calculated as averages of segmental values.

Mitral annular plane systolic excursion (MAPSE) was measured as the difference of the distance from the apex to the lateral mitral annulus in end-diastole and end-systole in 4-chamber view.

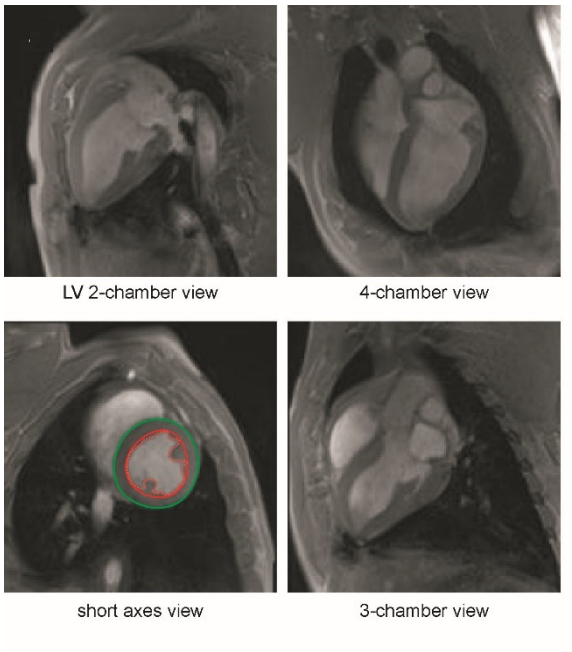

Figure 2.2: Functional cine images and their evaluation. Diastolic images of cine FLASH series in LV 2-chamber, 4-chamber, 3-chamber and mid-ventricular short-axis views. Subepicardial (green line) and subendocardial (red line) contouring in short axis images was employed to derive LV volume vs. time curves, wall thickness and left ventricular muscle mass. Image courtesy of Dr. U. Reiter, Dept. of Radiology, Medical University of Graz.

2.1.4.3 Phase contrast image data evaluation

Transmitral early (E) and late (A) diastolic, pulmonary venous systolic (S1, S2) and early diastolic (D) velocities, coronary sinus blood flow volume, and early diastolic lateral, septal and mean (E') mitral annular tissue velocities were evaluated from multi-planar images reconstructed from 4D flow data using a prototype software (4D Flow, Siemens Healthcare, Erlangen, Germany). Transmitral acceleration (AT) and deceleration (DT) times were assessed from average mitral velocity vs. time curves. E/A, E/E', (E/E')/EDV, and pulmonary venous S/D (with S as maximum of S1 and S2) ratios were calculated from peak through-plane velocities. Global myocardial perfusion was estimated from coronary sinus net forward blood volume divided by left ventricular muscle mass (181).

2.1.4.4 Global and segmental myocardial strain

Tagged images were evaluated semi-automatically by using a prototype software (Heart Deformation Analysis 2.0, Siemens Healthcare, Erlangen, Germany and University of

Auckland). A grid was aligned to the myocardial tags at end-diastole and propagated throughout all images of the cardiac cycle. Grids were manually corrected to the tags if necessary. Myocardial circumferential (CC) and radial strain (RR) and strain rates (CC rate, RR rate) were calculated by the software from the motion of grid lines at the basal, mid-ventricular and apical levels from the respective short axis slices. Longitudinal myocardial strain (LL) and strain rates (LL rate) were assessed from 4-chamber view images, while myocardial torsion and torsion rates were assessed from the strains of basal and apical short-axis slices. From time courses of strains, torsion and corresponding rates, end-systolic maxima/minima of strains and torsion as well as systolic and early diastolic maxima/minima of rates were determined. Furthermore, LV circumferential and radial strains and strain rates were calculated as means of basal, mid-ventricular and apical values.

2.1.4.5 T1 mapping

Segmental LV myocardial T1 times were derived by manually outlining T1 maps according to the AHA segmentation scheme, excluding blood pool, papillary muscles, trabeculae and epicardial structures. Regions were drawn to be as large as possible while avoiding inclusion of subendocardial and subepicardial tissue boundaries. Global LV myocardial T1 was calculated as mean of segmental values.

2.1.5 Echocardiography

Animals were first sedated in the stables with an intramuscular injection of midazolam, ketamine and azaperone. Echocardiography examination was then performed in the supine position, and required an additional operator to hyperextend the upper extremities throughout the procedure, in order to obtain access to good sonographic windows. Right-sided basal to mid-ventricular short and long axis view were acquired at least over three consecutive beats (Vivid I, GE Healthcare, Vienna, Austria). Analysis was performed offline via a commercially available software (Echopac, GE Healthcare, Vienna, Austria). LV end-diastolic wall-thickness and diameter were measured in the basal region both in short- and long-axis view. Relative wall thickness was defined as the ratio between LV wall thickness (sum of LV septum and LV posterior wall) and the LV end-diastolic diameter.

2.1.6 DOCA implantation - early-stage HFpEF model

Pigs were made hypertensive by implanting a subcutaneous deoxy-corticosterone acetate (DOCA) depot (100 mg/kg, 90 days release pellets, Innovative Research of America, Sarasota, FL, USA) into the inguinal region, combined to a high-salt (300g/day) and high-sugar (40g/day) diet, as previously published (182). Animals were first sedated with midazolam, ketamine and azaperone.

We additionally fed animals with potassium chloride (3g/day), in order to avoid DOCA-induced hypokalaemia and consequent arrhythmias. Given the negligible impact of the high-lipid diet on LV remodelling observed in our previous experience with the model, i.e. lack of fibrosis, we omitted it from the protocol. Figure 2.3 represents the protocol followed for this disease model.

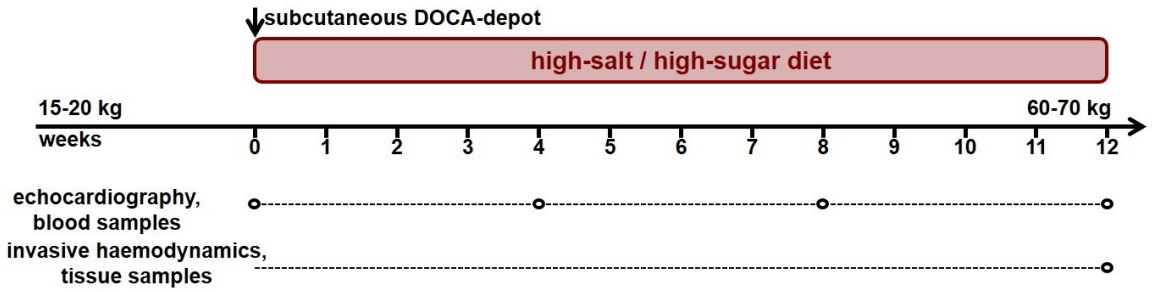

Figure 2.3: DOCA induced early-stage HFpEF, experimental protocol.

2.2 In vitro experiments

2.2.1 Histology

After in vivo measurements were completed, a thoracotomy was performed and a bolus of 100 mmol potassium was administered into the cavum of the LV to sacrifice each animal. For electron microscopic analysis of the myocardium, transmural biopsies were then collected from the lateral left ventricular wall and fixed in 1.5% glutaraldehyde, 1.5% paraformaldehyde in 0.15 M HEPES buffer. The samples were then stored in the fixative at 4°C until further processing. The processing steps included post-fixation in 1% osmium tetroxide solution, overnight staining in half-saturated uranyl acetate solution, dehydration in an ascending acetone series and finally embedding in epoxy resin. From the embedded samples, semi- and ultra-thin sections were obtained for stereological analysis, performed by Professor C. Mühlfeld and collaborators, Institute of Functional and Applied Anatomy, Hannover Medical School, Hannover, Germany.

2.2.2 Western blot

Western blot analysis of titin isoform and phosphorylation in the tissue samples was performed by Prof. N. Hamdani, Dept. of Cardiovascular Physiology, Ruhr University Bochum, Bochum, Germany.

2.2.2.1 Titin isoform separation

Titin isoforms were separated as described previously (183). Tissue samples were solubilized in 50 mM Tris sodium dodecyl sulfate (SDS) buffer (pH 6.8) containing 8 μg mL^{-1} leupeptin (Peptin Institute, Japan) and phosphatase inhibitor cocktail (PIC [P2880], 10 μL mL^{-1}; Sigma). Samples were heated for 3 minutes at 96°C and centrifuged. Then, samples (20 μg) were separated on agarose-strengthened 1.8 % sodium dodecyl sulfate-polyacrylamide gels. The gel was run at 5 mA constant current for 16 h.

2.2.2.2 Protein expression and phosphorylation by Western blot

Gel electrophoresis followed by Western blot was performed according to standard protocols to measure phosphorylation of cardiac protein titin. Custom-made, affinity-purified, anti-titin peptide antibodies (Eurogentec; Belgium) used in this study are summarized in Table 2.2. Positions in full-length human titin according to UniProtKB entry, Q8WZ42, are also reported.

Target-sequence	Titin-domain	Human-titin position	Dilution
EEGKS(PO3H2)LRFPLA and EEGKS(PO3H2)LSFPLA	N2Bus	S4010	1:500
DLLS(PO3H2)KESLLS	N2Bus	S4062	1:100
LFS(PO3H2)EWLRNI	N2Bus	S4099	1:500
EVVLKS(PO3H2)VLRK	PEVK	S11878	1:500
KLRPGS(PO3H2)GGEKPP	PEVK	S12022	1:500

Table 2.2: Antibodies used to assess phosphorylation of cardiac titin.

In addition, total titin phosphorylation was assessed by anti-phosphoserine/ phosphothreonine-specific antibodies recognizing all phosphorylated sites in titin (rabbit polyclonal; 1:1000, Eurogentec; Belgium). All these antibodies gave specific signals on Western blots. Titin phosphorylation level obtained with all these antibodies was indexed to PVDF stains for comparison of protein load.

2.3 Statistical analysis

All data are presented as mean ± standard error of the mean. Normally distributed data were compared using Student's paired or unpaired t-test. Non-normally distributed data were compared using the Mann-Whitney non-parametric test. Multiple comparison between experimental groups were performed by one or two-way analysis of variance (ANOVA), while comparison within related samples at different timepoints were performed by ANOVA for repeated measurements. Statistical analysis were performed using the commercially available software SigmaStat 3.5 (Systat Software GmbH, Erkrath, Germany). Pressure-volume relationships were compared by analysis of covariance (174) (IBM SPSS Statistics, International Business Machines Corporation Armonk, NY, USA). Post-hoc testing was performed by Tukey's test. A p-value < 0.05 was considered significant.

Chapter 3:

Temperature dependent modulation of LV systolic and diastolic function

MH is an established therapy to improve neurologic outcome in resuscitated patients (124, 184, 185). However, the recent Targeted Temperature Management (TTM) trial (125) did not demonstrate any difference between MH and NT in resuscitated patients, raising the question whether cooling or merely the avoidance of fever mediates neuroprotection and better patient outcome. The optimal target temperature for resuscitated patients is therefore unclear at present.

Temperature does not only impact on neurologic activity and recovery, but is an important determinant also of cardiovascular function. Cooling increased contractility in isolated rodent and human cardiac muscle strips (126, 127), isolated rat and rabbit hearts (128, 129), and in dogs (130) and pigs in vivo (131). Vice versa, hyperthermia (HT) decreased LV contractility in isolated cardiac muscle strips from rats (126) and in isolated dog hearts (132). In line with that, two small-scale clinical studies in patients with cardiogenic shock demonstrated an increase of cardiac index during intravascular cooling (133, 134). Experimental MH decreased infarct size, microvascular obstruction (186, 187) and mortality (188) in porcine models of myocardial infarction (186, 187) and subsequent cardiogenic shock (188). Furthermore, cooling preserved vascular resistance and pulmonary function and exerted anti-inflammatory effects during endotoxemia in pigs (170). These data imply that temperature management in resuscitated patients may affect outcome also by direct cardiac and systemic hemodynamic effects.

While the hemodynamic effects of MH vs. NT have been investigated in several experimental studies, a direct comparison of MH and HT in vivo has not been performed so far. We therefore induced HT (40.5 °C) and MH (33.0 °C) in anaesthetized pigs and assessed cardiac function in detail by pressure-volume analysis. To better estimate the relevance of temperature-dependent changes of cardiac function, we compared the effects of temperature to a standard clinical inotropic drug, i.e. dobutamine.

3.1 Specific Methods

3.1.1 Experimental setup

The experimental setup has been described before (135) and in Chapter 2.1.1. Briefly, Landrace pigs (n=9, 67±2 kg) were fasted overnight with free access to water and sedated with 0.5 mg/kg midazolam and 20 mg/kg ketamine. After administration of 1 mg/kg propofol, the animals were intubated, and anaesthesia was continued with 1 % sevoflurane, 35 µg/kg/h fentanyl, 1.25 mg/kg/h midazolam, 0.2 mg/kg/h pancuronium and 3 mg/kg/h ketamine.

3.1.2 Experimental protocol

Steady-state hemodynamics were acquired and averaged over three respiratory cycles. To generate pressure-volume relationships, afterload was increased briefly three times by inflating the intraaortic balloon catheter. During these recordings, the tidal volume was set to the respirator's minimum of 50 ml in order to minimize the effect of respirator-induced alterations of intrathoracic pressure.

Measurements were started at 40.5 °C (HT) and repeated at 38.0 °C (NT) and 33.0 °C (MH). At each temperature step, dobutamine was infused and titrated to double the steady state maximum LV dP/dt. A single dose of dobutamine was used, as we figured that a whole dose-response curve including maximum doses would cause ß-adrenoceptor desensitization and down-regulation. The increase of heart rate during dobutamine infusion can cause an acceleration of LV relaxation per se (189-191). After measurements at spontaneous heart rate at each temperature, we therefore increased heart rate to multiples of 20bpm up to the maximum rate followed by steady contractions before and during dobutamine. At each pacing step, steady-state measurements and aortic occlusions were repeated.

3.2 Results

The dose of dobutamine needed to double maximum LV dP/dt decreased with temperature from HT (2.1±0.1µg/kg/min) to NT (1.8±0.1µg/kg/min) and further to MH (1.5±0.1µg/kg/min, $p<0.05$ vs. HT). Maximum simulation rate followed by regular and steady LV contractions was 187±3 bpm at HT, 165±3bpm at NT ($p<0.05$ vs. HT) and 122±2bpm at MH ($p<0.05$ vs. NT). During dobutamine infusion, maximum heart rates increased (HT, NT and MH: 208±5, 187±3, 149±3bpm, all $p<0.05$).

3.2.1 Systemic hemodynamics

Mean aortic pressure decreased from HT to MH. Heart rate, cardiac output and CPO decreased with cooling from HT to NT and MH and were increased by dobutamine at each temperature step (table 1). Systemic vascular resistance increased with cooling from HT to MH and was decreased by dobutamine at each temperature. Central venous pressure decreased slightly with cooling and during dobutamine infusion.

Table 3.1: Systemic hemodynamics and oxygen consumption. LV = left ventricle, -dob = before dobutamine infusion, +dob = during dobutamine infusion. [a]p < 0.05 vs. hyperthermia, [b]p < 0.05 vs. normothermia, [c]p < 0.05 vs. -dob at temperature step.

		hyperthermia (40.5 °C)	normothermia (38.0 °C)	mild hypothermia (33.0 °C)
heart rate (bpm)	**-dob**	98 ± 4	89 ± 4[a]	65 ± 2[a,b]
	+dob	122 ± 3[c]	114 ± 3[a,c]	83 ± 4[a,b,c]
cardiac output (l min^{-1})	**-dob**	6.7 ± 0.3	6.1 ± 0.3	4.4 ± 0.2[a,b]
	+dob	8.4 ± 0.3[c]	7.8 ± 0.3[c]	6.0 ± 0.3[a,b,c]
mean aortic pressure (mmHg)	**-dob**	74 ± 3	68 ± 3	65 ± 2[a]
	+dob	77 ± 4	71 ± 4	69 ± 2[a]
central venous pressure (mmHg)	**-dob**	5 ± 0	4 ± 0[a]	4 ± 0[a]
	+dob	3 ± 0[c]	3 ± 0[c]	3 ± 0
cardiac power output (W)	**-dob**	1.1 ± 0.1	0.9 ± 0.1[a]	0.6 ± 0.0[a,b]
	+dob	1.4 ± 0.1[c]	1.2 ± 0.1[a,c]	0.9 ± 0.1[a,b,c]
systemic vascular resistance (dyn s cm^{-5})	**-dob**	840 ± 48	856 ± 56	1152 ± 64[a,b]
	+dob	720 ± 56[c]	704 ± 40[c]	880 ± 24[a,b,c]
whole body oxygen consumption (ml kg^{-1} min^{-1})	**-dob**	395 ± 19	314 ± 24[a]	199 ± 16[a,b]
	+dob	378 ± 20	335 ± 22[a,c]	230 ± 16[a,b,c]
mixed venous oxygen saturation (%)	**-dob**	53 ± 2	60 ± 2[a]	66 ± 2[a,b]
	dob	66 ± 2[c]	68 ± 1[c]	74 ± 2[a,b,c]

3.2.2 LV systolic function

Cooling from HT to MH decreased LV maximum pressure while both the rate of contraction (i. e., LV maximum dP/dt) and LV ejection fraction (EF) increased ($p<0.05$ vs. HT). The end-systolic pressure-volume relationship (ESPVR) was progressively shifted leftwards with cooling from HT to MH (Fig. 1 and Fig. 2a), and the calculated LV end-systolic volume at an end-systolic pressure of 100 mmHg (LV VPes100) decreased (Fig. 3a). In other words, the leftward shift of the ESPVR implicated an unchanged Ees and a decreased V_0 (table 2). Dobutamine infusion further decreased LV VPes100 at each temperature step. The effect of decreasing temperature on LV VPes100 (HT to NT: -28±3%, NT to MH: -20±5%) was of comparable effect size as dobutamine at a given temperature (HT:-28±4%, NT: -27±6%, MH: -27±9%, Fig. 3b).

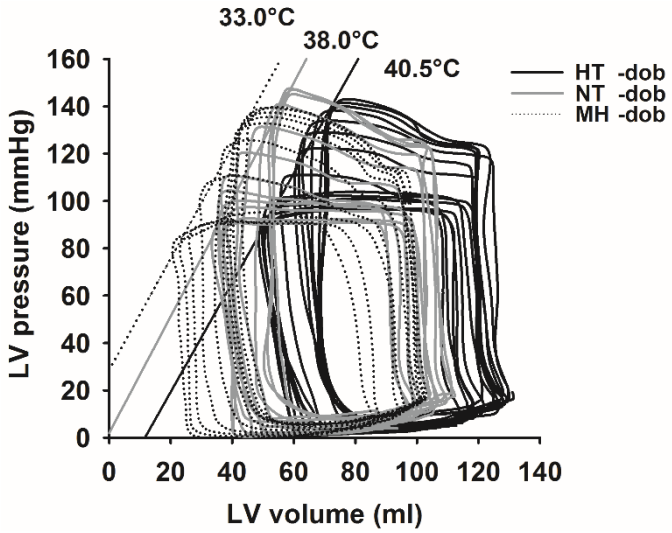

Figure 3.1: Original tracings of left ventricular pressure–volume loops during transient aortic occlusion at 40.5, 38.0 and 33.0 °C. There is a progressive leftward shift of the loops from hyperthermia to mild hypothermia, such that a given end-systolic pressure is reached at lower end-systolic volumes, indicating increased contractility. Lines indicate the end-systolic pressure–volume relationship. LV = left ventricle, -dob = before dobutamine infusion

Figure 3.2: LV end-systolic pressure-volume relationships (ESPVR): (a) the ESPVR is progressively shifted leftwards from hyper- (HT) to normothermia (NT) and from normo- to mild hypothermia(MH). The ESPVR during dobutamine infusion is shifted leftwards compared to the ESPVR before dobutamine at all three temperature steps (b-d). LV = left ventricle, -dob = before dobutamine infusion, +dob = during dobutamine infusion

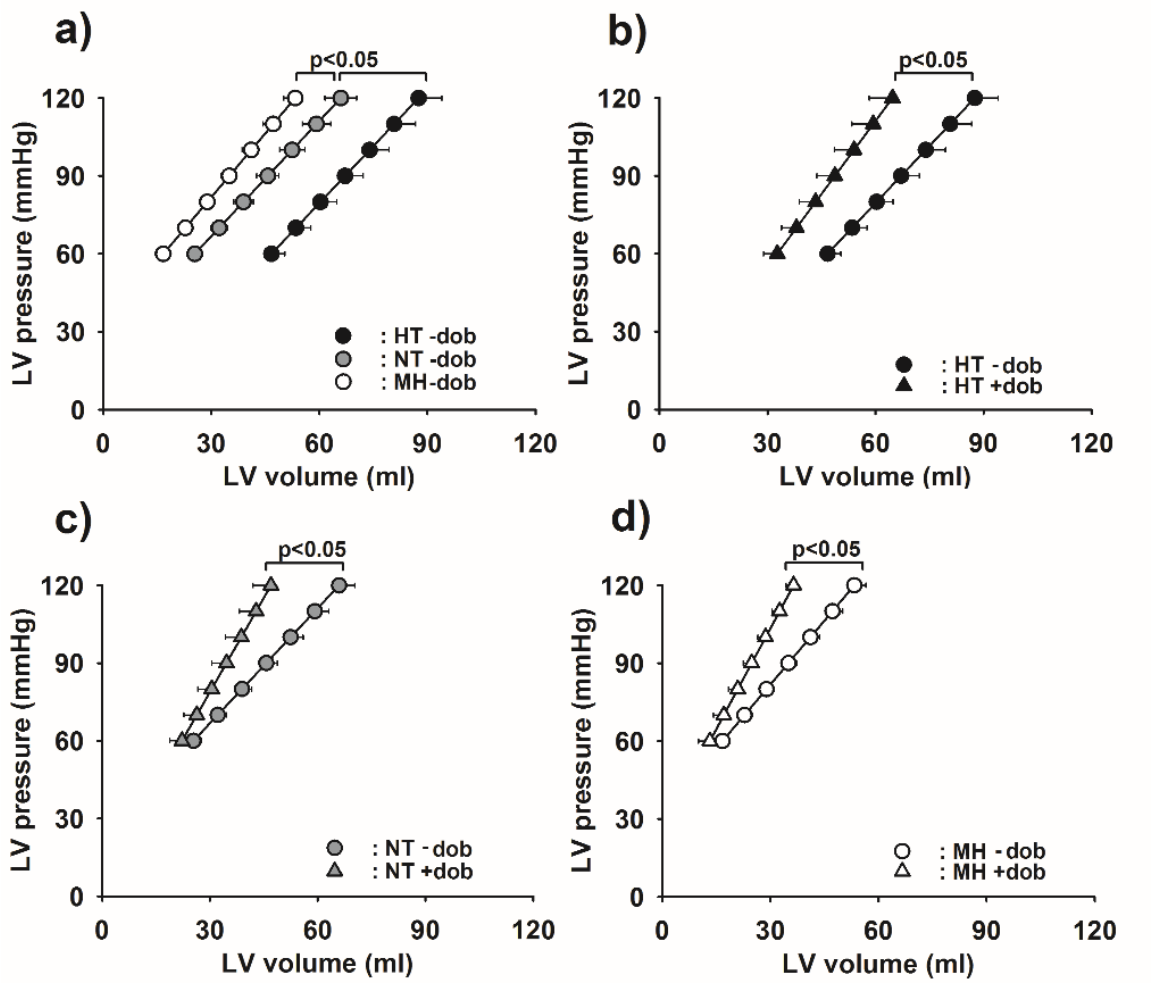

Figure 3.3: a) The LV end-systolic volume at an end-systolic pressure of 100 mmHg (LV VPes100) decreased with cooling from hyper- (HT) to mild hypothermia (MH), indicating increased contractility with lower temperatures. LV VPes100 was further decreased by dobutamine at all temperature steps. -dob = before dobutamine infusion, +dob = during dobutamine infusion *: p<0.05 vs. hyperthermia, §: p<0.05 vs. normothermia, †: p<0.05 vs. -dob at temperature step. b) The relative increase of LV contractility with cooling was comparable to the effect of dobutamine infusion at each temperature step. The overall effect from HT to MH exceeded the effect of dobutamine. *: p<0.05 vs. dobutamine steps

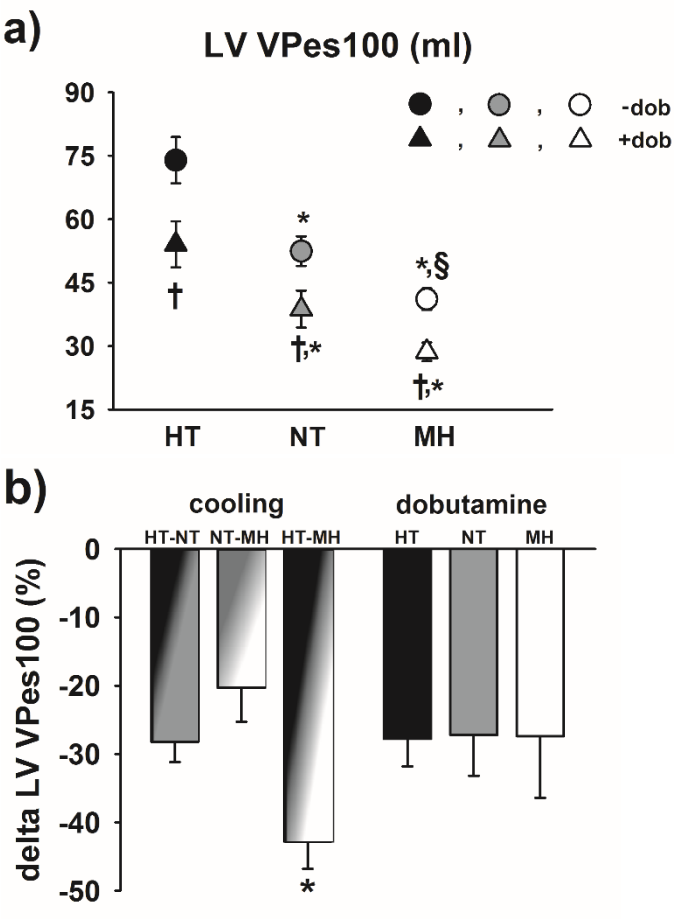

3.2.3 LV diastolic function

From HT to MH, LV end-diastolic volume decreased progressively, along with a lower maximum rate of LV pressure fall (dP/dtmin) and a prolonged isovolumic relaxation constant (τ) (Table 2). The EDPVR at spontaneous heart rate during NT was shifted rightwards by HT and leftwards by MH (Fig. 4a), and while dobutamine had no effect at NT or HT, it reverted the leftward shift of the EDPVR at MH (fig. 4b-d). Dobutamine infusion decreased the isovolumic relaxation constant at MH (Table 2).

Table 3.2: LV systolic and diastolic function. LV = left ventricle, -dob = before dobutamine infusion, +dob = during dobutamine infusion. [a]$p < 0.05$ vs. HT, [b]$p < 0.05$ vs. NT, [c]$p < 0.05$ vs. -dob at temperature step.

		HT (40.5 °C)	NT (38.0 °C)	MH (33.0 °C)
maximum LV pressure (mmHg)	**-dob**	92±2	84±2[a]	81±2[a]
	+dob	97±3	96±2[c]	97±3[c]
end-diastolic LV pressure (mmHg)	**-dob**	11±1	9±1[a]	9±1[a]
	+dob	9±0[c]	9±1	7±0[a,b,c]
maximum rate LV pressure increase (mmHg s^{-1})	**-dob**	1256±66	1457±74	1800±94[a,b]
	+dob	2470±162[c]	3071±146[a,c]	3570±140[a,b,c]
maximum rate LV pressure decrease (mmHg s^{-1})	**-dob**	-1760±60	-1349±66[a]	-640±35[a,b]
	+dob	-1965±81[c]	-1401±62[a]	-995±56[a,b,c]
LV isovolumic relaxation constant (□□ (ms)	**-dob**	31±0	40±1[a]	105±5[a,b]
	+dob	27±0	40±1[a]	71±4[a,b,c]
end-diastolic LV volume (ml)	**-dob**	129±7	109±8[a]	95±5[a,b]
	+dob	116±9[c]	102±7[a]	99±5[a]
LV ejection fraction (%)	**-dob**	53±2	64±1[a]	71±2[a,b]
	+dob	61±2[c]	68±2[a]	74±2[a]
LV stroke volume (ml)	**-dob**	68±3	70±4	67±3
	+dob	69±4	69±3	73±4
LV VPed10, end-diastolic volume at 10 mmHg (ml)	**-dob**	124±6	112±6[a]	97±5[a,b]
	+dob	121±7	110±6[a]	111±4[a,c]
end-systolic elastance (Ees)	**-dob**	1.57±0.15	1.58±0.14	1.74±0.15
	+dob	2.14±0.27[c]	2.63±0.27[a,c]	2.90±0.32[a,c]
volume axis intercept (V_0)	**-dob**	5.81±2.13	-15.11±3.21[a]	-19.95±3.92[a,b]
	+dob	0.74±3.51[c]	-2.49±2.67[a,c]	-10.03±5.34[a,b,c]

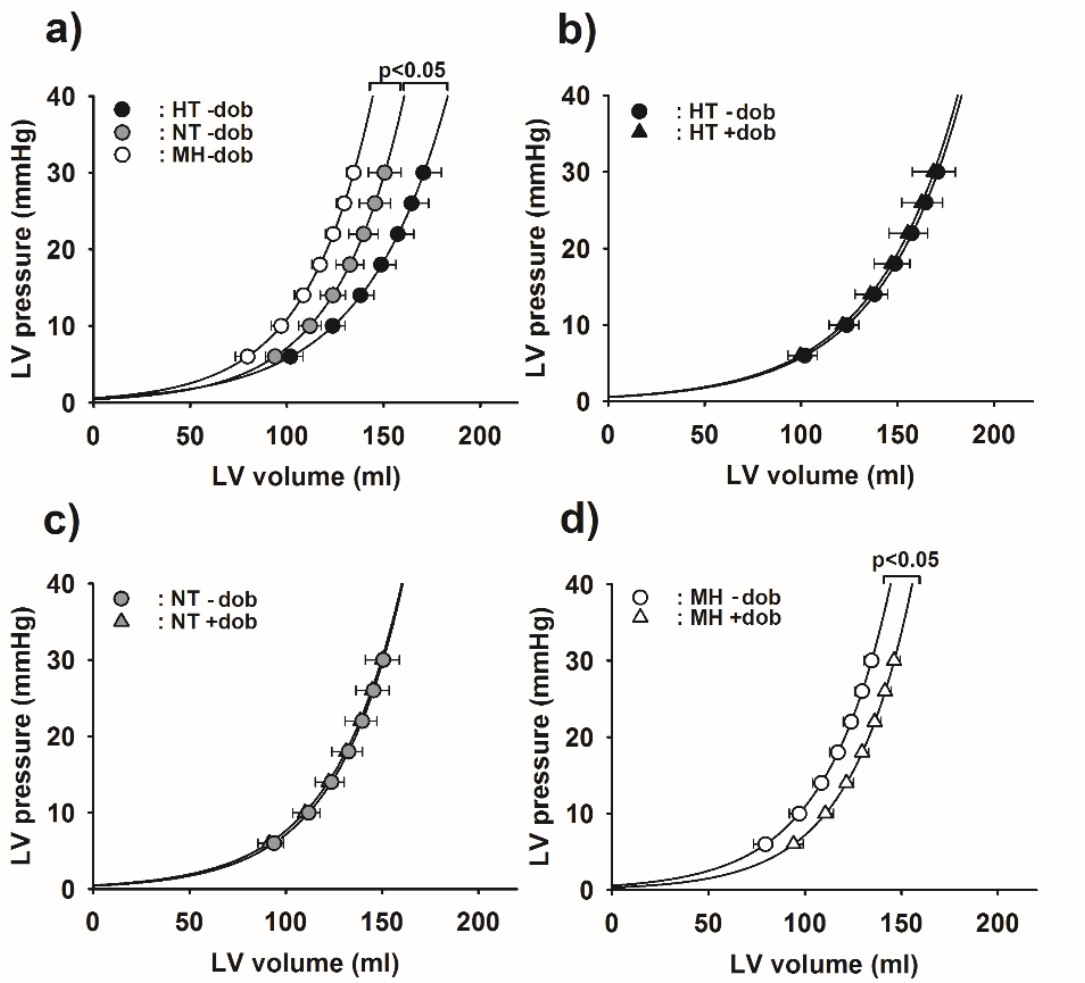

Figure 3.4: left ventricular end-diastolic pressure-volume relationships (EDPVR): (a) the EDPVR is progressively shifted leftwards from hyper- (HT) to normothermia (NT) and from NT to mild hypothermia (MH). The EDPVR during dobutamine infusion superimposed the EDPVR before dobutamine at HT (b) and NT (c). During MH, dobutamine re-shifted the EDPVR rightwards (d). LV = left ventricle, -dob = before dobutamine infusion, +dob = during dobutamine infusion

During HT and NT, pacing above 140 bpm decreased LV VPed10. During MH, such decrease of LV VPed10 was observed already at 100 bpm (Fig. 5a). Dobutamine infusion did not change this relationships during HT and NT (Fig. 5b-c), but increased LV VPed10 at each heart rate during MH (Fig. 5d).

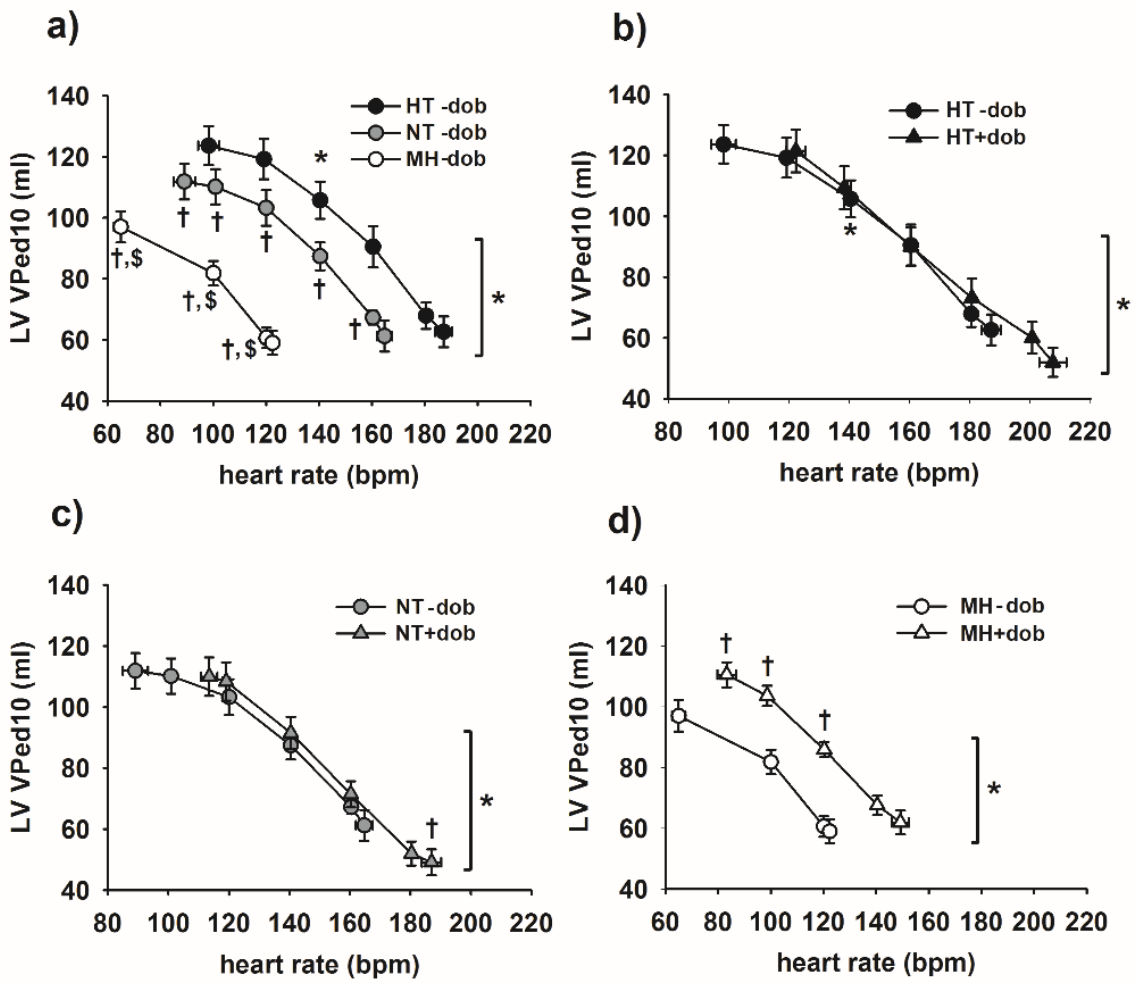

Figure 3.5: the LV end-diastolic volume at an end-diastolic pressure of 10 mmHg (LV VPed10) decreased from hyper- (HT) to normothermia (NT) and from NT to mild hypothermia (MH) at a given heart rate (a). The LV VPed10 during dobutamine infusion superimposed values before dobutamine at HT (b) and NT (c) at a given heart rate. During MH, the LV VPed10 was higher during dobutamine infusion at a given heart rate (d). -dob = before dobutamine infusion, +dob = during dobutamine infusion. (a) *: $p<0.05$ vs. spontaneous heart rate at temperature step, †: $p<0.05$ vs. HT at corresponding heart rate, §: $p<0.05$ vs. NT at corresponding heart rate. (b, c, d) *: $p<0.05$ vs. spontaneous heart rate, †: $p<0.05$ vs. -dob at corresponding heart rate

3.2.4 Blood gases and oxygen consumption

Whole body oxygen consumption decreased by approximately 50% with cooling from HT to MH (Table 1). Mixed venous oxygen saturation (O_2-Sat_{ven}) increased progressively during cooling from HT to MH. At each temperature step, dobutamine further increased O_2-Sat_{ven}. A given value of O_2-Sat_{ven} was reached at lower CPO values during cooling (Fig. 6). Arterial pH values, base excess, lactate and haemoglobin remained within the normal range during the protocol.

Figure 3.6: Cooling from hyper- to normo- and to mild hypothermia decreased while dobutamine increased cardiac power output (CPO). Both interventions increased mixed venous O_2 saturation. -dob = before dobutamine infusion, +dob = during dobutamine infusion.*: $p<0.05$ vs. hyperthermia, §: $p<0.05$ vs. normothermia, †: $p<0.05$ vs. -dob at temperature step.

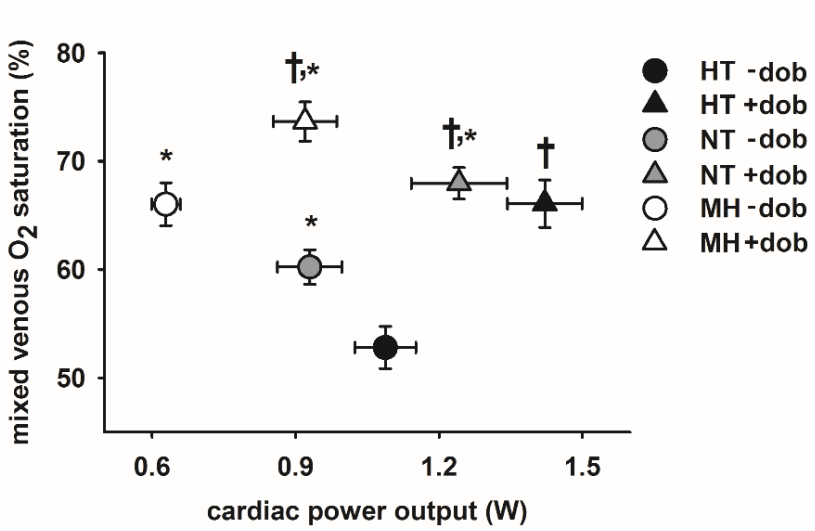

3.3 Discussion

After the results of the TTM trial (125) were published, the optimal target temperature in resuscitated patients after cardiac arrest, i.e., fever control or cooling to MH, has become a matter of debate. As most patients suffer from cardiac arrest on the background of a pre-existing cardiac disease (192) and temperature is an important determinant of cardiac function (77), we set out to compare systemic hemodynamic and cardiac effects of HT, NT and MH in closed-chest pigs in vivo. To illustrate the relevance of these effects, we performed a comparison to the standard positive inotrope dobutamine.

3.3.1 Systemic hemodynamics

Cooling from HT to NT and MH in the present study progressively decreased heart rate and cardiac output, while systemic vascular resistance increased from NT to MH. In contrast, dobutamine infusion increased heart rate and cardiac output by ≈ 25% and decreased systemic vascular resistance. These changes were reported already decades ago and had been discussed such that HT enhances and MH depresses cardiac function (193, 194). However, studies in isolated cardiac muscle strips, isolated hearts and in vivo have repeatedly demonstrated that either HT exerts a negative (126, 132, 195-197) or MH exerts a positive inotropic effect (127, 130, 131, 198) on left ventricular function. This discrepancy can be explained by the profound effect of temperature on whole body metabolic demand. Systemic oxygen consumption decreased by ≈ 50% from HT to MH in the present study, and even at a lower cardiac output mixed venous oxygen saturation – the net indicator of systemic oxygen supply-demand balance – increased. Systemic hemodynamic variables therefore fall too short to characterize LV function at different temperatures, and we therefore performed LV pressure-volume analysis.

3.3.2 LV systolic function

As shown in Fig. 1, lowering temperature induced a progressive leftward shift of the LV pressure-volume loop and the end-systolic pressure-volume relationship (ESPVR) (Fig. 2a). At lower temperatures, the LV ejected to smaller end-systolic volumes at a given end-systolic pressure (LV VPes100, circles in Fig. 3a), which indicates increased contractility. At each temperature step, the ESPVR was shifted further leftwards by dobutamine (Fig. 2b-d). Fig. 3b illustrates the effect size of cooling and dobutamine on LV VPes100. It becomes obvious that cooling from HT to NT increased LV contractility to the same amount as

dobutamine at HT, although both heart rate and cardiac output changed in opposite directions. This effect continued from NT to MH, and overall from HT to MH cooling was a more powerful inotrope than the dose of dobutamine applied in the present study.

While pressure-volume analysis and the decrease of LV VPes100 indicate a relevant inotropic effect of cooling, LV maximum dP/dt increases to a much smaller extent with cooling than with dobutamine. To some degree, the decrease of LV end-diastolic volume with lower temperatures may have counteracted the increase of maximum dP/dt, as this parameter is preload-dependent (199). In addition, the mechanism of positive inotropy differs between catecholamines and cooling. Beta-adrenergic receptor stimulation via the cyclic AMP-PKA pathway increases the cardiomyocyte calcium transient and hastens the rate of calcium release and reuptake into the sarcoplasmic reticulum (200). This translates into both increased force and speed of myocardial contraction and relaxation. In contrast, MH does not alter the cardiomyocyte calcium transient (127), but rather increases myofilament calcium responsiveness by an increase of calcium activated force (201) and possibly also by increased calcium sensitivity. A temperature-dependent decrease of SERCA activity and decreased cross-bridge detachment rates in turn prolong active LV relaxation (202, 203). Increased contractility during cooling therefore is not reflected by the speed (maximum dP/dt), but rather by the force of contraction (LV VPes100).

3.3.3 LV diastolic function

As reported before (131, 135), cooling from NT to MH prolonged the isovolumic relaxation constant τ and decreased minimum dP/dt; these changes were opposite when NT was compared to HT in the present study. Similarly, the end-diastolic pressure-volume relationship (EDPVR) was shifted leftwards during MH and rightwards during HT (Fig. 4a). We previously suggested that the prolongation of relaxation during MH is so profound that it limits LV filling and compliance and thereby induces a leftward shift of the EDPVR despite spontaneous bradycardia (135). In line with this concept, infusion of dobutamine during MH in the present study shortened τ and re-shifted the EDPVR nearly back to normothermic values (Fig. 4d). In contrast, the effect of dobutamine on τ at HT and MH was minor. As τ increases with load (204), the increase of LV pressure during dobutamine infusion may have masked a shortening of τ. In addition, larger doses of ß-adrenergic agonists may be needed to accelerate LV relaxation to supraphysiologic rates at NT and HT compared to the correction of subphysiologic rates at MH. In line with that, dobutamine did not impact on the shift of the EDPVR between NT and HT (Fig. 4b-c). It is also conceivable

that HT increases LV compliance by direct myofilamental effects, for example by post-translational modification of myofilamental and/or cytoskeletal proteins (205).

The increase of heart rate during dobutamine infusion can cause an acceleration of LV relaxation per se (189-191). We therefore increased heart rate to multiples of 20bpm up to the maximum at each temperature before and during dobutamine infusion and indexed the single EDPVRs by the volume at an end-diastolic pressure of 10 mmHg (LV VPed10, Table 1 and Fig. 5a). Right atrial pacing at 140 bpm and higher decreased LV VPed10 both at HT and NT, while at MH, this occurred already at 100 bpm (Fig. 5a). The relationship between LV VPed10 and heart rate remained unaffected by dobutamine at HT and NT, but was shifted upwards towards a higher LV compliance at MH (Fig. 5d). This indicates that incomplete LV relaxation during MH decreases LV compliance independent of heart rate effects on relaxation. In summary, we conclude that dobutamine improves LV compliance at MH by hastening a profoundly slowed relaxation. Vice versa, when LV relaxation rates are normal during NT, higher doses of dobutamine would be needed to impact on LV compliance during higher heart rates.

3.3.4 Systemic oxygen supply-demand balance

The SHOCK trial determined a critical level of CPO below which metabolic and oxygen demand are no longer met and mortality steeply increases in patients with cardiogenic shock (178, 206). The acute balance of systemic oxygen supply and demand in turn is reflected by mixed venous oxygen saturation (O_2-Sat_{ven}), which has prognostic value in patients undergoing heart surgery (207, 208). As cooling decreases oxygen demand and increases O_2-Sat_{ven} (Table 1), the critical level of CPO in patients with cardiogenic shock may strongly depend on temperature. We therefore plotted O_2-Sat_{ven} as a function of CPO in the present study (Fig. 6). When dobutamine was started at HT, O_2-Sat_{ven} increased by more than 10% due to an increased cardiac output. The same increase was present when the animals were cooled to MH, however, the corresponding CPO was less than half than at HT+dobutamine infusion. Given that catecholamines can empty cardiomyocyte energy stores during limited blood flow, are arrhythmogenic and considered as toxic in general, cooling appears as a promising synergistic or even alternative therapy to improve an oxygen supply-demand imbalance in cardiogenic shock.

3.4 Limitations

A limitation of our study lies in the fact that we investigated the cardiovascular effects of high and low temperatures in pigs with normal cardiac function. However, we have previously demonstrated the stability of our experimental setup (135, 169, 170) in several experimental settings of acute cardiac dysfunction, comprising a model of resuscitation after electrically induced ventricular fibrillation (168).

In addition, we are aware of the fact that in the clinical setting the priority would not be given to LV "contractility", as defined in this study, but to remedies enhancing CO and global perfusion pressure. However, despite a decreased CO with cooling, the pronounced decrease of demand (more than 50% of WB-O2) lead to an improved relationship between CPO and mixed venous oxygen saturation, with higher O2-Sat_{ven} at a given CPO, enhancing global perfusion pressure. We are therefore convinced of the relevance of our findings in the clinical arena and we believe that the combination of increased LV contractility and hypometabolic state induced by cooling can be beneficial in patients with acutely reduced cardiac reserve.

3.5 Clinical implications and conclusions

We demonstrate that temperature is a powerful determinant of systemic hemodynamics and cardiac systolic and diastolic function. The inotropic effects of temperature, in particular already between HT and NT, have the magnitude of standard inotropic support by dobutamine. As cooling increases also systemic vascular resistance, it may save both positive inotropes and vasopressors, as already indicated in clinical studies (209, 210). In addition, the lusitropic effect of dobutamine hastens LV relaxation and reverses the decrease of LV compliance during MH, pointing towards a possible synergistic effect of MH and ß-adrenergic stimulation in resuscitated patients. Finally, the hypometabolic state during cooling allows the heart to meet systemic oxygen demand at a much lower amount of external work, which may provide acutely failing hearts with time to recover. These data imply that in resuscitated patients already prevention of fever can improve LV function, but that further cooling would provide additional benefit in an unstable hemodynamic situation.

Chapter 4:

LV mechanics and myocardial perfusion in a porcine model of early-stage HFpEF: a CMR imaging study

4.1 Introduction

Heart failure with preserved ejection fraction (HFpEF) evolves by accumulation of risk factors over time and still lacks a guideline therapy, in part due to the complex pathophysiology and a shortage of relevant animal models (39). An increased left ventricular stiffness at rest is the hemodynamic hallmark of the disease (70). However, most patients become symptomatic preferably during exercise, and the mechanisms leading the transition from mere diastolic dysfunction to heart failure symptoms are unclear at present.

Several small-scale clinical studies, in the past years, have been investigating hemodynamic response of severe hypertensive and early-HFpEF patients to dynamic exercise (78, 81, 82, 84, 97), showing that the reduced diastolic reserve function consists of several components, ranging from a loss of relaxation enhancement, to reduced suction and further pronounced stiffness (Chapter 1.4.2). Furthermore, a recent study in hypertensive patients at risk for HFpEF has shown an intriguing correlation between reduced coronary flow reserve, LV functional impairment, circulating markers of myocardial fibrosis and exercise tolerance (211). It was therefore postulated that limited myocardial perfusion and contractility reserve may induce subendocardial ischemia and fibrosis, and play a major role in the transition from diastolic dysfunction to exercise intolerance (212).

The DOCA-salt-induced hypertensive pig has been introduced as a large animal model for mineralocorticoid-induced hypertension (213-215). DOCA-salt-induced hypertension in the pig is associated with a pronounced phenotype, comprising concentric LV hypertrophy (216, 217), increased peripheral vascular resistance (218-221), and contractile impairment of vascular smooth muscle cells (222, 223). We recently established a model of early stage HFpEF, combining DOCA-salt-induced hypertension with western diet. We have shown that this model (182) is characterized by left atrial (LA) dilatation, a stiff LV (as shown by a leftward shift of the EDPVR associated with myocyte hypertrophy), titin isoform shift and reduced total-titin phosphorylation in the sub-endocardial layer, and increased LV end-diastolic pressures at lower cardiac output (182). These characteristics resemble important HFpEF patients' features, and make it an attractive model to investigate dynamic response of LV to stress.

Cardiac magnetic resonance (CMR) imaging is the gold standard for non-invasive assessment of cardiac and myocardial function and morphology [18-21]. CMR techniques such as cine imaging, myocardial tagging and 4D flow imaging at rest and during stress as well as myocardial T1 mapping make it possible to investigate cardiac function, evaluate

stress-induced differences, and identify myocardial tissue alterations in a single investigation.

In this chapter, we therefore aimed to evaluate comprehensive CMR imaging of the previously established model of early HFpEF, in comparison with weight-matched control pigs at rest and during dobutamine stress, to identify potential mechanisms contributing to exercise intolerance in early-stage HFpEF.

4.1 Specific Methods

The study was approved by the local Bioethics Committee of Vienna, Austria (BMWF-66.010/0091-II/3b/2013) and conformed to the guide for the care and use of laboratory animals, US National Institute of Health (NIH Publication No. 85–23, revised 1996). Arterial hypertension was induced in six animals (65±2 kg) by subcutaneous implantation of DOCA pellets (as described in Chapter 2, paragraph 2.1.6) in combination with a high-salt, high-sugar, high-potassium diet. After 12 weeks of treatment, animals were examined by cardiac magnetic resonance (CMR) imaging at rest and during dobutamine stress. Seven weight-matched healthy animals (58±9) served as controls. One animal in the DOCA-salt-treated group (hereafter, DOCA) was excluded because of florid pericarditis.

4.1.1 Experimental setup

After 12 weeks of treatment, animals were sedated by intramuscular administration of ketamine (20 mg·kg-1), midazolam (0.25 mg·kg-1) and azaperone (5 mg·kg-1). Anaesthesia was induced by 30-60 mg propofol to allow endotracheal intubation. Pigs were mechanically ventilated and anaesthesia was maintained with sevoflorane (1.5-2.5%), fentanyl (35 µg·kg^{-1}·h^{-1}), midazolam (1.2 mg·kg^{-1}·h^{-1}), ketamine (2-8 mg·kg^{-1}·h^{-1}) and pancuronium (0.2 mg·kg^{-1}·h^{-1}). Sheaths were placed in a carotid artery to monitor the arterial blood pressure and in the jugular veins to adjust the infusion rate to volume need. Further details are given in Chapter 2, paragraph 2.1.4.

4.1.2 Experimental protocol

The protocol consisted of two imaging sessions, one at rest and one during stress-test, with dobutamine titrated to increase heart rate of approximately 25% (2-8 µg·kg-1·min-1). Each session consisted of assessment of cardiac and myocardial function, blood flow and LV T1 times. At the end of the protocol and in a subgroup of 8 animals (5 DOCA and 3 controls), the heart was explanted and tissue samples harvested for stereological analysis of LV free wall layers.

4.1.3 LV stereology

The following parameters were assessed by the method of point counting (224): volume fraction of interstitium (VV(int/lv)), volume fraction of cardiomyocytes (VV(myo,lv)=1-

VV(int/lv)), of blood vessels (VV(ves/lv)) and of collagen fibrils either related to the left ventricle (VV(coll/lv)) or to the interstitium (VV(coll/int)) as reference volume. The total myocyte (V(myo,lv)), collagen V(coll,lv) and blood vessel V(ves,lv) content in the myocardium were obtained by multiplying LVMM with VV(myo/lv), VV(coll/lv), and VV(ves/lv), respectively. More details are described in Chapter 2, paragraph 2.2.1.

4.2 Results

The baseline characteristics of DOCA and control animals are summarized in Table 4.1. DOCA pigs did not differ from controls by heart rate, body weight and body surface index, while systolic, diastolic and mean arterial pressure were higher at rest, resulting in a higher rate-pressure product. This difference disappeared during dobutamine stress, indicating a failure of DOCA animals to increase mean arterial pressure compared to controls. The dose of dobutamine needed to increase heart rate of 25% was lower in the DOCA animals compared to controls (2.8±0.9 $10^{-5}\cdot\mu g\cdot kg^{-1}\cdot min^{-1}$ vs 5.3±2.0 $10^{-5}\cdot\mu g\cdot kg^{-1}\cdot min^{-1}$, $p<0.05$).

Table 4.1: Baseline characteristics of control and DOCA animals**.** BSA = body surface area, HR = heart rate, mBP = mean blood pressure, sBP = systolic blood pressure, dBP = diastolic blood pressure, RPP = rate pressure product.*: $p<0.05$ vs rest, §: $p<0.05$ vs control at rest.

	Control		**DOCA**	
parameter	**rest**	**stress**	**rest**	**stress**
weight (kg)	58±9	-	65±2	-
BSA (m^2)	1.05±0.10	-	1.14±0.03	-
HR (min^{-1})	89±5	114±3*	86±8	110±13*
mBP (mmHg)	87±7	95±13	106±8§	101±12
sBP (mmHg)	103±8	116±9*	125±6§	120±11
dBP (mmHg)	75±9	82±16	96±10§	86±12
RPP ($mmHg\cdot min^{-1}$)	92±8	132±11*	108±14§	132±17*

4.2.1 Left ventricular geometry and function

Table 4.2 summarizes the major parameters of LV geometry and LV function. DOCA animals showed higher LV muscle mass (LVMM, 111±9 $g \cdot m^{-2}$ vs 84±7 DOCA vs controls, $p<0.05$) and increased end-diastolic and end-systolic wall thickness (WT_{ED} and WT_{ES}) at both rest and stress, indicating LV concentric hypertrophy with preserved ejection fraction. LV wall thickening and mitral annular plane systolic excursion (MAPSE) differed between groups only at rest. LV end-systolic (ESV) and end-diastolic volume (EDV), stroke volume and cardiac index did not differ at rest between groups. Dobutamine increased LV ejection-fraction and decreased LV end-systolic volume in both groups. However, cardiac index increased less in DOCA pigs (DOCA vs controls, 37±12% vs 63±23%, $p<0.05$), and the LV end-diastolic volume significantly decreased during stress only in the DOCA animals (DOCA vs controls, -20±11% vs -5±11%; $p<0.05$). Finally, the isovolumic relaxation time (IVRT) was prolonged in the DOCA pigs compared to controls only at rest, while did not differ during stress.

Table 4.2: LV geometry and function. WTED = end-diastolic wall thickness, WTES = end-systolic wall thickness, WTH = wall thickening, MAPSE = mitral annular plane systolic excursion, EF = left ventricular ejection fraction, EDV = left ventricular end-diastolic volume, ESV = left ventricular end-systolic volume, SV = left ventricular stroke volume, CI = left ventricular cardiac index. *: $p<0.05$ vs rest, §: $p<0.05$ vs control at rest, †: $p<0.05$ vs control during stress.

	Control		**DOCA**	
parameter	**rest**	**stress**	**rest**	**stress**
WT_{ED} ($mm \cdot m^{-2}$)	6.3±1.2	6.2±1.4	8.3±0.8§	9.3±1.6†
WT_{ES} ($mm \cdot m^{-2}$)	9.6±1.6	11.8±2.2*	13.0±1.4§	15.5±1.9*,†
WTH ($mm \cdot m^{-2}$)	3.3±0.8	5.6±1.7*	4.8±0.9§	6.2±1.1
MAPSE (mm)	11.1±3.6	15.0±3.7	6.9±1.2§	13.5±4.9*
EF (%)	52±3	69±7*	53±5	70±2*
EDV ($ml \cdot m^{-2}$)	124±15	117±12	125±18	102±26*
ESV ($ml \cdot m^{-2}$)	59±9	36±10*	59±10	30±9*
SV ($ml \cdot m^{-2}$)	65±8	81±9*	66±11	71±17
CI ($l\ min^{-1} \cdot m^{-2}$)	5.8±0.9	9.4±1.1*	5.8±1.0	7.8±1.2*,†
IVRT (ms)	80±15	78±16	99±10§	93±17

4.2.2 Transmitral and myocardial tissue velocities

Early diastolic myocardial tissue peak velocity (E') was lower in DOCA at rest and during stress (table 4.3), transposing to higher E/E' at rest and stress (Figure 4.1). Transmitral inflow pattern did not differ between groups (Table 4.3). (E/E′)/EDV was higher in DOCA pigs both at rest (3.6±0.9 vs 2.7±0.5, p<0.05) and during stress (4.8±1.6 vs 3.1±0.6, p<0.05).

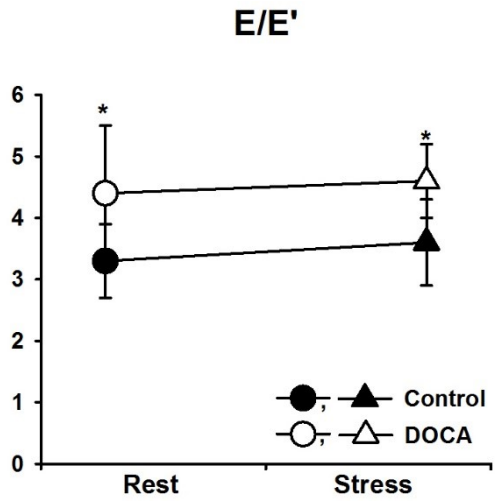

Figure 4.1: Ratio between E wave and early diastolic myocardial tissue peak velocity (E') at rest and stress in the two groups.*p<0.05 between groups.

	Control		DOCA	
parameter	**rest**	**stress**	**rest**	**stress**
E ($cm \cdot s^{-1}$)	63±6	78±9*	56±10	70±11*
A ($cm \cdot s^{-1}$)	47±11	48±9	43±12	43±13
E/A	1.4±0.5	1.7±0.5	1.4±0.4	1.7±0.5*
AT (ms)	87±17	79±9	83±14	70±9
DT (ms)	152±50	163±66	169±67	153±16
E'_{sep} ($cm \cdot s^{-1}$)	18±4	20±6	11±3§	14±2
E'_{lat} ($cm \cdot s^{-1}$)	21±5	25±6	14±3	16±3†
E' ($cm \cdot s^{-1}$)	20±4	23±6	13±2§	15±2†

Table 4.3: Summary of transmitral and tissue velocities parameters. E = early diastolic transmitral peak velocity, A = late diastolic transmitral peak velocity, AT= acceleration time, DT= deceleration time, E'sept = early diastolic septal wall mitral annular tissue velocity, E'lat = early diastolic lateral wall mitral annular tissue velocity, E' = average early diastolic mitral annular tissue velocity. *: p<0.05 vs rest, §: p<0.05 vs control at rest, †: p<0.05 vs control during stress.

4.2.3 Pulmonary venous velocities

Alterations in the pulmonary venous flow pattern, with higher D-wave and lower S/D ratio in the DOCA animals compared to controls, were present only at rest, and disappeared during stress (Table 4.4).

	Control		DOCA	
parameter	**rest**	**stress**	**rest**	**stress**
S1 ($cm \cdot s^{-1}$)	33±9	48±4*	39±18	46±5
S2 ($cm \cdot s^{-1}$)	40±10	49±9*	44±18	44±5
D ($cm \cdot s^{-1}$)	37±10	56±11*	57±17§	58±6
S/D	1.1±0.2	0.9±0.2*	0.8±0.2§	0.8±0.2

Table 4.4: Pulmonary venous velocities. S1 = early systolic pulmonary venous peak velocity, S2 = systolic pulmonary venous peak velocity, D = early diastolic pulmonary venous peak velocity, S = maximal systolic pulmonary venous peak velocity. *: $p<0.05$ vs rest, §: $p<0.05$ vs control at rest.

4.2.4 Global Myocardial perfusion and perfusion reserve

Coronary sinus blood flow volume was increased in the DOCA pigs at rest (1.6±0.5 ml/m^2 vs 2.4±0.6 ml/m^2 control vs DOCA, $p<0.05$) but failed to further increase during stress (2.7±1.0 ml/m^2 vs 2.8±0.5 ml/m^2, control vs DOCA). However, as a result of the higher LVMM in DOCA pigs, global myocardial perfusion (GMP) did not differ between groups at rest. On the contrary, during stress GMP increased less in DOCA pigs, resulting in reduced myocardial perfusion reserve (MPR, Figure 4.2).

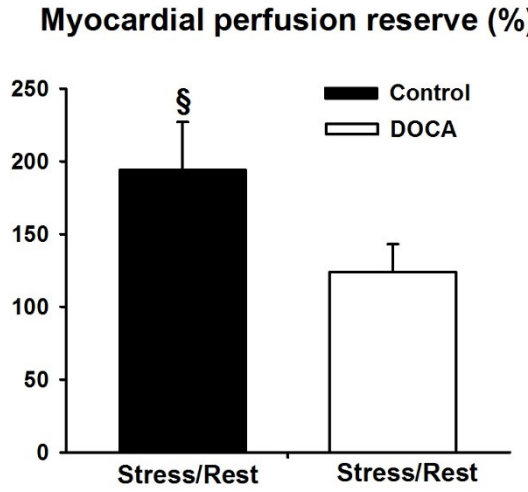

Figure 4.2: Myocardial perfusion reserve (MPR). §: $p<0.05$ between groups.

4.2.5 LV myocardial strains and torsion

One control pig was excluded from the analysis for poor image quality. Circumferential, radial and longitudinal strain and strain rate as well as torsion and torsion rates were evaluated. Results are summarized in table 4.5.

Significant differences were detected only with regard to longitudinal strain rate (LL rate) and torsion. Whereas systolic LL $rate_{min}$ did not differ between groups at rest, it was smaller in DOCA animals during stress. Systolic torsion $rate_{max}$ showed the opposite behavior, being significantly higher in DOCA pigs at rest but not during stress. Diastolic torsion $rate_{min}$ did not differ significantly between groups; however, the torsion $rate_{min}$ failed to properly increase during stress in the DOCA group (DOCA, $0\pm5°\cdot s^{-1}$; control, $-19\pm11°\cdot s^{-1}$; $p<0.05$).

	Control		**DOCA**	
parameter	**rest**	**stress**	**rest**	**stress**
$CC_{min,LV}$ (%)	-16±1	-17±2	-17±2	-18±3
$RR_{max,LV}$ (%)	34±12	39±11	33±4	35±5
$LL_{min,LV}$ (%)	-13±2	-13±3	-12±1	-11±2
$torsion_{max}$ (°)	4.6±1.4	5.7±1.6	6.1±0.9	7.0±1.2
CC $rate_{min,LV}$ ($\%\cdot s^{-1}$)	-90±11	-139±19*	-96±13	-155±16*
RR $rate_{max,LV}$ ($\%\cdot s^{-1}$)	185±52	337±66*	188±36	309±81*
LL $rate_{min}$ ($\%\cdot s^{-1}$)	-77±11	-120±15*	-68±6	-95±13*,†
torsion $rate_{max}$ ($°\cdot s^{-1}$)	29±3	47±15*	44±8§	62±17
CC $rate_{max,LV}$ ($\%\cdot s^{-1}$)	83±4	119±30*	89±11	129±20*
RR $rate_{min,LV}$ ($\% s^{-1}$)	-190±81	-229±90	-192±41	-222±53
LL $rate_{max}$ ($\%\cdot s^{-1}$)	51±19	71±17	47±10	58±10
torsion $rate_{min}$ ($°\cdot s^{-1}$)	-24±6	-43±13*	-28±9	-28±7

Table 4.5: LV strain and torsion. CCmin,LV = minimal left ventricular circumferential strain, RRmax,LV = maximal left ventricular radial strain, LLmin,LV = minimal left ventricular longitudinal strain, torsionmax = maximal left ventricular torsion, CC ratemin,LV = systolic minimum circumferential strain rate, RR ratemax,LV = systolic maximal radial strain rate, LL ratemin = systolic minimal longitudinal strain rate, torsion ratemin = systolic minimal torsion rate, CC ratemax,LV = early diastolic maximal circumferential strain rate, RR ratemin,LV = early diastolic minimal radial strain rate, LL ratemax = early diastolic maximal longitudinal strain rate, torsion ratemax = early diastolic maximal torsion rate. *: $p<0.05$ vs rest, §: $p<0.05$ vs control at rest, †: $p<0.05$ vs control during stress.

4.2.6 Global LV myocardial T1 times

After image-quality evaluation, five DOCA and six control animals were included in this analysis. Global LV T1-times did not differ between groups (DOCA, 1174±27 ms; controls, 1201±39 ms), indicating no detectable difference in myocardial magnetic relaxation proprieties between the two groups.

4.2.7 Stereological analysis

We collected and analysed samples from five DOCA and three control pigs. At the stereological analysis, volume fractions of the interstitium and of blood vessels did not differ between the DOCA and control group. Volume fractions of collagen with respect to both the LV and the interstitium were significantly increased in the DOCA group (Figure 4.3). Total myocyte volume (V(myo/lv), DOCA, 104±16 ml; controls, 67±1 ml; $p<0.05$), total collagen volume (V(col/lv), DOCA, 3.8±1.0 ml; controls, 1.5±0.4 ml; $p<0.05$) and total blood vessel volume (V(ves/lv), DOCA, 7.1±1.2 ml; controls, 3.7±1.1 ml; $p<0.05$) were higher in the DOCA pigs than in the control pigs.

Figure 4.3: Stereological analysis of the LV volume fractions of collagen in DOCA and control animals.

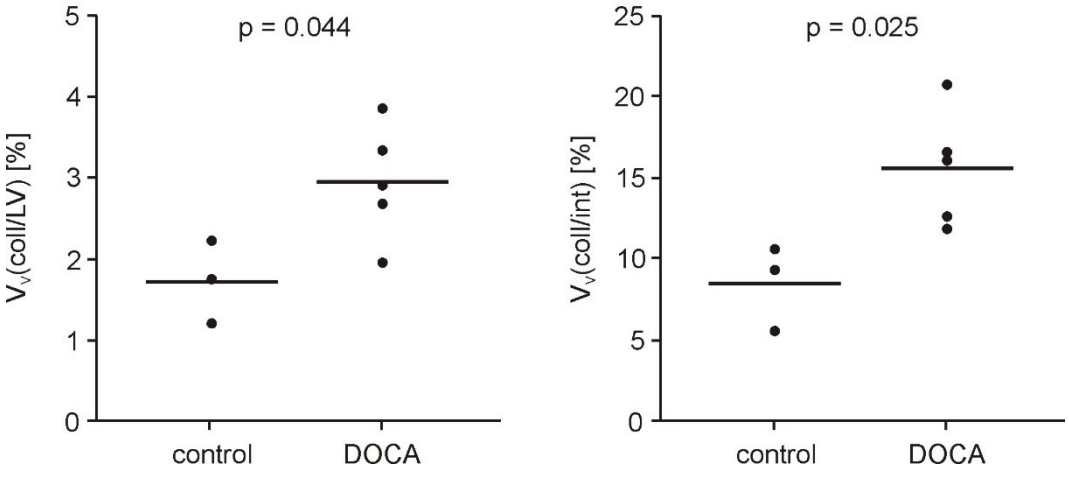

4.3 Discussion

In this study, we evaluated comprehensive CMR imaging of a porcine model of early HFpEF in comparison with weight-matched control pigs, at rest and during dobutamine stress. DOCA pigs showed concentric LV hypertrophy, impaired LV filling at both rest and stress, and altered myocardial muscle mechanics, in particular longitudinal strain rate and torsion. Under stress, DOCA pigs failed to increase cardiac index as much as controls, while showing a reduced myocardial perfusion reserve. Finally, native T1 mapping failed to detect the significant collagen elevation showed by stereological analysis.

4.3.1 Left ventricular geometry and myocardial structure

DOCA pigs developed concentric LV hypertrophy, with increased wall thickness and muscle mass (Table 4.2), as previously reported by our and other groups in both Landrace and Yucatan miniature swine (182, 213, 216, 217). 3D reconstruction of LV histology by stereological analysis of the collected samples showed both cardiomyocyte hypertrophy and increased levels of collagen (i.e., a higher collagen volume relative to the interstitial space, relative to LV myocardium and as absolute volume, Figure 4.3), indicating a transition state from LV hypertrophy to HFpEF (225-227). The latter finding is in contrast with our previous study, where picrosirius red staining did not show any collagen increase in DOCA pigs compared to controls (182), and may be attributable to the different quantitative accuracy of these two experimental approaches. In addition, native T1 mapping failed to detect any significant collagen increase in the DOCA animals, while normally T1 time is reported to be increased with higher myocardial collagen (228, 229). In this regard, being the effective time obtained by T1 mapping the result of the magnetic relaxation time of all compartments in the voxel, the increased volume fraction of cardiomyocytes may have decreased T1 times, masking the elevated levels of collagen in the relatively small interstitium.

4.3.2 Left ventricular function and mechanics

In our study, the abovementioned structural changes in the DOCA pigs were paralleled by functional and mechanical alterations. As expected during β-adrenergic stress, LV ejection fraction increased and ESV decreased in both groups. However, EDV significantly decreased during stress in DOCA pigs, inhibiting stroke volume and cardiac index from properly increasing with the heart rate. A similar response was reported in patients with

HFpEF during dynamic exercise (78, 230). Other signs of subtle systolic dysfunction in our DOCA animals were an impaired MAPSE at rest, indicating an altered longitudinal function, and a lower LL $rate_{min}$ during stress compared to controls. This is in line with echocardiographic studies in HFpEF patients that showed reduced longitudinal and circumferential strain (87), and a failure to enhance global longitudinal strain rate during stress (231). However, and differently from our DOCA animals, in those patients EF failed to increase during stress, indicating somehow a later stage of disease. These results address once again the contribution of subtle LV systolic dysfunction to the overall progression from the hypertensive heart disease to the HFpEF phenotype (87, 232, 233).

The DOCA animals showed no alteration in the transmitral inflow pattern (Table 4.3). However, early diastolic myocardial tissue peak velocity was lower in DOCA at rest and during stress, transposing to higher E/E' (Figure 4.1). This is in line with studies in both early-stage HFpEF and hypertensive patients (103, 230, 234). The alterations observed in the pulmonary venous flow patterns in DOCA pigs, with lower S/D ratio at rest and with a failure to increase systolic and diastolic pulmonary venous peak velocities during stress, are indicating an impaired relaxation (235, 236) and can be as well related to the increased E/E' (236).

In addition, a recent study (230) showed a marked increase of (E/E')/EDV during exercise in HFpEF patients and correlated this index of diastolic stiffness with decreased exercise tolerance. Similarly, in the DOCA pigs the observed increased (E/E')/EDV appears to be related to the prolonged IVRT at rest (83, 234, 237) and/or subtle stress-induced myocardial ischemia (95), as indicated by the lower global myocardial perfusion reserve during dobutamine in the hypertrophied LV myocardium. This would be in line with a recent study in hypertensive patients at risk for HFpEF, showing a correlation between reduced coronary flow reserve, LV functional impairment, circulating markers of myocardial fibrosis and exercise tolerance (211).

Finally, torsion and systolic torsion $rate_{max}$ were higher in DOCA than control pigs, as a result of the increased lever arm for epicardial fibers in the context of a concentric remodelled LV (238). On the other hand, diastolic torsion $rate_{min}$ significantly increased during β-adrenergic stimulation in the control group, but not in DOCA animals, indicating reduced intraventricular pressure gradients and impaired LV untwisting enhancement during stress, as already described in elderly patients (239, 240).

4.3.3 Blood supply and myocardial perfusion

In this study, DOCA animals showed an increased coronary sinus blood flow volume at rest, likely in order to maintain myocardial perfusion in the hypertrophied myocardium. This functional finding was paralleled by a larger absolute vessel volume compartment V(ves/lv) compared to controls by stereological analysis. However, these compensatory mechanisms were to some extent challenged by the dobutamine stress test, unmasking an impaired myocardial perfusion reserve. Our findings are therefore in line with the vasodilator reserve impairment observed in HFpEF patients during exercise (99).

4.4 Limitations

Several limitations of the present study need to be acknowledged. The study had a small sample size; therefore, it was not possible to assess correlations between studied parameters. Moreover, samples for stereological analysis were collected in a sub-group of animals only from the LV lateral wall and, for reasons of feasibility, not by a random sampling scheme.

All CMR measurements were performed under mechanical ventilation. Breathing motion was typically suppressed by averaging, except for the MOLLI sequence. Automated motion correction, however, enabled appropriate reconstruction of T1 maps. 4D flow data were acquired with one velocity encoding optimized for LV intra-cavity blood flow, and all flow results were determined a posteriori from this dataset. The multiple acquisitions of smaller data sets with optimized velocity encoding and optimized resolution might have improved the accuracy of results but would have further prolonged investigation time.

Finally, invasive intra-cardiac hemodynamic measurements were not performed during CMR examinations, as appropriate MR-compliant equipment was not available.

4.5 Conclusion

The present study has characterized cardiac and myocardial function at rest and during stress in a previously established large animal model of early-stage HFpEF. Aside numerous functional alterations at rest, such as altered myocardial muscle mechanics and left ventricular filling characteristics, we observed an impaired increase of cardiac index during dobutamine stress that was paralleled by a reduced myocardial perfusion reserve. Exercise induced myocardial ischemia may therefore be a contributor to LV dysfunction in the early stage of the disease, and may serve as an early marker of transition from diastolic dysfunction to symptomatic heart failure. Of note, myocardial T1 mapping could not detect elevated levels of myocardial collagen found by stereology in our early-stage HFpEF model.

Chapter 5:

Effects of soluble guanylate cyclase (sGC) stimulation and phosphodiesterase (PDE) 5A inhibition on myocardial function

5.1 Introduction

Heart failure is the leading cause of mortality worldwide. Heart failure patients have either a reduced or a preserved LV ejection fraction (HFpEF), and the prevalence of these two clinical phenotypes is equally distributed (13, 30). HFpEF patients share the same poor prognosis of patients with reduced ejection fraction. However, in striking contrast with their clinical counterpart, there are no available therapeutic options improving their outcome (13) (Chapter 1.3.2).

The pathophysiology of HFpEF is complex and poorly understood (33). On a cellular level, a pronounced lack of cGMP and subsequent low PKG-activity have been demonstrated in myocardial biopsies from HFpEF patients (111). This is considered as a major contributor in the pathogenesis of HFpEF (55), because reduced PKG-mediated phosphorylation of the myofilamental protein titin leads to increased cardiomyocyte passive tension (241) and reduced LV capacitance. In the past years, cGMP-enhancing drugs have therefore emerged as possible therapeutic approach to this condition.

Stimulators of soluble guanylate cyclase (sGC) represent a new class of drugs, which impact on the nitric oxide (NO) – sGC – cGMP – PKG pathway. Their effects on vascular function have been studied extensively within the last decade (159) and clinical benefit has been demonstrated in patients affected by pulmonary arterial hypertension (242, 243). However, little is known about their effect on LV compliance in disease conditions associated with lowered myocardial cGMP levels.

Pharmacological inhibitors of PDE5A, such as sildenafil, represent another class of drugs impacting on the cGMP – PKG pathway. Sildenafil increased LV capacitance in HFpEF patients with pulmonary hypertension, as evidenced by lower pulmonary capillary wedge pressures at higher LV end-diastolic diameters (156). In addition, sildenafil acutely increased LV compliance in young, normotensive and old, hypertensive dogs (146). However, these promising results did not translate in an improved exercise capacity or clinical status in HFpEF patients treated with sildenafil in the RELAX trial (45). One of the reasons for this failure may be related to the inability of PDE5A inhibition to recruit enough cGMP in the myocardium, as a result of the low expression of PDE5A within the heart (244). In this regard, the combination of PDE5A inhibition with a direct stimulator of the sGC could represent a way to solve this therapeutic conundrum.

We previously established a risk factor-based porcine model of hypertensive heart disease – early-stage HFpEF with a loss of LV capacitance similar to that reported in patients with

HFpEF(182). In this model, decreased LV compliance was associated with a reduction in total titin phosphorylation and a shift toward the stiffer titin N2B-isoform (182).

In this study, we aimed to investigate the effects of the sGC-stimulator BAY 41-8543 on systemic hemodynamics and LV function in both healthy pigs and in our porcine model of early-stage HFpEF in vivo. We hypothesized that administration of BAY 41-8543, alone or in combination with PDE5A inhibition via sildenafil, would increase LV titin phosphorylation and thereby increase LV compliance measured by pressure-volume analysis.

In the final section of this chapter, we report data from a series of recently performed preliminary experiments in which we tested the hypothesis that acute intracoronary infusion of nitroglycerin (NTG) or atrial natriuretic peptide (ANP), at doses not affecting systemic vascular resistance, would exert direct myocardial effects and improve LV compliance in healthy myocardium.

5.2 Specific Methods

The experimental protocols were approved by the local bioethics committee of Vienna, Austria (BMWF-66.010/0127-II/3b/2011 and BMWF-66.010/0091-II/3b/2013), and conforms with the Guide for the Care and Use of Laboratory Animals published by the US National Institute of Health (NIH Publication No. 85-23, revised 1996).

5.2.1 Experimental models: healthy and DOCA-salt-treated hypertensive pigs

Sixteen healthy female Landrace pigs (60±3 kg) were sedated with an intramuscular injection of 0.5 mg kg-1 midazolam and 20 mg kg-1 ketamine, followed by 1 mg kg-1 propofol to allow for intubation with an endotracheal tube. Anaesthesia was maintained with 1 % sevoflurane, 35 μg kg-1 h-1 fentanyl, 1.25 mg kg-1 h-1 midazolam, and 0.2 mg kg-1 h-1 pancouronium. Pigs were then instrumented for invasive measurements, and the complete experimental setup is described in Chapter 2.1.1.

In an additional series, female Landrace pigs (n=15, 61±2 kg) were made hypertensive by implanting a subcutaneous DOCA depot into the inguinal region, combined to a high-salt and high-sugar diet (hereafter simply DOCA), as described in Chapter 2.1.6 and previously published (182). At 4, 8 and 12 weeks of treatment the animals were sedated, underwent non-invasive blood pressure measurement (tail-cuff) and transthoracic echocardiography (Vivid I, GE Healthcare, Vienna, Austria). Parasternal long- and short-axis 2D-views were recorded. At 12 weeks, pigs were anaesthetized and instrumented, and invasive measurement were performed. In comparison to previous studies from our group, these chronic hypertensive pigs were more sensitive to alterations of loading conditions, i.e. aortic occlusions, showing some hemodynamic instability and being prone to arrhythmias. We therefore added 3 mg/kg/h ketamine to the anaesthesia regimen, in order to achieve a deeper narcosis.

5.2.2 Experimental protocol - healthy pigs

5.2.2.1 Invasive hemodynamic group

In a first group of nine pigs, the hemodynamic effect of BAY 41-8543 was investigated by pressure volume analysis. All animals were allowed to stabilize for at least 30 minutes after instrumentation. Steady-state hemodynamics were acquired over three respiratory cycles at

spontaneous heart rate. Descending aorta occlusions at the respirator´s minimum tidal volume (50ml) were performed in triplicate to vary loading conditions and obtain pressure-volume relationships. Heart rate was then increased to multiples of 20 bpm by right atrial pacing up to the maximum rate followed by steady contractions. At each pacing step, steady-state and aortic occlusions (in triplicate) data were collected. All measurements were done at baseline conditions as well as during infusion of 1 and 3 µg kg-1 min-1 BAY 41-8543, respectively. Each dose was administered for 30 minutes before measurements were recorded.

5.2.2.2 Sequential biopsies group

In a second group of seven animals, a lateral thoracotomy was performed and the LV was exposed in a pericardial cradle. After stabilisation for 30 min, a pouch suture was prepared on the LV lateral wall, 2-3 transmural LV biopsies were taken from the beating heart and the pouch suture was immediately closed. Next, 3 µg kg-1 min-1 BAY 41-8543 were infused for 30 minutes, and further biopsies were taken as described above. All biopsies were carefully rinsed, immediately frozen into liquid nitrogen and stored at -80 °C.

5.2.3 Experimental protocol - DOCA animals

In a group of 7 pigs (64±3 kg), following baseline measurements, the sGC stimulator BAY 41-8543 was infused intravenously at 1 and 3 µg/kg/min over 20 min, respectively and data collection repeated at each infusion step. In the remaining 8 pigs (58±2 kg), following baseline measurements, the PDE5A inhibitor sildenafil was given as a 0.25mg/kg intravenous slow bolus with data collection 20 minutes later. In a subgroup of n=4, sildenafil was followed by on top infusion of the sGC stimulator BAY 41-8543 (1 and 3 µg/kg/min over 20 min, intravenously).

5.2.4 Phosphorylation of cardiac titin

Total phosphorylation of the two major titin isoforms (N2B and N2BA) in the LV samples obtained from healthy pigs before and during BAY 41-8543 was measured. Phosphosite-specific polyclonal antibodies directed towards relevant residues in the N2Bus (S4010, S4062, S4099) and PEVK-regions (S12022, S11878) were used to quantify titin-domain phosphorylation by western blot analyses. Further details are described in Chapter 2.2.2.

5.2.5 Intracoronary infusion of NTG and ANP-preliminary experiments

Five anaesthetized, closed-chest pigs (59±2kg) were acutely instrumented with a left ventricular (LV) pressure-volume catheter, a Swan-Ganz catheter and an aortic ballon catheter. Two 5F coronary catheters were positioned in the right and left coronary ostia via femoral access. Pressure-volume relationships were derived from short aortic occlusions. Following baseline measurements, NTG was infused bicoronarily at 10, 30 and 100 ng/kg/min over 20 min, respectively. After 30 min wash-out, the same protocol was repeated with ANP at 1, 3 and 10 ng/kg/min.

5.3 Results

5.3.1 Healthy pigs

5.3.1.1 Systemic hemodynamics

Heart rate and cardiac output increased, while mean aortic pressure and systemic vascular resistance decreased during infusion of BAY 41-8543 (Table 1). Mean pulmonary arterial pressure and pulmonary vascular resistance remained unchanged during the infusion of BAY 41-8543.

Table 5.1: Systemic hemodynamics and LV function at spontaneous heart rate during baseline and continuous infusion of 1 and 3 µg kg^{-1} min^{-1} BAY-8543, respectively. *: $p<0.05$ vs baseline, †: $p<0.05$ vs 1 µg/kg/min. LV: left ventricular, Ees: end-systolic elastance, V0: Volume axis intercept, VPes100: end-systolic volume at end-systolic pressure of 100 mmHg, VPed10: end-diastolic volume at end-diastolic pressure of 10 mmHg.

	baseline	**1 µg kg^{-1} min^{-1} BAY 41-8543**	**3 µg kg^{-1} min^{-1} BAY 41-8543**
heart rate (bpm)	85 ± 3	96 ± 3	103 ± 5*
cardiac output ($l\ min^{-1}$)	5.7 ± 0.2	6.6 ± 0.3*	7.1 ± 0.2*
mean aortic pressure (mmHg)	88 ± 2	75 ± 2*	62 ± 2*,†
systemic vascular resistance ($mmHg\ l^{-1}\ min^{-1}$)	14.9 ± 0.8	10.8 ± 0.6*	7.9 ± 0.3*,†
mean pulmonary pressure (mmHg)	19 ± 1	18 ± 1	18 ± 1
pulmonary vascular resistance ($mmHg\ l^{-1}\ min^{-1}$)	1.9 ± 0.2	1.8 ± 0.3	1.5 ± 0.2
LV maximum pressure (mmHg)	103 ± 2	90 ± 3*	83 ± 2*,†
LV maximum dP/dt ($mmHg\ s^{-1}$)	1820 ± 64	1821 ± 78	1747 ± 79
cardiac power output (W)	1.11 ± 0.04	1.09 ± 0.05	0.99 ± 0.04*
Ees ($mmHg\ ml^{-1}$)	1.7 ± 0.1	1.4 ± 0.1	1.6 ± 0.1
V_0 (ml)	-2.0 ± 6.4	-17.1 ± 11.7	-3.4 ± 8.6
LV VPes100 (ml)	61 ± 6	63 ± 5	67 ± 3

LV end-systolic volume (ml)	60 ± 6	56 ± 6	52 ± 3
LV ejection fraction (%)	54 ± 2	56 ± 2	58 ± 2
LV end-diastolic pressure (mmHg)	8 ± 1	7 ± 1	8 ± 1
LV end-diastolic volume (ml)	127 ± 8	125 ± 9	123 ± 4
τ (ms)	41 ± 2	40 ± 1	40 ± 1
LV minimum dP/dt (mmHg s^{-1})	-1796 ± 52	-1489 ± 50*	-1134 ± 37*,†
LV VPed10 (ml)	132 ± 8	140 ± 8	133 ± 3

5.3.1.2 LV dimensions and LV systolic function

LV end-diastolic volume, LV end-systolic volume, LV ejection fraction and LV maximum dP/dt did not change significantly during infusion of BAY 41-8543 (Table 5.1), while LV maximum pressure was lower compared to baseline. Cardiac power output (CPO) slightly decreased during infusion of BAY 41-8543 (Table 5.1). Although the ESPVR was shifted slightly rightward in individual animals (Fig. 5.1), the average ESPVR during infusion of BAY 41-8543 superimposed the ESPVR obtained during baseline conditions at spontaneous heart rate (Fig. 2). Neither Ees nor V0 changed significantly, resulting in an unchanged LV VPes100 (Table 5.1).

Figure 5.1: Original registrations of left ventricular pressure-volume data obtained in one animal during inflation of the aortic balloon catheter at baseline conditions (a) and infusion of 1 and 3 µg kg-1 min-1 (b, c). All registrations were recorded at spontaneous heart rate. ESPVR: end-systolic pressure-volume relationship. EDPVR: end-diastolic pressure-volume relationship.

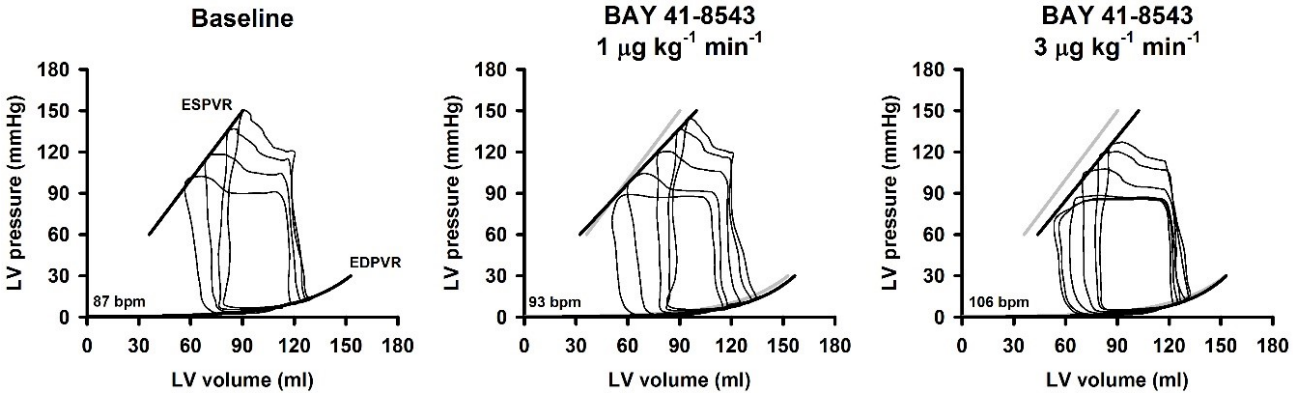

5.3.1.3 LV diastolic function

LV end-diastolic pressure remained unchanged. The absolute value of LV minimum dP/dt decreased with increasing doses of BAY 41-8543, while the time constant of isovolumic relaxation, τ, remained unchanged (Table 5.1). At spontaneous heart rate, the EDPVR during infusion of BAY 41-8543 superimposed the EDPVR obtained at baseline conditions (Fig. 5.1 and 5.2), so that LV VPed10 was not different (Table 5.1).

Figure 5.2: Pressure-volume relationships in n=9 healthy pigs. The end-systolic pressure-volume relationship (ESPVR) as well as the end-diastolic pressure-volume relationship (EDPVR) remained unchanged during infusion of 1 and 3 μg kg^{-1} min^{-1} BAY 41-8543 compared to baseline, respectively.

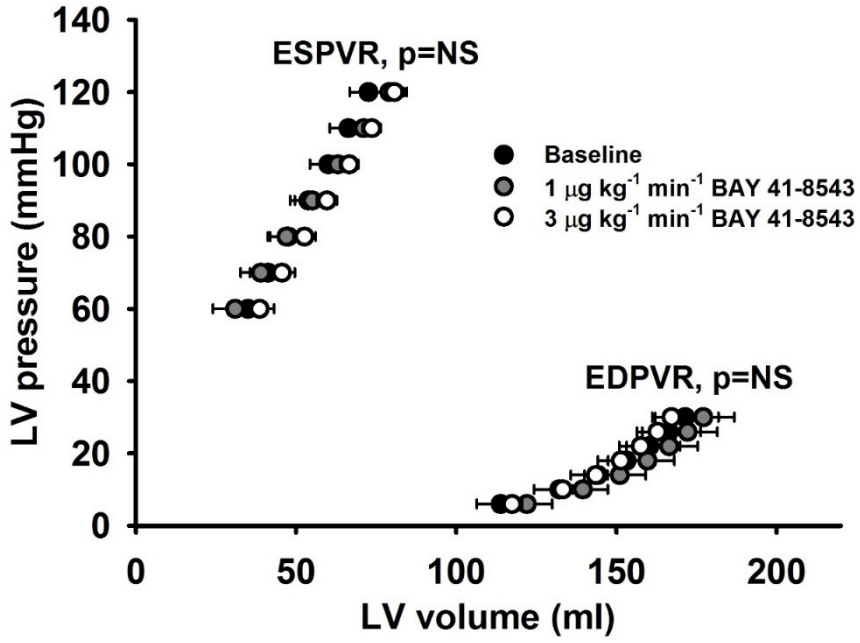

5.3.1.4 Effects of right atrial pacing

The response to right atrial pacing during infusion of BAY 41-8543 is shown in Fig.5.3. Cardiac output increased during pacing. LV maximum pressure was lower at any heart rate during infusion of BAY 41-8543 compared to baseline. There were no differences compared to baseline with respect to LV end-diastolic pressure, volume and LV VPed10. LV VPes100 decreased with increasing heart rate during baseline measurements but not during infusion of BAY 41-8543.

Figure 5.3: Hemodynamic parameters in n=9 healthy pigs. Cardiac output was higher during infusion of BAY 41-8543 compared to baseline (a), while LV maximum pressure was lower at any heart rate (b). There were no differences compared to baseline with respect to LV end-diastolic pressure, volume and LV VPed10 (c-e). LV VPes100 decreased with increasing heart rate during baseline measurements but not during infusion of BAY 41-8543, revealing a slight negative inotropic effect of sGC-stimulation (f). *: $p<0.05$ vs. spontaneous heart rate; †: vs. baseline

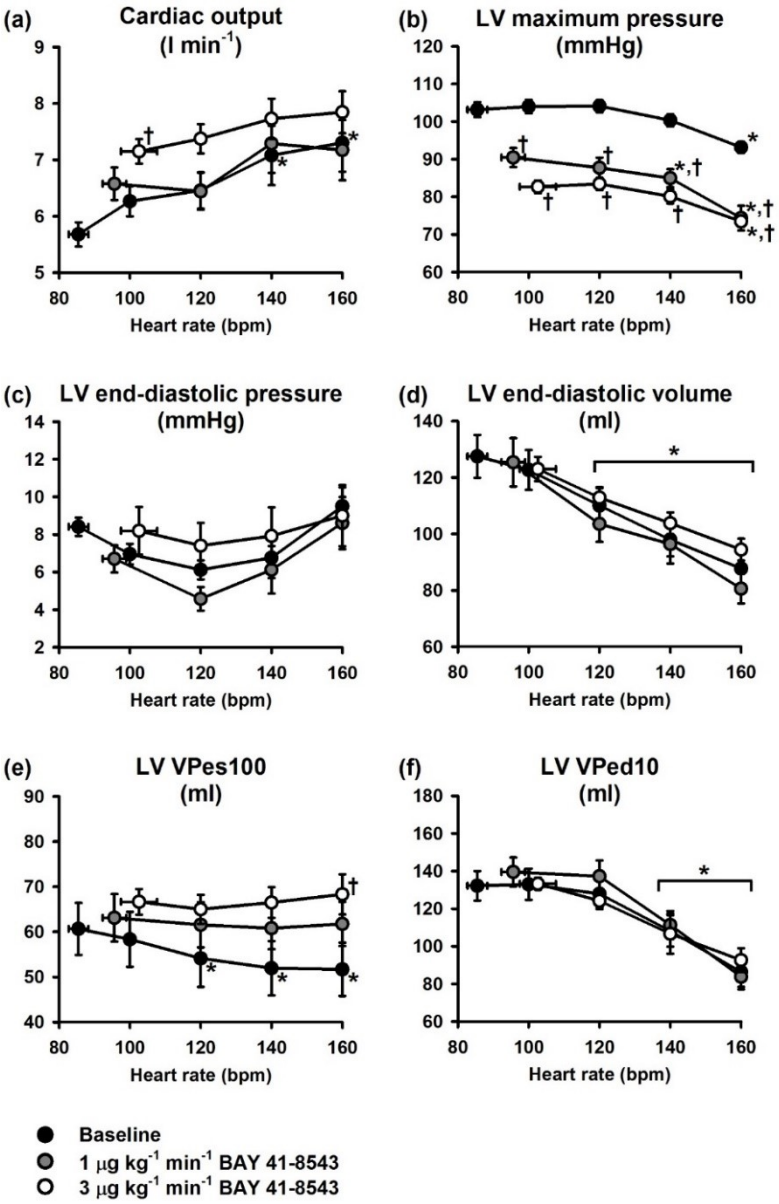

5.3.1.5 Myocardial tissue samples

Both total phosphorylation of the two major titin isoforms (N2B and N2BA, Fig. 5.4A) and phosphorylation of relevant residues in the N2Bus (S4010, S4062, S4099) and PEVK-regions (S12022) regions were not significantly affected by infusion of BAY 41-8543 (Fig. 5.4C-F). Only the N2B-phosphorylation at the PEVK-residue S11878 was slightly increased (Fig. 5.4B).

Figure 5.4: Western blot analyses (each n=7) showed that total phosphorylation of the two major titin isoforms (A) remained unchanged during infusion of BAY 41-8543. Only phosphorylation of the N2B-isoform at the PEVK S11878 residue was increased, while all other relevant residues within the N2Bus and PEVK-titin regions were not affected by BAY 41-8543 (B-F). *: $p<0.05$ vs. baseline

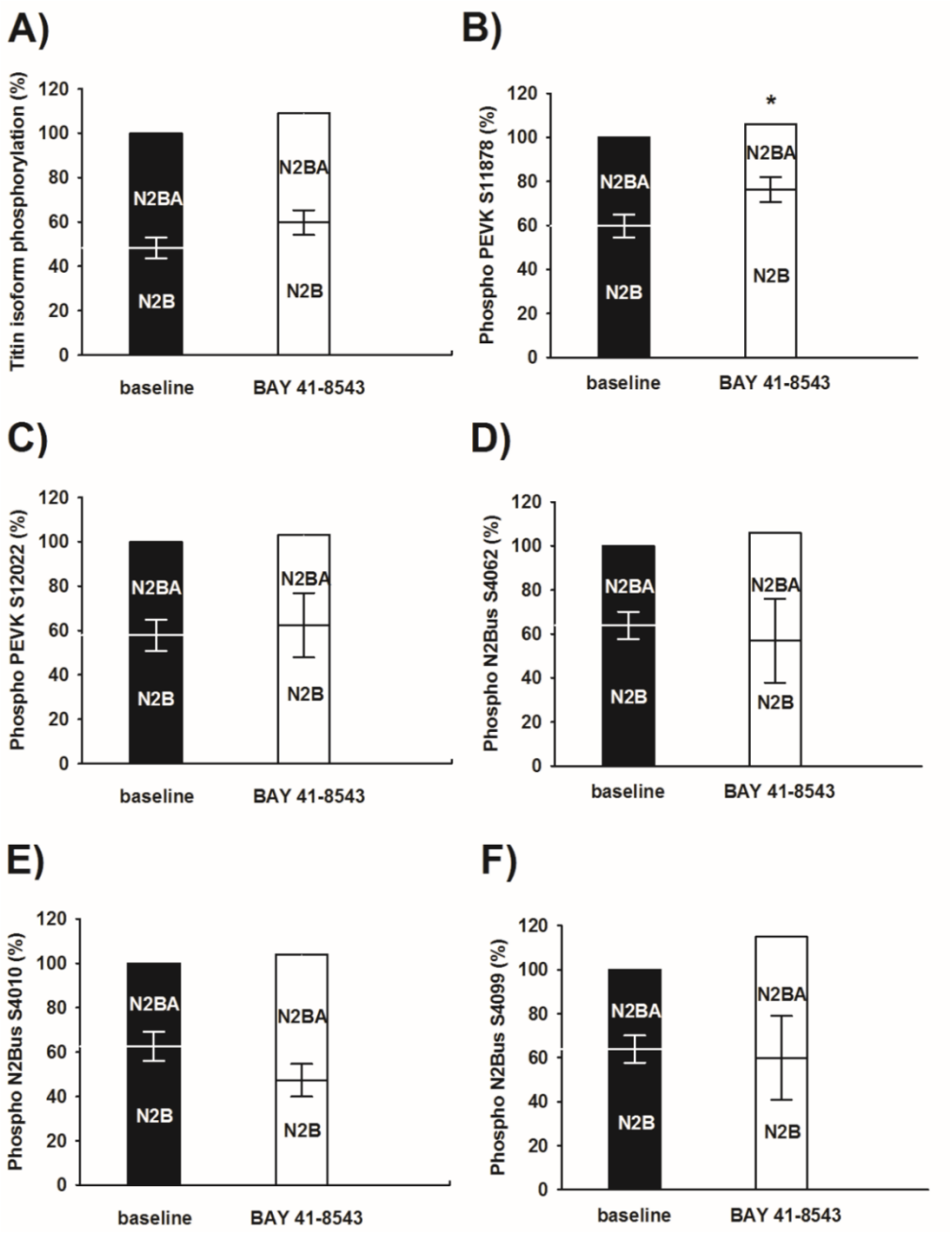

5.3.2 DOCA pigs

5.3.2.1 Echocardiography

Starting at 8 weeks of DOCA treatment, the animals developed LV concentric hypertrophy compared to historic controls. At the end of the protocol, they had higher LV wall thickness (Figure 5.5A-B) at similar LV end-diastolic diameters (Figure 5.5C), meaning a higher relative wall thickness (Figure 5.5D), in line with what previously reported by our group (182).

Figure 5.5: Echocardiographic follow-up of LV remodelling in the hypertensive animals (n=15) vs. controls (n=41). We first plotted septal wall thickness (A), posterior wall thickness (B), end-diastolic diameter (C) and relative wall thickness (RWT) as a function of body weight in an historic control group, and fit the regression through the data point. At 8 weeks and further at 12 weeks, the average values of all these parameters in the hypertensive animals fell out of the prediction band, indicating LV concentric hypertrophy.

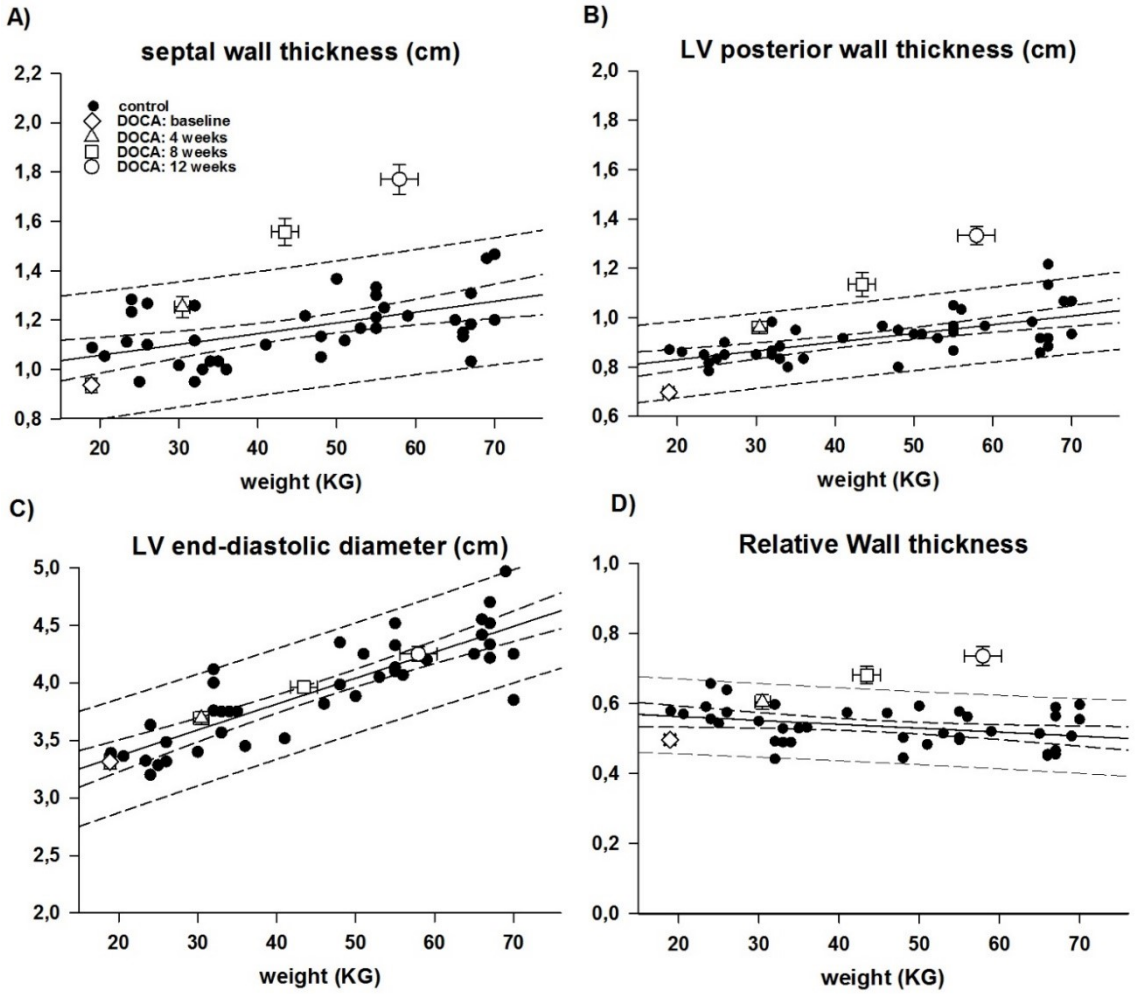

5.3.2.2 Systemic hemodynamics

In the first group of animals (Table 5.2A), during infusion of BAY 41-8543 heart rate and cardiac output did not change, while mean aortic pressure decreased subsequent to decreased systemic vascular resistance. BAY 41-8543 did not impact on pulmonary arterial pressure. In the second group (Table 5.2B), after sildenafil bolus heart rate and cardiac output did not change, while mean aortic pressure and systemic vascular resistance decreased. Pulmonary arterial pressure significantly decreased, as a result of a drop in pulmonary vascular resistance (271±23 vs 206±16 dyn s cm^{-5}). On top of sildenafil BAY 41-8543 infusion (Table 5.2C) further dropped mean aortic pressure and systemic vascular resistance.

Table 5.2A: Invasive hemodynamics at baseline and during BAY 41-8543 infusion. *: $p<0.05$ vs baseline, †: $p<0.05$ vs 1µg/kg/min BAY 41-8543.

	(n=7)	**BAY 41-8543**	
	baseline	**1µg/kg/min**	**3µg/kg/min**
heart rate (bpm)	89 ± 4	88 ± 4	89 ± 6
cardiac output (l/min)	6.3 ± 0.3	6.4 ± 0.4	6.6 ± 0.4
mean arterial pressure (mmHg)	73 ± 3	65 ± 2*	57 ± 2*,†
systemic vascular resistance (dyn s cm^{-5})	886 ± 49	768 ± 43	625 ± 34*,†
pulmonary arterial pressure (mmHg)	19 ± 1	18 ± 1	18 ± 1

Table 5.2B: Invasive hemodynamics at baseline and during sildenafil infusion. *: $p<0.05$ vs baseline

	(n=8)	
	baseline	**sildenafil**
heart rate (bpm)	85 ± 2	91 ± 4
Cardiac output (l/min)	5.3 ± 0.1	5.7 ± 0.2
mean arterial pressure (mmHg)	90 ± 5	71± 4*
systemic vascular resistance (dyn s cm^{-5})	1321 ± 93	949 ± 50*
pulmonary arterial pressure (mmHg)	18 ± 2	15 ± 1*

Table 5.2C: Invasive hemodynamics at baseline, during sildenafil infusion and during on-top-of-sildenafil BAY 41-8543 infusion in a subgroup of animals. *: $p<0.05$ vs baseline

	(n=4)		**BAY 41-8543**	
	baseline	**sildenafil**	**1µg/kg/min**	**3µg/kg/min**
heart rate (bpm)	84 ± 5	83 ± 5	90 ± 4	95±3
Cardiac output (l/min)	5.4 ± 0.1	5.5 ± 0.3	5.7 ± 0.2	5.9±0.1
mean arterial pressure (mmHg)	84 ± 5	63± 5	59 ± 4*	59±4*
systemic vascular resistance (dyn s cm^{-5})	1187 ± 90	857 ± 62	774 ± 54*	741±47*
pulmonary arterial pressure (mmHg)	20 ± 3	16 ± 2*	17 ± 3	17±2

5.3.2.3 LV systolic function

The infusion of BAY 41-8543 decreased LV maximum pressure and the rate of contraction (i. e., LV maximum dP/dt), while the LV ejection fraction did not change (Table 5.3A). In line with that, the end-systolic pressure volume relationships (ESPVR) before and during infusion of BAY 41-8543 were superimposable (Figure 5.6A).

Sildenafil bolus (Table 5.3B) had a comparable effect on LV maximum pressure, rate of contraction and ejection fraction. However, the ESPVR was rightward shifted by sildenafil compared to baseline (Figure 5.6), indicating a negative inotropic effect. On top of sildenafil BAY 41-8543 infusion (Table 5.3C) further dropped LV maximum pressure, but did not impact the indexes of LV systolic function (Figure 5.6C).

Table 5.3A: Parameters of LV systolic and diastolic function at baseline and during BAY 41-8543 infusion

	(n=7)	**BAY 41-8543**	
	baseline	**1µg/kg/min**	**3µg/kg/min**
LV maximum pressure (mmHg)	93 ± 1	87 ± 2	82 ± 1*
LVPed (mmHg)	11 ± 2	10 ± 2	12 ± 1
LV maximum dP/dt (mmHg s^{-1})	1617 ± 71	1335 ± 70*	1218 ± 88*,†
LV minimum dP/dt (mmHg s^{-1})	-1304 ± 66	-1143 ± 85*	-967 ± 63*,†
LV-EF (%)	67 ± 2	65 ± 3	66 ± 3
tau (ms)	42 ± 2	42 ± 2	41 ± 1
LVVed (ml)	107 ± 4	114 ± 8	113 ± 4

Table 5.3B: Parameters of LV systolic and diastolic function at baseline, during sildenafil infusion and during on top BAY 41-8543 infusion

	(n=8)	
	baseline	**sildenafil**
LV maximum pressure (mmHg)	107 ± 5	88 ± 3*
LVPed (mmHg)	13 ± 1	9 ± 1*
LV maximum dP/dt ($mmHg\ s^{-1}$)	1444 ± 140	1279 ± 159*
LV minimum dP/dt ($mmHg\ s^{-1}$)	-1837 ± 114	-1424 ± 81*
LV-EF (%)	59 ± 1	61 ± 2
tau (ms)	40 ± 1	40 ± 1
LVVed (ml)	108 ± 5	106 ± 7

Table 5.3C. Parameters of LV systolic and diastolic function at baseline, during sildenafil infusion and during on top BAY 41-8543 infusion in a subgroup of animals

	(n=4)		**BAY 41-8543 (n=4)**	
	baseline	**sildenafil**	**1µg/kg/min**	**3µg/kg/min**
LV maximum pressure (mmHg)	101 ± 5	82 ± 3	79 ± 1*	79±1*
LVPed (mmHg)	13 ± 1	10 ± 1*	10 ± 1*	10±1*
LV maximum dP/dt (mmHg s^{-1})	1140 ± 140	923 ± 159*	891 ± 1*	908±1*
LV minimum dP/dt (mmHg s^{-1})	-1639 ± 114	-1237 ± 81*	-1218 ± 1*	-1189±1*
LV-EF (%)	59 ± 1	62 ± 2	62 ± 1	61±1
tau (ms)	42± 1	41 ± 1	38 ± 1	38±1
LVVed (ml)	110 ± 5	111 ± 7	107 ± 1	101±1

5.3.2.4 LV diastolic function

BAY 41-8543 decreased the rate of relaxation (i. e., LV minimum dP/dt), while the isovolumic relaxation constant tau, end-diastolic pressure and end-diastolic volume did not change (Table 5.3A). In line with that, the EDPVR before and during infusion of BAY 41-8543 were superimposable (Figure 5.6A). Sildenafil bolus had similar impact on rate of relaxation and tau (Table 5.3B), but additionally dropped the end-diastolic pressure at a constant end-diastolic volume, as confirmed by a trendwise rightward shift of the EDPVR (Figure 5.6B). On top of sildenafil BAY 41-8543 infusion had no further effect on diastolic function (Table 5.3C and Figure 5.6C).

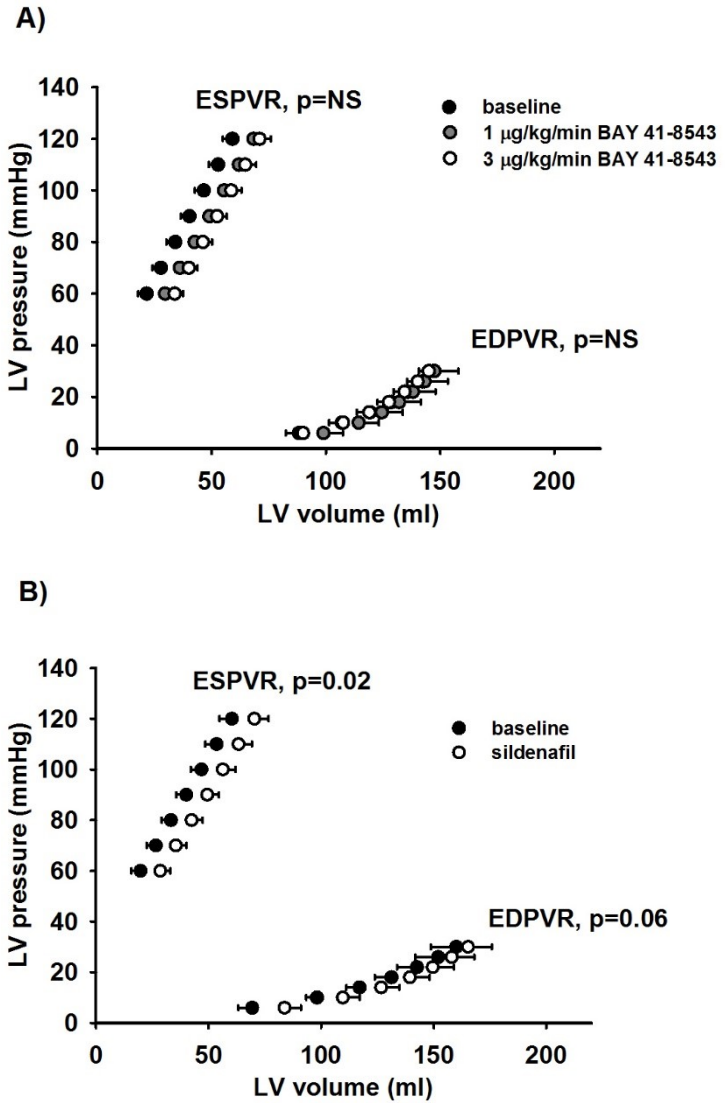

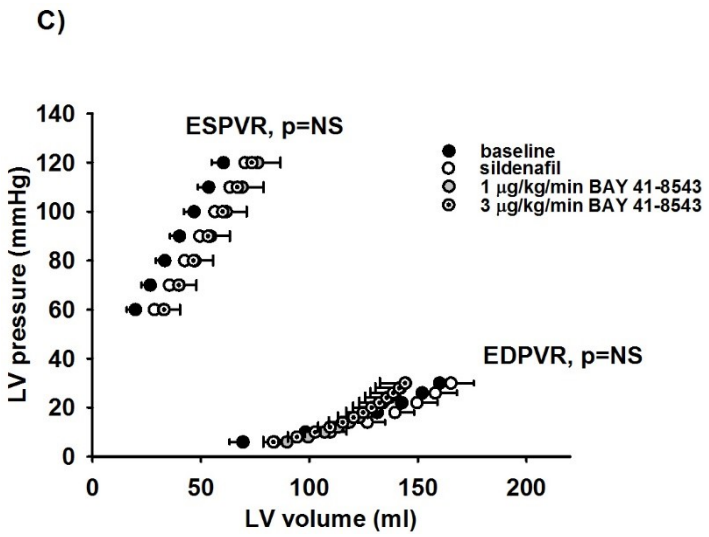

Figure 5.6: Pressure-volume relationships at baseline and (A) during during low/high dose BAY 41-8543 (n=7). Neither the ESPVR, nor the EDPVR were affected by the drug. In the second group of animals (B), during sildenafil infusion the ESPVR was shifted rightwards compared to baseline, indicating a negative inotropic effect. The EDPVR showed only a trend ($p<0.06$) towards an increase of compliance (n=8). On top of sildenafil infusion of BAY 41-8543 in a subgroup (n=4) exerted no additional effect on LV compliance or contractility (C).

5.3.2.5 Effects of right atrial pacing

Pacing at higher heart rates decreased the diastolic duration time (t-dia, Figure 5.7A – C), while the isovolumic relaxation constant tau (τ) decreased (Figure 5.7D-F), resulting in a decreased ratio between t-dia and τ (Figure 5.7G-I). There was no impact of any treatment on these parameters. Left ventricular end-diastolic volume at 10 mmHg pressure (LV-VPed10) was higher during sildenafil infusion throughout the pacing staircase, but not during BAY 41-8543 infusion (Figure 5.7L-M). On top of sildenafil BAY 41-8543 infusion exerted no additional effect (Figure 5.7N).

Both the highest dose of BAY 41-8543 (Figure 5.8A) and sildenafil bolus (Figure 5.8B) increased LV-Vpes100 at each pacing step, indicating a negative inotropic effect. On top of sildenafil BAY 41-8543 infusion exerted no additional effect (Figure 5.8C).

Figure 5.7: Parameters of diastolic function during right atrial pacing at increasing heart rates. First column: effect of BAY 41-8543 in the first group of animals (n=5), second column: effect of sildenafil in the second group of animals (n=8), third column: effect of on top of sildenafil BAY 41-8543 infusion in a subgroup of animals (n=4). The diastolic duration time (t-dia) decreased at higher heart rates (A – C). The isovolumic relaxation constant tau (τ) was not affected by any treatment (D-F), resulting in an unchanged ratio between t-dia and τ (G-I). Left ventricular end-diastolic volume at 10 mmHg pressure (LV-VPed10) was higher during sildenafil infusion throughout the pacing staircase, but not during BAY 41-8543 infusion (L-M). On top of sildenafil BAY 41-8543 infusion exerted no additional effect (N). *: $p<0.05$ vs spontaneous heart rate, †: $p<0.05$ vs baseline at corresponding heart rate, §: $p<0.05$ vs sildenafil at corresponding heart rate.

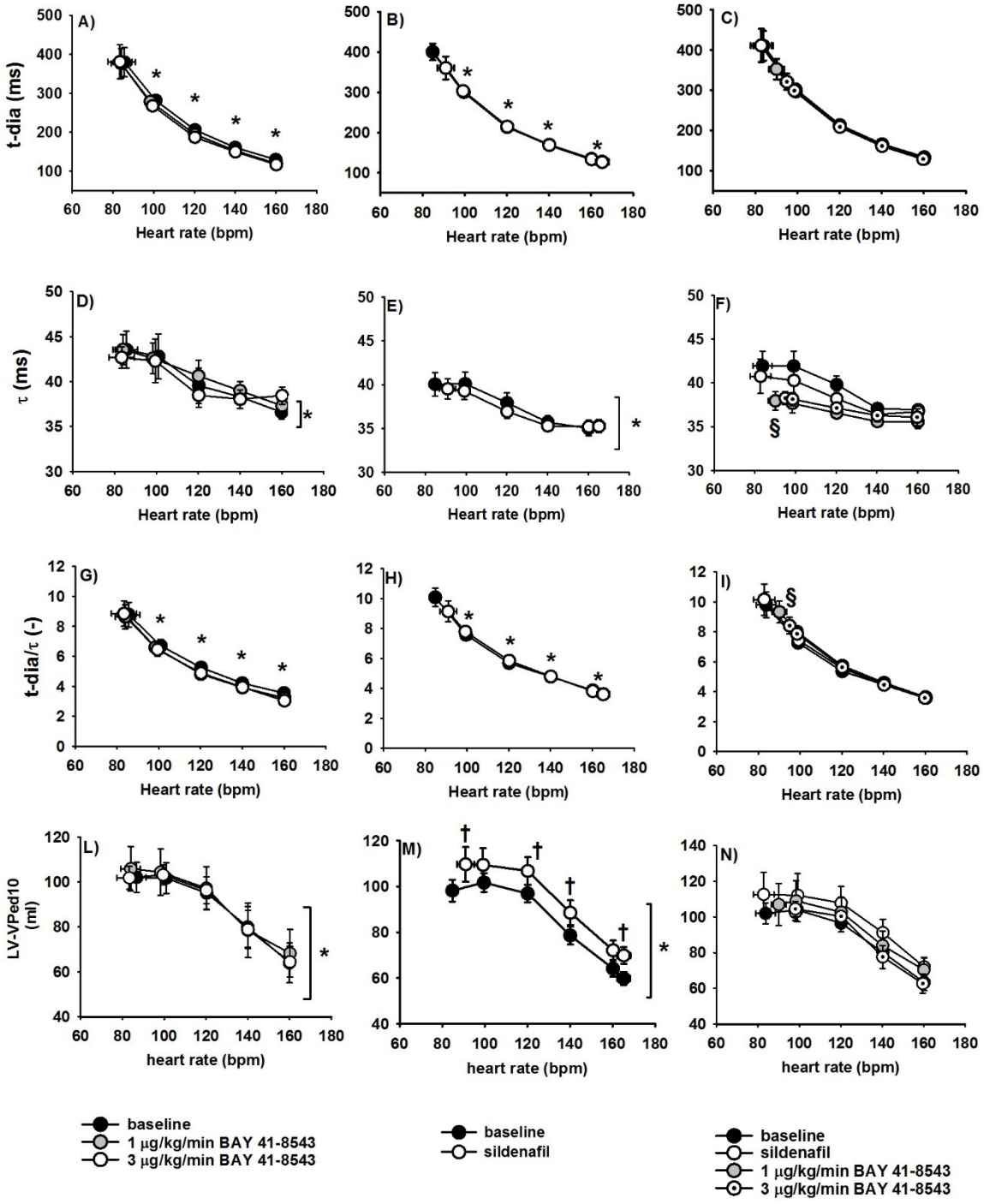

Figure 5.8: LV end-systolic volume at 100mmHg of pressure (LV-VPes100) during right atrial pacing at increasing heart rates. Both the highest dose of BAY 41-8543 (A) and of sildenafil (B) increased LV-Vpes100, indicating a negative inotropic effect. On top of sildenafil BAY 41-8543 infusion exerted no additional effect (C). . *: $p<0.05$ vs spontaneous heart rate, †: $p<0.05$ vs baseline at corresponding heart rate

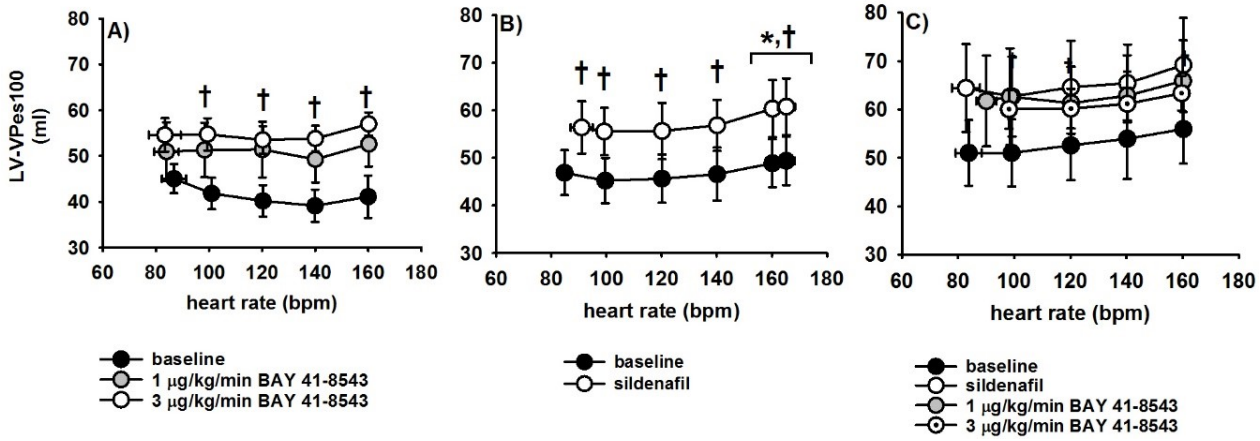

5.3.3 Effect of intracoronary infusion of NTG and ANP on myocardial function (preliminary data)

As mentioned in the introduction, drugs were titrated not to affect systemic vascular resistance. In fact, LV peak pressure slightly decreased at the highest dose compared to baseline (NTG: 87±3 vs 94±4, ANP: 85±4 vs 96±6 mmHg, $p<0.05$) while systemic vascular resistance was not altered during NTG infusion and to a minor extent during the highest dose of ANP (11.1±0.6 vs 12.7±0.7 mmHg/l/min, $p<0.05$). The maximum rate of positive LV pressure change, LV dP/dtmax, decreased and the calculated end-systolic volume at 100 mmHg end-systolic pressure increased dose-dependently, indicating a negative inotropic effect. The EDPVR (Figure 5.9) before and during infusion of NTG and ANP were shifted rightwards compared to the respective baseline.

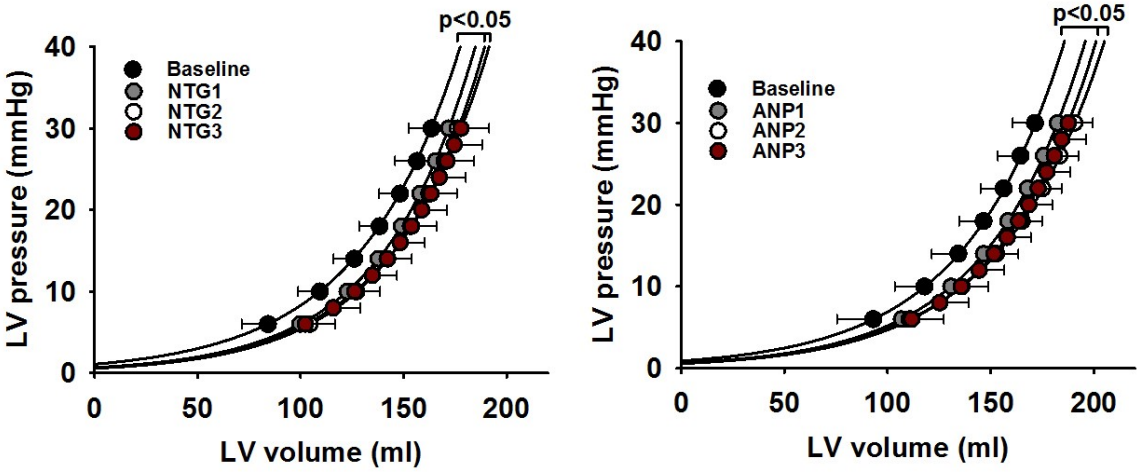

Figure 5.9: LV end-diastolic pressure-volume relationships during bicoronary infusion of NTG and ANP, at increasing doses. A progressive rightward shift of the EDPVR is shown when infusing both NTG and ANP.

5.4 Discussion

We studied the impact of the sGC-stimulator BAY 41-8543 on myocardial function in both healthy and hypertensive animals. We observed a pronounced loss of systemic vascular resistance, while diastolic function remained largely unaffected. In line with that, total titin phosphorylation remained unchanged and phosphorylation of relevant residues in the elastic I-band regions N2Bus and PEVK was not affected systematically by BAY 41-8543 infusion in healthy pigs. In a separate group of hypertensive animals, sildenafil trend-wise increased LV compliance, while on top of sildenafil BAY 41-8543 infusion did not exert any additional effect.

5.4.1 Effects of BAY 41-8543, sildenafil and their combination on systemic hemodynamics

BAY 41-8543 and sildenafil induced a pronounced vasodilation, further enhanced by the infusion of BAY 41-8543 on top of sildenafil in the DOCA pigs. Systemic vascular resistance dropped as a result of two different mechanisms of action: BAY 41-8543 increases the conversion of GTP in cGMP in smooth muscle cells by stimulating the activity of sGC molecules (245), while sildenafil raises cGMP concentration in the smooth muscle cell via inhibition of the enzyme responsible for its breakdown, PDE5A (138). Elevated cGMP-levels activate PKG, which in turn phosphorylates a number of proteins leading to reduced intracellular Ca^{2+}-concentration, lower Ca^{2+}-sensitivity and finally vascular relaxation (245). The effect of BAY 41-8543 or other sGC stimulators on systemic vascular resistance was previously reported in both rodents, mice (245) and rats (158, 246, 247), and large animals, pigs (248) and dogs (249). The sGC stimulator riociguat exerted the same effect on systemic vascular resistance in patients affected by pulmonary hypertension (164, 250).

BAY 41-8543 induced reflex tachycardia and progressively increased cardiac output only in the healthy group, but not in the DOCA group. In contrast to our results, in patients with HFpEF and pulmonary hypertension, oral riociguat increased cardiac index at the early time point of 6 hours (250). Similarly, in a phase IIb clinical study in patients with pulmonary hypertension caused by systolic LV dysfunction, the oral administration of the sGC stimulator riociguat increased cardiac index and stroke volume without any increase in heart rate at 16 weeks (164). The difference between our study and the studies available in literature may be explained by the deep regimen of anaesthesia induced in the animals, in order to obtain stable and reproducible conditions for our measurements.

The beneficial effect of sGC-stimulating compounds and PDE5A inhibitors has been shown in several experimental (160, 247, 251, 252) and clinical (92, 243, 253, 254) settings of pulmonary arterial hypertension. In our study, we observed no change in pulmonary vascular resistance during BAY 41-8543 infusion, in both healthy and hypertensive animals, but a clear drop after the sildenafil bolus. The lack of effect of BAY 41-8543 on pulmonary vascular resistance is line with what previously reported in a canine model of experimental heart failure with slightly elevated pulmonary pressure (249). Furthermore, in two small-scale clinical studies, both acute (250) and chronic (164) administration of oral riociguat did not decrease systolic pulmonary arterial pressure.

5.4.2 Effects of BAY 41-8543, sildenafil and their combination on LV systolic function

In the healthy pigs, we could not detect alterations of the ESPVR during infusion of BAY 41-8543 at spontaneous heart rate. If any, the numerically higher values of LV VPes100 at spontaneous heart rate would indicate a minor rightward shift of the ESPVR and thus a negative inotropic effect. In line with that, CPO decreased by approximately 10% during infusion of the higher dose of BAY 41-8543. In addition, LV maximum dP/dt did not increase in spite of reflex tachycardia, i. e. endogenous sympathetic activation. Finally, the response of LV VPes100 to increasing heart rate was blunted during infusion of BAY 41-8543. Taken together, these findings point towards a slight negative inotropic effect during profound sGC-stimulation in healthy pigs.

To our knowledge, there are no data in literature on the effect of acute infusion of sGC stimulators or PDE5A inhibitors as assessed by pressure volume analysis in heart failure patients. On the same line of what observed in the healthy group at higher rates, both the highest dose of BAY 41-8543 and sildenafil infusion increased systolic capacitance, as evidenced by a rightwardshift of the ESPVR and an increase of LV VPes100. These changes are consistent with a negative inotropic effect, as also suggested by the decrease of a load-dependent index such as the LV maximum dP/dt in both treatment groups.

It is now widely accepted that the ESPVR is non-linear and not completely load-independent (174). The rightwardshift of the ESPVR observed during BAY41-8543 and sildenafil infusion might therefore be a consequence, at least in part, of the decreased afterload. Despite we cannot exclude a contribution of the decreased afterload, there are several evidences in literature leading us to believe that our findings reflect a direct effect on passive tension properties of the cardiomyocytes.

First of all, experimental data in-vitro indicate that NO donors exert a negative inotropic effect in cardiac myocytes (255) and that this is mediated by downstream PKG (147). The mechanism behind this effect is not clearly elucidated, but would be mediated by reduced myofilamental Ca^{2+}-sensitivity via Troponin I-phosphorylation (148) and by reduced Ca^{2+}-transients via L-type Ca^{2+}-channel phosphorylation (149). Secondly, in line with our study, infusion of sildenafil, alone and in combination with BNP, increased systolic compliance in young, normotensive and old, hypertensive dogs (146). In a similar study, infusion of ANP in dogs reduced LV contractility before and after induction of heart failure (175). Finally, a recently published prospective ancillary study of the RELAX trial, showed a reduction of LV contractility in HFpEF patients after 24 weeks treatment with sildenafil (256). This reduction was of modest entity, but it correlated with changes in exercise capacity, suggesting that the lack of clinical improvement in this cohort of patients may be mechanistically linked to the negative inotropic effect of sildenafil.

5.4.3 Effects of BAY 41-8543, sildenafil and their combination on LV diastolic function

In contrast to our initial hypothesis, BAY 41-8543, alone or in combination with sildenafil had no impact on the LV EDPVR, as indicated also by no change in end-diastolic pressure and end-diastolic volume, and by the lack of any effect on the LV VPed10 along the pacing staircase. Sildenafil alone, had a trend-wise effect on the EDPVR, decreasing LV end-diastolic pressure at a constant end-diastolic volume, and clearly increased LV VPed10 along the pacing staircase. Other groups have previously demonstrated the impact of cGMP-enhancing therapies – other than sGC stimulators- on LV end-diastolic capacitance. In mice, administration of the PDE5A inhibitor sildenafil attenuated the loss of LV end-diastolic capacitance in the early stage after transaortic banding (155). The EDPVR of young, normotensive and old, hypertensive dogs was acutely shifted to the right by infusion of sildenafil together with BNP (146). Furthermore, in patients presenting with chest pain but no evidence of coronary disease, the intracoronary infusion of the NO-donor sodium nitroprusside resulted in an acute increase of LV end-diastolic capacitance (151). In a similar way, substance P increased LV end-diastolic distensibility in healthy subjects and transplant recipients undergoing coronary angiography (257). Finally, the administration of sildenafil in HFpEF patients with pulmonary hypertension resulted in higher LV capacitance (156). As a further proof of the importance of this pathway on LV compliance, a previous study in patients with dilated cardiomyopathy showed that the higher compliance induced by the

infusion of the Angiotensin Converting Enzyme inhibitor enalapril, was prevented by the infusion of nitric oxide synthase inhibitor L N(G)-monomethyl-L-arginine (L-NMMA) (258). Our findings on the effect of sildenafil are therefore in line with the literature, while the lack of effect of BAY 41-8543 is somehow unexpected. There are several reasons that may explain this negative finding.

First of all, the dose of 3 µg/kg/min may have been too low to enhance cGMP within the cardiomyocyte. The pronounced vascular unloading obtained at this dose may be a limitation in the attempt to obtain a direct myocardial effect. A higher dose would have not been possible, rendering the animals hemodynamically unstable. An intracoronary infusion of the drug could therefore appear more desirable. However, the relatively long half-life of BAY 41-8543 (approximately 1h) would lead to a systemic accumulation of the drug (259).

Finally, there is raising evidence in literature that the intracellular cGMP is tightly compartmentalized within the cardiomyocyte (157). Indeed, cGMP derived from PDE5-inhibition and from sGC stimulation are not detectable at the sarcolemmal membrane, and therefore have a different compartmentalization than pGC-derived cGMP (260). The mechanisms underlying the regulation of cGMP concentration, PKG activity and its myofilament target proteins are still not fully understood.

5.4.4 Effects of sGC stimulation on cardiac titin

In line with the neutral effects on diastolic function in-vivo, total titin phosphorylation was not affected by BAY 41-8543 infusion in the present study. As mentioned in Chapter 1.5.3, titin is a molecular spring regulating passive tension of cardiomyocyte, and contributing to LV coil and recoil. Titin´s elastic proprieties are not only regulated by the proportion of stiff and smooth isoform, N2B and N2BA, within the myofilament (114), but can be also posttranslational modulated by several processes such as phosphorylation (112) of residues in the regions N2Bus and PEVK. PKG and PKA were shown to be involved in these processes, reducing passive stiffness of skinned and isolated myofibrils‘in human failing and non failing left ventricles (115) via phosphorylation of residues within the N2Bus domain region (112). In the present study, we considered the most frequently reported in literature residues, Ser4010, Ser4062 and Ser4099 in the N2Bus region (115, 261) and Ser11878 and Ser12022 in the PEVK region (118, 183) as possible targets of acute sGC stimulation. These in vitro findings were supported by in vivo studies in young, normotensive and old, hypertensive dogs (146), in which the acute infusion of sildenafil and sildenafil + BNP increased LV compliance in a graded manner, along with increased total phosphorylation of

titin. However, the graded increase of LV compliance in vivo during sildenafil and on top BNP infusion was not paralleled by a further increase of total titin phosphorylation, suggesting that also mechanisms other than titin phosphorylation may be involved. In this regard, both the in-vivo and in-vitro findings of our study show that the stimulation of sGC via BAY-418543 infusion is not able to recruit such an effect in healthy pigs. An explanation for the discrepancy between the present data and those on sildenafil and BNP may be due to the recruitment of different subcellular microdomains of cGMP by PDE5-inhibition, pGC or sGC stimulation in the cardiomyocyte (157). Indeed, cGMP derived from PDE5-inhibition and from sGC stimulation are not detectable at the sarcolemma membrane, and therefore have a different compartmentalization than pGC-derived cGMP (260). This can result in intracellular gradients of PKG stimulation and may therefore induce a different modulation of myofilament proteins.

5.5 Limitations

A sGC stimulator triggers only the activity of the non-oxidized version of sGC (Fe^{2+}). Assuming that a large proportion of sGC was oxidized, a sGC-activator could have been more effective compared to a sGC-stimulator. However, both the negative inotropic effect and the potent vasodilation observed in our study indicate the presence of non-oxidized sGC in cardiomyocytes and smooth muscle cells.

Moreover, acute sGC stimulation might not be effective to increase LV end-diastolic capacitance, while protective effects might only emerge in a delayed manner by, for instance, an effect on titin isoform composition. Thus, the long-term effects of BAY 41-8543 administration on LV diastolic function remain to be investigated.

Finally, we reported data on titin phosphorylation during BAY 41-8543 infusion only in healthy pigs. A series of sequential biopsies during BAY 41-8543 infusion in our early-stage HFpEF model is undergoing, and will further support the in vivo results.

5.6 Preliminary experiments on myocardial effect of NTG and ANP

After the unexpected negative results of sGC stimulation in both healthy and DOCA animals, we have decided to approach the experimental hypothesis starting from the effect of the two major upstream of the cGMP-PKG-titin pathway. We therefore administered a NO-donor (NTG) and a natriuretic peptide (ANP), in order to assess the differential effect of cGMP stimulation via sGC and pGC. We infused these compounds directly in the coronaries in the attempt to reach the myocardial concentration needed to recruit an effect, reducing at the minimum the effect on systemic vasculature. In Chapter 1, we already discussed the conceptual implications of the paradigm shift from the vasculature as a target to the heart itself, especially considering the sensitivity of HFpEF patients to load changes. These preliminary data show that the acute pharmacological stimulation of cGMP-dependent signalling, via both pGC and sGC, improves LV end-diastolic distensibility in healthy pigs in vivo. The molecular mechanisms mediating such acute modulation of LV distensibility are under investigation via a phosphoproteomic approach in sequential biopsies and may represent pharmacological targets to increase the preload reserve in HFpEF patients.

5.7 Conclusion

Acute stimulation of sGC by BAY 41-8543 induced no effect on LV compliance in both healthy and hypertensive pigs. In parallel to these findings, sGC stimulation did not have an impact on total titin phosphorylation status and specific phosphorylation sites. On the contrary, PDE5A inhibition by sildenafil trendwise increased LV compliance in hypertensive pigs. However, on top of sildenafil administration of BAY 41-8543 did not exert any additional effect on LV compliance. These data argue against the concept that acute potentiation of cGMP-dependent signaling can recruit a preload reserve, neither in healthy nor in hypertrophied LV myocardium. Effects of long-term sGC-stimulation with oral compounds in disease conditions associated with lowered myocardial cGMP levels, i. e., heart failure with preserved ejection fraction, remain to be investigated.

Chapter 6:

Summary and Conclusion

Heart failure with preserved ejection fraction is a syndrome characterized by high prevalence, a complex and poorly understood pathophysiology and a lack of treatment influencing its natural history. Diastolic dysfunction is a major mechanism of disease, deriving from the contribution of multiple elements, related to both active mechanisms of relaxation, reduced mid-diastolic suction and passive myocardial elastic proprieties.

In Chapter 3 of the current work, we have studied the mechanisms behind temperature-dependent modulation of LV systolic function, relaxation and compliance in healthy closed-chest pigs by pressure-volume analysis. We have previously shown that mild hypothermia (33 °C) induces acute LV diastolic dysfunction by impaired active relaxation, while substantially increasing LV contractility. In this study, we investigated the effect of hyperthermia (40.5°C) and mild hypothermia, and compared it with a standard inotropic drug used in the intensive-care unit, i.e. dobutamine. We show that LV contractility increased with cooling, while the end-diastolic pressure-volume relationship (EDPVR) was progressively shifted leftwards from HT to NT and from NT to MH, indicating a loss of LV compliance at lower temperatures. The effect of cooling on contractility is comparable to a clinically relevant dose of dobutamine, while fostering LV relaxation with dobutamine at 33°C reverses the loss of LV capacitance, making relaxation complete. These findings address the role of MH in a condition of impaired contractile function, i.e. cardiogenic shock, and underline the possible synergistic role of β-adrenergic stimulation and cooling.

As mentioned above, an increased LV stiffness at rest is characteristic of the disease. However, most patients become symptomatic preferably during exercise, and a limited myocardial perfusion and contractility reserve may play a role. In Chapter 4, we therefore describe an CMR imaging study to investigate LV function and perfusion during dobutamine stress in a previously established porcine model of early-stage HFpEF, induced by DOCA implantation, high-salt and high-sugar diet. Aside numerous functional alterations at rest, such as altered myocardial muscle mechanics, in particular longitudinal shortening and torsion, and left ventricular filling characteristics, an impaired increase of cardiac index during dobutamine stress was paralleled by a reduced myocardial perfusion reserve. Exercise induced myocardial ischemia may therefore be a contributor to LV dysfunction in HFpEF.

With regard to the pathogenesis, HFpEF evolves from the accumulation of a multitude of cardiovascular comorbidities over time, leading to increased systemic inflammation, oxidative stress and coronary microvascular endothelial inflammation. Nitric oxide (NO) bioavailability is reduced because of microvascular inflammation, and NO-cyclic GMP-

protein kinase G pathway was shown to be impaired in HFpEF patients, with an important impact on the elastic proprieties and function of the major myofilament protein titin. Enhancement of PKG activity has therefore emerged in the past years as a possible therapeutic approach. In Chapter 5, we have tested a compound, which enhances PKG activity via acute pharmacological stimulation of the soluble guanylate cyclase (sGC), BAY 41-8543. In healthy pigs, BAY 41-8543 did not exert any beneficial effect on LV compliance, as confirmed by the unchanged phosphorylation state of titin, but rather exerted a slight negative inotropic effect. In DOCA animals, only phosphodiesterase V inhibition via sildenafil, but not sGC stimulation or their combination, increased LV compliance. However, both the treatments clearly decreased LV contractility. These data argue against the concept that acute potentiation of cGMP-dependent signaling via a direct sGC stimulator can recruit a preload reserve, neither in healthy nor in hypertrophied LV myocardium. In a final series of preliminary experiments, we tested the differential impact of NO-mediated (via nitroglycerin infusion, acting on sGC) versus NO-independent stimulation (via atrial natriuretic peptide infusion, acting on pGC) of the cGMP-PKG-titin pathway. Acute bicoronary infusion of these substances, at doses not affecting systemic vascular resistance, rightward shifts the EDPVR in a dose-dependent manner, increasing LV compliance. These data address the need of switching the focus in HFpEF therapy from the vasculature to the heart itself, especially considering the sensitivity of these patients to load changes. The molecular mechanisms underlying the observed acute LV compliance changes and the PKG downstream targets remain to be clarified in future studies.

Chapter 7:

Appendix

7.1 Contribution of coworkers

Colleagues and collaborators contributing to this work are reported in the appropriate sections. I´m thankful for their precious support. Apart from the exceptions described in this section, I am directly responsible for the planning, execution and analyses of all the experiments as well as for the interpretation of results and the preparation of this thesis.

All experiments described in this thesis were conducted between 2012 and 2015 at the Medical University of Graz (Dept. of Experimental Surgery, Institute of Bio-medical Research or the Center for Medical Research).

Dr. Michael Schwarzl, Dr. Martin Manninger, Dr. Stefan Huber, Dr. Birgit Zirngast, Prof. Heinrich Mächler, Dr. Jochen Verderber, Dr. David Zweiker (all Medical University of Graz, Austria) assisted in the in vivo experiments.

Dr. Ursula Reiter and Dr. Gert Reiter planned the sequences, acquired and analysed the cardiac MR images. In addition, they drafted a manuscript (under submission) on the work summarized and described in Chapter 4.

Prof. Paul Steendijk (Leiden University Medical Center, Leiden, The Netherlands) provided the CircLab software and supported the interpretation of pressure-volume data, with regard to special issues.

Blood samples were analysed in the Clinical Institute of Medical and Chemical Laboratory Diagnostics, Medical University of Graz (Prof. Truschnig-Wilders).

Prof. Nazha Hamdani performed western blots for titin isoform composition and titin phosphorylation in Prof. Wolfgang Linke's lab (Ruhr University Bochum, Germany).

Prof. Mühlfeld and collaborators performed the stereological analysis of myocardial tissue samples in his laboratories (Institute of Functional and Applied Anatomy, Hannover Medical School, Hannover, Germany).

7.2 Research Funding

The author was supported by the Austrian Science Fund's PhD-programme "DK-MOLIN – Molecular Fundamentals of Inflammation" (FWF; W 1218). Additional funding was provided by the European Union Seventh Framework Programme (FP7/2007–2013) under Grant Agreement No. 261057 (EUTRAF) and unrestricted research grants from Philips Healthcare, Vienna, Austria and Bayer Healthcare AG, Wuppertal, Germany.

7.3 References

1. McMurray JJ, Adamopoulos S, Anker SD, Auricchio A, Bohm M, Dickstein K, et al. ESC Guidelines for the diagnosis and treatment of acute and chronic heart failure 2012: The Task Force for the Diagnosis and Treatment of Acute and Chronic Heart Failure 2012 of the European Society of Cardiology. Developed in collaboration with the Heart Failure Association (HFA) of the ESC. European heart journal. 2012;33(14):1787-847.
2. Yancy CW, Jessup M, Bozkurt B, Butler J, Casey DE, Jr., Drazner MH, et al. 2013 ACCF/AHA guideline for the management of heart failure: executive summary: a report of the American College of Cardiology Foundation/American Heart Association Task Force on practice guidelines. Circulation. 2013;128(16):1810-52.
3. Meta-analysis Global Group in Chronic Heart F. The survival of patients with heart failure with preserved or reduced left ventricular ejection fraction: an individual patient data meta-analysis. European heart journal. 2012;33(14):1750-7.
4. Packer M, Poole-Wilson PA, Armstrong PW, Cleland JG, Horowitz JD, Massie BM, et al. Comparative effects of low and high doses of the angiotensin-converting enzyme inhibitor, lisinopril, on morbidity and mortality in chronic heart failure. ATLAS Study Group. Circulation. 1999;100(23):2312-8.
5. Tang AS, Wells GA, Talajic M, Arnold MO, Sheldon R, Connolly S, et al. Cardiac-resynchronization therapy for mild-to-moderate heart failure. The New England journal of medicine. 2010;363(25):2385-95.
6. Effect of enalapril on survival in patients with reduced left ventricular ejection fractions and congestive heart failure. The SOLVD Investigators. The New England journal of medicine. 1991;325(5):293-302.
7. The Cardiac Insufficiency Bisoprolol Study II (CIBIS-II): a randomised trial. Lancet. 1999;353(9146):9-13.
8. Pitt B, Zannad F, Remme WJ, Cody R, Castaigne A, Perez A, et al. The effect of spironolactone on morbidity and mortality in patients with severe heart failure. Randomized Aldactone Evaluation Study Investigators. The New England journal of medicine. 1999;341(10):709-17.
9. Zannad F, McMurray JJ, Krum H, van Veldhuisen DJ, Swedberg K, Shi H, et al. Eplerenone in patients with systolic heart failure and mild symptoms. The New England journal of medicine. 2011;364(1):11-21.
10. Yusuf S, Pfeffer MA, Swedberg K, Granger CB, Held P, McMurray JJ, et al. Effects of candesartan in patients with chronic heart failure and preserved left-ventricular ejection fraction: the CHARM-Preserved Trial. Lancet. 2003;362(9386):777-81.
11. Cleland JG, Tendera M, Adamus J, Freemantle N, Polonski L, Taylor J, et al. The perindopril in elderly people with chronic heart failure (PEP-CHF) study. European heart journal. 2006;27(19):2338-45.
12. Massie BM, Carson PE, McMurray JJ, Komajda M, McKelvie R, Zile MR, et al. Irbesartan in patients with heart failure and preserved ejection fraction. The New England journal of medicine. 2008;359(23):2456-67.
13. Borlaug BA, Paulus WJ. Heart failure with preserved ejection fraction: pathophysiology, diagnosis, and treatment. European heart journal. 2011;32(6):670-9.
14. Paulus WJ, Tschope C, Sanderson JE, Rusconi C, Flachskampf FA, Rademakers FE, et al. How to diagnose diastolic heart failure: a consensus statement on the diagnosis of heart failure with normal left ventricular ejection fraction by the Heart Failure and Echocardiography Associations of the European Society of Cardiology. European heart journal. 2007;28(20):2539-50.
15. De Keulenaer GW, Brutsaert DL. Systolic and diastolic heart failure are overlapping phenotypes within the heart failure spectrum. Circulation. 2011;123(18):1996-2004; discussion 5.

16. Borlaug BA, Redfield MM. Diastolic and systolic heart failure are distinct phenotypes within the heart failure spectrum. Circulation. 2011;123(18):2006-13; discussion 14.
17. Smiseth OA, Torp H, Opdahl A, Haugaa KH, Urheim S. Myocardial strain imaging: how useful is it in clinical decision making? European heart journal. 2015.
18. Solomon SD, Dobson J, Pocock S, Skali H, McMurray JJ, Granger CB, et al. Influence of nonfatal hospitalization for heart failure on subsequent mortality in patients with chronic heart failure. Circulation. 2007;116(13):1482-7.
19. Tavazzi L, Senni M, Metra M, Gorini M, Cacciatore G, Chinaglia A, et al. Multicenter prospective observational study on acute and chronic heart failure: one-year follow-up results of IN-HF (Italian Network on Heart Failure) outcome registry. Circulation Heart failure. 2013;6(3):473-81.
20. Borlaug BA. Heart failure with preserved and reduced ejection fraction: different risk profiles for different diseases. European heart journal. 2013;34(19):1393-5.
21. Mosterd A, Hoes AW. Clinical epidemiology of heart failure. Heart. 2007;93(9):1137-46.
22. Ho KK, Pinsky JL, Kannel WB, Levy D. The epidemiology of heart failure: the Framingham Study. Journal of the American College of Cardiology. 1993;22(4 Suppl A):6A-13A.
23. Gerber Y, Weston SA, Redfield MM, Chamberlain AM, Manemann SM, Jiang R, et al. A contemporary appraisal of the heart failure epidemic in Olmsted County, Minnesota, 2000 to 2010. JAMA Intern Med. 2015;175(6):996-1004.
24. Stewart S, MacIntyre K, Hole DJ, Capewell S, McMurray JJ. More 'malignant' than cancer? Five-year survival following a first admission for heart failure. European journal of heart failure. 2001;3(3):315-22.
25. Jhund PS, Macintyre K, Simpson CR, Lewsey JD, Stewart S, Redpath A, et al. Long-term trends in first hospitalization for heart failure and subsequent survival between 1986 and 2003: a population study of 5.1 million people. Circulation. 2009;119(4):515-23.
26. Bleumink GS, Knetsch AM, Sturkenboom MC, Straus SM, Hofman A, Deckers JW, et al. Quantifying the heart failure epidemic: prevalence, incidence rate, lifetime risk and prognosis of heart failure The Rotterdam Study. European heart journal. 2004;25(18):1614-9.
27. Nichols GA, Reynolds K, Kimes TM, Rosales AG, Chan WW. Comparison of Risk of Re-hospitalization, All-Cause Mortality, and Medical Care Resource Utilization in Patients With Heart Failure and Preserved Versus Reduced Ejection Fraction. Am J Cardiol. 2015;116(7):1088-92.
28. Cheng RK, Cox M, Neely ML, Heidenreich PA, Bhatt DL, Eapen ZJ, et al. Outcomes in patients with heart failure with preserved, borderline, and reduced ejection fraction in the Medicare population. American heart journal. 2014;168(5):721-30.
29. Quiroz R, Doros G, Shaw P, Liang CS, Gauthier DF, Sam F. Comparison of characteristics and outcomes of patients with heart failure preserved ejection fraction versus reduced left ventricular ejection fraction in an urban cohort. Am J Cardiol. 2014;113(4):691-6.
30. Owan TE, Hodge DO, Herges RM, Jacobsen SJ, Roger VL, Redfield MM. Trends in prevalence and outcome of heart failure with preserved ejection fraction. The New England journal of medicine. 2006;355(3):251-9.
31. Blackledge HM, Tomlinson J, Squire IB. Prognosis for patients newly admitted to hospital with heart failure: survival trends in 12 220 index admissions in Leicestershire 1993-2001. Heart. 2003;89(6):615-20.
32. Cowie MR, Wood DA, Coats AJ, Thompson SG, Suresh V, Poole-Wilson PA, et al. Survival of patients with a new diagnosis of heart failure: a population based study. Heart. 2000;83(5):505-10.
33. Borlaug BA. The pathophysiology of heart failure with preserved ejection fraction. Nat Rev Cardiol. 2014;11(9):507-15.
34. Redfield MM, Jacobsen SJ, Burnett JC, Jr., Mahoney DW, Bailey KR, Rodeheffer RJ. Burden of systolic and diastolic ventricular dysfunction in the community: appreciating the scope of the heart failure epidemic. Jama. 2003;289(2):194-202.

35. Devereux RB, Roman MJ, Liu JE, Welty TK, Lee ET, Rodeheffer R, et al. Congestive heart failure despite normal left ventricular systolic function in a population-based sample: the Strong Heart Study. Am J Cardiol. 2000;86(10):1090-6.
36. Andersson C, Vasan RS. Epidemiology of heart failure with preserved ejection fraction. Heart failure clinics. 2014;10(3):377-88.
37. Maurer MS, King DL, El-Khoury Rumbarger L, Packer M, Burkhoff D. Left heart failure with a normal ejection fraction: identification of different pathophysiologic mechanisms. J Card Fail. 2005;11(3):177-87.
38. Senni M, Paulus WJ, Gavazzi A, Fraser AG, Diez J, Solomon SD, et al. New strategies for heart failure with preserved ejection fraction: the importance of targeted therapies for heart failure phenotypes. European heart journal. 2014;35(40):2797-815.
39. Shah SJ, Katz DH, Selvaraj S, Burke MA, Yancy CW, Gheorghiade M, et al. Phenomapping for novel classification of heart failure with preserved ejection fraction. Circulation. 2015;131(3):269-79.
40. Vasan RS, Levy D. The role of hypertension in the pathogenesis of heart failure. A clinical mechanistic overview. Archives of internal medicine. 1996;156(16):1789-96.
41. Fonarow GC, Stough WG, Abraham WT, Albert NM, Gheorghiade M, Greenberg BH, et al. Characteristics, treatments, and outcomes of patients with preserved systolic function hospitalized for heart failure: a report from the OPTIMIZE-HF Registry. Journal of the American College of Cardiology. 2007;50(8):768-77.
42. Vasan RS, Benjamin EJ, Levy D. Prevalence, clinical features and prognosis of diastolic heart failure: an epidemiologic perspective. Journal of the American College of Cardiology. 1995;26(7):1565-74.
43. Ceia F, Fonseca C, Mota T, Morais H, Matias F, de Sousa A, et al. Prevalence of chronic heart failure in Southwestern Europe: the EPICA study. European journal of heart failure. 2002;4(4):531-9.
44. Chinali M, Joffe SW, Aurigemma GP, Makam R, Meyer TE, Goldberg RJ. Risk factors and comorbidities in a community-wide sample of patients hospitalized with acute systolic or diastolic heart failure: the Worcester Heart Failure Study. Coron Artery Dis. 2010;21(3):137-43.
45. Redfield MM, Chen HH, Borlaug BA, Semigran MJ, Lee KL, Lewis G, et al. Effect of phosphodiesterase-5 inhibition on exercise capacity and clinical status in heart failure with preserved ejection fraction: a randomized clinical trial. Jama. 2013;309(12):1268-77.
46. Guder G, Frantz S, Bauersachs J, Allolio B, Wanner C, Koller MT, et al. Reverse epidemiology in systolic and nonsystolic heart failure: cumulative prognostic benefit of classical cardiovascular risk factors. Circulation Heart failure. 2009;2(6):563-71.
47. Maisel WH, Stevenson LW. Atrial fibrillation in heart failure: epidemiology, pathophysiology, and rationale for therapy. Am J Cardiol. 2003;91(6A):2D-8D.
48. Kenchaiah S, Evans JC, Levy D, Wilson PW, Benjamin EJ, Larson MG, et al. Obesity and the risk of heart failure. The New England journal of medicine. 2002;347(5):305-13.
49. Fang ZY, Prins JB, Marwick TH. Diabetic cardiomyopathy: evidence, mechanisms, and therapeutic implications. Endocrine reviews. 2004;25(4):543-67.
50. Seferovic PM, Paulus WJ. Clinical diabetic cardiomyopathy: a two-faced disease with restrictive and dilated phenotypes. European heart journal. 2015;36(27):1718-27, 27a-27c.
51. Bitter T, Faber L, Hering D, Langer C, Horstkotte D, Oldenburg O. Sleep-disordered breathing in heart failure with normal left ventricular ejection fraction. European journal of heart failure. 2009;11(6):602-8.
52. Ather S, Chan W, Bozkurt B, Aguilar D, Ramasubbu K, Zachariah AA, et al. Impact of noncardiac comorbidities on morbidity and mortality in a predominantly male population with heart failure and preserved versus reduced ejection fraction. Journal of the American College of Cardiology. 2012;59(11):998-1005.
53. Brouwers FP, de Boer RA, van der Harst P, Voors AA, Gansevoort RT, Bakker SJ, et al. Incidence and epidemiology of new onset heart failure with preserved vs. reduced ejection

fraction in a community-based cohort: 11-year follow-up of PREVEND. European heart journal. 2013;34(19):1424-31.
54. Bhatia RS, Tu JV, Lee DS, Austin PC, Fang J, Haouzi A, et al. Outcome of heart failure with preserved ejection fraction in a population-based study. The New England journal of medicine. 2006;355(3):260-9.
55. Paulus WJ, Tschope C. A novel paradigm for heart failure with preserved ejection fraction: comorbidities drive myocardial dysfunction and remodeling through coronary microvascular endothelial inflammation. Journal of the American College of Cardiology. 2013;62(4):263-71.
56. Vaccarino V. Ischemic heart disease in women: many questions, few facts. Circ Cardiovasc Qual Outcomes. 2010;3(2):111-5.
57. Ekman I, Cleland JG, Andersson B, Swedberg K. Exploring symptoms in chronic heart failure. European journal of heart failure. 2005;7(5):699-703.
58. Swedberg K, Komajda M, Bohm M, Borer JS, Ford I, Dubost-Brama A, et al. Ivabradine and outcomes in chronic heart failure (SHIFT): a randomised placebo-controlled study. Lancet. 2010;376(9744):875-85.
59. McMurray JJ, Packer M, Desai AS, Gong J, Lefkowitz MP, Rizkala AR, et al. Angiotensin-neprilysin inhibition versus enalapril in heart failure. The New England journal of medicine. 2014;371(11):993-1004.
60. Hernandez AF, Hammill BG, O'Connor CM, Schulman KA, Curtis LH, Fonarow GC. Clinical effectiveness of beta-blockers in heart failure: findings from the OPTIMIZE-HF (Organized Program to Initiate Lifesaving Treatment in Hospitalized Patients with Heart Failure) Registry. Journal of the American College of Cardiology. 2009;53(2):184-92.
61. Pitt B, Pfeffer MA, Assmann SF, Boineau R, Anand IS, Claggett B, et al. Spironolactone for heart failure with preserved ejection fraction. The New England journal of medicine. 2014;370(15):1383-92.
62. Pfeffer MA, Claggett B, Assmann SF, Boineau R, Anand IS, Clausell N, et al. Regional variation in patients and outcomes in the Treatment of Preserved Cardiac Function Heart Failure With an Aldosterone Antagonist (TOPCAT) trial. Circulation. 2015;131(1):34-42.
63. Solomon SD, Zile M, Pieske B, Voors A, Shah A, Kraigher-Krainer E, et al. The angiotensin receptor neprilysin inhibitor LCZ696 in heart failure with preserved ejection fraction: a phase 2 double-blind randomised controlled trial. Lancet. 2012;380(9851):1387-95.
64. Jhund PS, Claggett B, Packer M, Zile MR, Voors AA, Pieske B, et al. Independence of the blood pressure lowering effect and efficacy of the angiotensin receptor neprilysin inhibitor, LCZ696, in patients with heart failure with preserved ejection fraction: an analysis of the PARAMOUNT trial. European journal of heart failure. 2014;16(6):671-7.
65. Gheorghiade M, Greene SJ, Butler J, Filippatos G, Lam CS, Maggioni AP, et al. Effect of Vericiguat, a Soluble Guanylate Cyclase Stimulator, on Natriuretic Peptide Levels in Patients With Worsening Chronic Heart Failure and Reduced Ejection Fraction: The SOCRATES-REDUCED Randomized Trial. Jama. 2015;314(21):2251-62.
66. Edelmann F, Gelbrich G, Dungen HD, Frohling S, Wachter R, Stahrenberg R, et al. Exercise training improves exercise capacity and diastolic function in patients with heart failure with preserved ejection fraction: results of the Ex-DHF (Exercise training in Diastolic Heart Failure) pilot study. Journal of the American College of Cardiology. 2011;58(17):1780-91.
67. Shah AM, Pfeffer MA. The many faces of heart failure with preserved ejection fraction. Nat Rev Cardiol. 2012;9(10):555-6.
68. Edelmann F, Wachter R, Schmidt AG, Kraigher-Krainer E, Colantonio C, Kamke W, et al. Effect of spironolactone on diastolic function and exercise capacity in patients with heart failure with preserved ejection fraction: the Aldo-DHF randomized controlled trial. Jama. 2013;309(8):781-91.
69. Pieske B, Butler J, Filippatos G, Lam C, Maggioni AP, Ponikowski P, et al. Rationale and design of the SOluble guanylate Cyclase stimulatoR in heArT failurE Studies (SOCRATES). European journal of heart failure. 2014;16(9):1026-38.

70. Zile MR, Baicu CF, Gaasch WH. Diastolic heart failure--abnormalities in active relaxation and passive stiffness of the left ventricle. The New England journal of medicine. 2004;350(19):1953-9.
71. Borlaug BA, Olson TP, Lam CS, Flood KS, Lerman A, Johnson BD, et al. Global cardiovascular reserve dysfunction in heart failure with preserved ejection fraction. Journal of the American College of Cardiology. 2010;56(11):845-54.
72. Zile MR, Gaasch WH, Carroll JD, Feldman MD, Aurigemma GP, Schaer GL, et al. Heart failure with a normal ejection fraction: is measurement of diastolic function necessary to make the diagnosis of diastolic heart failure? Circulation. 2001;104(7):779-82.
73. Topol EJ, Traill TA, Fortuin NJ. Hypertensive hypertrophic cardiomyopathy of the elderly. The New England journal of medicine. 1985;312(5):277-83.
74. van Heerebeek L, Borbely A, Niessen HW, Bronzwaer JG, van der Velden J, Stienen GJ, et al. Myocardial structure and function differ in systolic and diastolic heart failure. Circulation. 2006;113(16):1966-73.
75. Zile MR, Gottdiener JS, Hetzel SJ, McMurray JJ, Komajda M, McKelvie R, et al. Prevalence and significance of alterations in cardiac structure and function in patients with heart failure and a preserved ejection fraction. Circulation. 2011;124(23):2491-501.
76. Lam CS, Roger VL, Rodeheffer RJ, Bursi F, Borlaug BA, Ommen SR, et al. Cardiac structure and ventricular-vascular function in persons with heart failure and preserved ejection fraction from Olmsted County, Minnesota. Circulation. 2007;115(15):1982-90.
77. Templeton GH, Wildenthal K, Willerson JT, Reardon WC. Influence of temperature on the mechanical properties of cardiac muscle. Circulation research. 1974;34(5):624-34.
78. Borlaug BA, Jaber WA, Ommen SR, Lam CS, Redfield MM, Nishimura RA. Diastolic relaxation and compliance reserve during dynamic exercise in heart failure with preserved ejection fraction. Heart. 2011;97(12):964-9.
79. Weisfeldt ML, Frederiksen JW, Yin FC, Weiss JL. Evidence of incomplete left ventricular relaxation in the dog: prediction from the time constant for isovolumic pressure fall. The Journal of clinical investigation. 1978;62(6):1296-302.
80. Borlaug BA, Nishimura RA, Sorajja P, Lam CS, Redfield MM. Exercise hemodynamics enhance diagnosis of early heart failure with preserved ejection fraction. Circulation Heart failure. 2010;3(5):588-95.
81. Tan YT, Wenzelburger F, Lee E, Heatlie G, Frenneaux M, Sanderson JE. Abnormal left ventricular function occurs on exercise in well-treated hypertensive subjects with normal resting echocardiography. Heart. 2010;96(12):948-55.
82. Tan YT, Wenzelburger F, Lee E, Nightingale P, Heatlie G, Leyva F, et al. Reduced left atrial function on exercise in patients with heart failure and normal ejection fraction. Heart. 2010;96(13):1017-23.
83. Yu CM, Lin H, Yang H, Kong SL, Zhang Q, Lee SW. Progression of systolic abnormalities in patients with "isolated" diastolic heart failure and diastolic dysfunction. Circulation. 2002;105(10):1195-201.
84. Tan YT, Wenzelburger F, Lee E, Heatlie G, Leyva F, Patel K, et al. The pathophysiology of heart failure with normal ejection fraction: exercise echocardiography reveals complex abnormalities of both systolic and diastolic ventricular function involving torsion, untwist, and longitudinal motion. Journal of the American College of Cardiology. 2009;54(1):36-46.
85. Borlaug BA, Lam CS, Roger VL, Rodeheffer RJ, Redfield MM. Contractility and ventricular systolic stiffening in hypertensive heart disease insights into the pathogenesis of heart failure with preserved ejection fraction. Journal of the American College of Cardiology. 2009;54(5):410-8.
86. Yip GW, Zhang Q, Xie JM, Liang YJ, Liu YM, Yan B, et al. Resting global and regional left ventricular contractility in patients with heart failure and normal ejection fraction: insights from speckle-tracking echocardiography. Heart. 2011;97(4):287-94.

87. Kraigher-Krainer E, Shah AM, Gupta DK, Santos A, Claggett B, Pieske B, et al. Impaired systolic function by strain imaging in heart failure with preserved ejection fraction. Journal of the American College of Cardiology. 2014;63(5):447-56.
88. Lam CS, Roger VL, Rodeheffer RJ, Borlaug BA, Enders FT, Redfield MM. Pulmonary hypertension in heart failure with preserved ejection fraction: a community-based study. Journal of the American College of Cardiology. 2009;53(13):1119-26.
89. Damy T, Kallvikbacka-Bennett A, Goode K, Khaleva O, Lewinter C, Hobkirk J, et al. Prevalence of, associations with, and prognostic value of tricuspid annular plane systolic excursion (TAPSE) among out-patients referred for the evaluation of heart failure. J Card Fail. 2012;18(3):216-25.
90. Melenovsky V, Hwang SJ, Lin G, Redfield MM, Borlaug BA. Right heart dysfunction in heart failure with preserved ejection fraction. European heart journal. 2014;35(48):3452-62.
91. Guazzi M, Borlaug BA. Pulmonary hypertension due to left heart disease. Circulation. 2012;126(8):975-90.
92. Guazzi M, Vicenzi M, Arena R, Guazzi MD. Pulmonary hypertension in heart failure with preserved ejection fraction: a target of phosphodiesterase-5 inhibition in a 1-year study. Circulation. 2011;124(2):164-74.
93. Kawaguchi M, Hay I, Fetics B, Kass DA. Combined ventricular systolic and arterial stiffening in patients with heart failure and preserved ejection fraction: implications for systolic and diastolic reserve limitations. Circulation. 2003;107(5):714-20.
94. Tartiere-Kesri L, Tartiere JM, Logeart D, Beauvais F, Cohen Solal A. Increased proximal arterial stiffness and cardiac response with moderate exercise in patients with heart failure and preserved ejection fraction. Journal of the American College of Cardiology. 2012;59(5):455-61.
95. Phan TT, Abozguia K, Nallur Shivu G, Mahadevan G, Ahmed I, Williams L, et al. Heart failure with preserved ejection fraction is characterized by dynamic impairment of active relaxation and contraction of the left ventricle on exercise and associated with myocardial energy deficiency. Journal of the American College of Cardiology. 2009;54(5):402-9.
96. Phan TT, Shivu GN, Abozguia K, Davies C, Nassimizadeh M, Jimenez D, et al. Impaired heart rate recovery and chronotropic incompetence in patients with heart failure with preserved ejection fraction. Circulation Heart failure. 2010;3(1):29-34.
97. Abudiab MM, Redfield MM, Melenovsky V, Olson TP, Kass DA, Johnson BD, et al. Cardiac output response to exercise in relation to metabolic demand in heart failure with preserved ejection fraction. European journal of heart failure. 2013;15(7):776-85.
98. Haykowsky MJ, Brubaker PH, John JM, Stewart KP, Morgan TM, Kitzman DW. Determinants of exercise intolerance in elderly heart failure patients with preserved ejection fraction. Journal of the American College of Cardiology. 2011;58(3):265-74.
99. Borlaug BA, Melenovsky V, Russell SD, Kessler K, Pacak K, Becker LC, et al. Impaired chronotropic and vasodilator reserves limit exercise capacity in patients with heart failure and a preserved ejection fraction. Circulation. 2006;114(20):2138-47.
100. Cole CR, Blackstone EH, Pashkow FJ, Snader CE, Lauer MS. Heart-rate recovery immediately after exercise as a predictor of mortality. The New England journal of medicine. 1999;341(18):1351-7.
101. Sengupta PP, Khandheria BK, Narula J. Twist and untwist mechanics of the left ventricle. Heart failure clinics. 2008;4(3):315-24.
102. Benjamin EJ, Levy D, Anderson KM, Wolf PA, Plehn JF, Evans JC, et al. Determinants of Doppler indexes of left ventricular diastolic function in normal subjects (the Framingham Heart Study). Am J Cardiol. 1992;70(4):508-15.
103. Kasner M, Westermann D, Lopez B, Gaub R, Escher F, Kuhl U, et al. Diastolic tissue Doppler indexes correlate with the degree of collagen expression and cross-linking in heart failure and normal ejection fraction. Journal of the American College of Cardiology. 2011;57(8):977-85.

104. van Heerebeek L, Hamdani N, Handoko ML, Falcao-Pires I, Musters RJ, Kupreishvili K, et al. Diastolic stiffness of the failing diabetic heart: importance of fibrosis, advanced glycation end products, and myocyte resting tension. Circulation. 2008;117(1):43-51.
105. Badenhorst D, Maseko M, Tsotetsi OJ, Naidoo A, Brooksbank R, Norton GR, et al. Cross-linking influences the impact of quantitative changes in myocardial collagen on cardiac stiffness and remodelling in hypertension in rats. Cardiovascular research. 2003;57(3):632-41.
106. Sharma K, Kass DA. Heart failure with preserved ejection fraction: mechanisms, clinical features, and therapies. Circulation research. 2014;115(1):79-96.
107. Glezeva N, Baugh JA. Role of inflammation in the pathogenesis of heart failure with preserved ejection fraction and its potential as a therapeutic target. Heart Fail Rev. 2014;19(5):681-94.
108. Kalogeropoulos A, Georgiopoulou V, Psaty BM, Rodondi N, Smith AL, Harrison DG, et al. Inflammatory markers and incident heart failure risk in older adults: the Health ABC (Health, Aging, and Body Composition) study. Journal of the American College of Cardiology. 2010;55(19):2129-37.
109. Westermann D, Lindner D, Kasner M, Zietsch C, Savvatis K, Escher F, et al. Cardiac inflammation contributes to changes in the extracellular matrix in patients with heart failure and normal ejection fraction. Circulation Heart failure. 2011;4(1):44-52.
110. Franssen C, Chen S, Unger A, Korkmaz HI, De Keulenaer GW, Tschope C, et al. Myocardial Microvascular Inflammatory Endothelial Activation in Heart Failure With Preserved Ejection Fraction. JACC Heart Fail. 2015.
111. van Heerebeek L, Hamdani N, Falcao-Pires I, Leite-Moreira AF, Begieneman MP, Bronzwaer JG, et al. Low myocardial protein kinase G activity in heart failure with preserved ejection fraction. Circulation. 2012;126(7):830-9.
112. Linke WA, Hamdani N. Gigantic business: titin properties and function through thick and thin. Circulation research. 2014;114(6):1052-68.
113. Linke WA. Sense and stretchability: the role of titin and titin-associated proteins in myocardial stress-sensing and mechanical dysfunction. Cardiovascular research. 2008;77(4):637-48.
114. Cazorla O, Freiburg A, Helmes M, Centner T, McNabb M, Wu Y, et al. Differential expression of cardiac titin isoforms and modulation of cellular stiffness. Circulation research. 2000;86(1):59-67.
115. Kruger M, Kotter S, Grutzner A, Lang P, Andresen C, Redfield MM, et al. Protein kinase G modulates human myocardial passive stiffness by phosphorylation of the titin springs. Circulation research. 2009;104(1):87-94.
116. Yamasaki R, Wu Y, McNabb M, Greaser M, Labeit S, Granzier H. Protein kinase A phosphorylates titin's cardiac-specific N2B domain and reduces passive tension in rat cardiac myocytes. Circulation research. 2002;90(11):1181-8.
117. Hamdani N, Paulus WJ. Myocardial titin and collagen in cardiac diastolic dysfunction: partners in crime. Circulation. 2013;128(1):5-8.
118. Hidalgo C, Hudson B, Bogomolovas J, Zhu Y, Anderson B, Greaser M, et al. PKC phosphorylation of titin's PEVK element: a novel and conserved pathway for modulating myocardial stiffness. Circulation research. 2009;105(7):631-8, 17 p following 8.
119. Hohendanner F, Ljubojevic S, MacQuaide N, Sacherer M, Sedej S, Biesmans L, et al. Intracellular dyssynchrony of diastolic cytosolic [Ca(2)(+)] decay in ventricular cardiomyocytes in cardiac remodeling and human heart failure. Circulation research. 2013;113(5):527-38.
120. Janczewski AM, Lakatta EG. Modulation of sarcoplasmic reticulum Ca(2+) cycling in systolic and diastolic heart failure associated with aging. Heart Fail Rev. 2010;15(5):431-45.
121. Lancel S, Qin F, Lennon SL, Zhang J, Tong X, Mazzini MJ, et al. Oxidative posttranslational modifications mediate decreased SERCA activity and myocyte dysfunction in Galphaq-overexpressing mice. Circulation research. 2010;107(2):228-32.

122. Schwinger RH, Bohm M, Schmidt U, Karczewski P, Bavendiek U, Flesch M, et al. Unchanged protein levels of SERCA II and phospholamban but reduced Ca2+ uptake and Ca(2+)-ATPase activity of cardiac sarcoplasmic reticulum from dilated cardiomyopathy patients compared with patients with nonfailing hearts. Circulation. 1995;92(11):3220-8.
123. Xu A, Narayanan N. Effects of aging on sarcoplasmic reticulum Ca2+-cycling proteins and their phosphorylation in rat myocardium. The American journal of physiology. 1998;275(6 Pt 2):H2087-94.
124. Chamberlain D, Founding Members of the International Liaison Committee on R. The International Liaison Committee on Resuscitation (ILCOR)-past and present: compiled by the Founding Members of the International Liaison Committee on Resuscitation. Resuscitation. 2005;67(2-3):157-61.
125. Nielsen N, Wetterslev J, Cronberg T, Erlinge D, Gasche Y, Hassager C, et al. Targeted temperature management at 33 degrees C versus 36 degrees C after cardiac arrest. The New England journal of medicine. 2013;369(23):2197-206.
126. Hiranandani N, Varian KD, Monasky MM, Janssen PM. Frequency-dependent contractile response of isolated cardiac trabeculae under hypo-, normo-, and hyperthermic conditions. J Appl Physiol (1985). 2006;100(5):1727-32.
127. Weisser J, Martin J, Bisping E, Maier LS, Beyersdorf F, Hasenfuss G, et al. Influence of mild hypothermia on myocardial contractility and circulatory function. Basic research in cardiology. 2001;96(2):198-205.
128. Fukunami M, Hearse DJ. The inotropic consequences of cooling: studies in the isolated rat heart. Heart and vessels. 1989;5(1):1-9.
129. Mattheussen M, Mubagwa K, Van Aken H, Wusten R, Boutros A, Flameng W. Interaction of heart rate and hypothermia on global myocardial contraction of the isolated rabbit heart. Anesthesia and analgesia. 1996;82(5):975-81.
130. Nishimura Y, Naito Y, Nishioka T, Okamura Y. The effects of cardiac cooling under surface-induced hypothermia on the cardiac function in the in situ heart. Interactive cardiovascular and thoracic surgery. 2005;4(2):101-5.
131. Post H, Schmitto JD, Steendijk P, Christoph J, Holland R, Wachter R, et al. Cardiac function during mild hypothermia in pigs: increased inotropy at the expense of diastolic dysfunction. Acta physiologica. 2010;199(1):43-52.
132. Saeki A, Goto Y, Hata K, Takasago T, Nishioka T, Suga H. Negative inotropism of hyperthermia increases oxygen cost of contractility in canine hearts. American journal of physiology Heart and circulatory physiology. 2000;279(6):H2855-64.
133. Schmidt-Schweda S, Ohler A, Post H, Pieske B. Moderate hypothermia for severe cardiogenic shock (COOL Shock Study I & II). Resuscitation. 2013;84(3):319-25.
134. Stegman B, Aggarwal B, Senapati A, Shao M, Menon V. Serial hemodynamic measurements in post-cardiac arrest cardiogenic shock treated with therapeutic hypothermia. European heart journal Acute cardiovascular care. 2014.
135. Schwarzl M, Alogna A, Zirngast B, Steendijk P, Verderber J, Zweiker D, et al. Mild hypothermia induces incomplete left ventricular relaxation despite spontaneous bradycardia in pigs. Acta physiologica. 2015;213(3):653-63.
136. Kong Q, Blanton RM. Protein kinase G I and heart failure: Shifting focus from vascular unloading to direct myocardial antiremodeling effects. Circulation Heart failure. 2013;6(6):1268-83.
137. Hofmann F. The biology of cyclic GMP-dependent protein kinases. The Journal of biological chemistry. 2005;280(1):1-4.
138. Francis SH, Busch JL, Corbin JD, Sibley D. cGMP-dependent protein kinases and cGMP phosphodiesterases in nitric oxide and cGMP action. Pharmacological reviews. 2010;62(3):525-63.
139. Pfeifer A, Klatt P, Massberg S, Ny L, Sausbier M, Hirneiss C, et al. Defective smooth muscle regulation in cGMP kinase I-deficient mice. The EMBO journal. 1998;17(11):3045-51.

140. Rosenkranz AC, Hood SG, Woods RL, Dusting GJ, Ritchie RH. B-type natriuretic peptide prevents acute hypertrophic responses in the diabetic rat heart: importance of cyclic GMP. Diabetes. 2003;52(9):2389-95.
141. Calderone A, Thaik CM, Takahashi N, Chang DL, Colucci WS. Nitric oxide, atrial natriuretic peptide, and cyclic GMP inhibit the growth-promoting effects of norepinephrine in cardiac myocytes and fibroblasts. The Journal of clinical investigation. 1998;101(4):812-8.
142. Rosenkranz AC, Woods RL, Dusting GJ, Ritchie RH. Antihypertrophic actions of the natriuretic peptides in adult rat cardiomyocytes: importance of cyclic GMP. Cardiovascular research. 2003;57(2):515-22.
143. Wollert KC, Fiedler B, Gambaryan S, Smolenski A, Heineke J, Butt E, et al. Gene transfer of cGMP-dependent protein kinase I enhances the antihypertrophic effects of nitric oxide in cardiomyocytes. Hypertension. 2002;39(1):87-92.
144. Michael SK, Surks HK, Wang Y, Zhu Y, Blanton R, Jamnongjit M, et al. High blood pressure arising from a defect in vascular function. Proceedings of the National Academy of Sciences of the United States of America. 2008;105(18):6702-7.
145. Blanton RM, Takimoto E, Lane AM, Aronovitz M, Piotrowski R, Karas RH, et al. Protein kinase g ialpha inhibits pressure overload-induced cardiac remodeling and is required for the cardioprotective effect of sildenafil in vivo. Journal of the American Heart Association. 2012;1(5):e003731.
146. Bishu K, Hamdani N, Mohammed SF, Kruger M, Ohtani T, Ogut O, et al. Sildenafil and B-type natriuretic peptide acutely phosphorylate titin and improve diastolic distensibility in vivo. Circulation. 2011;124(25):2882-91.
147. Wegener JW, Nawrath H, Wolfsgruber W, Kuhbandner S, Werner C, Hofmann F, et al. cGMP-dependent protein kinase I mediates the negative inotropic effect of cGMP in the murine myocardium. Circulation research. 2002;90(1):18-20.
148. Pfitzer G, Ruegg JC, Flockerzi V, Hofmann F. cGMP-dependent protein kinase decreases calcium sensitivity of skinned cardiac fibers. FEBS letters. 1982;149(2):171-5.
149. Yang L, Liu G, Zakharov SI, Bellinger AM, Mongillo M, Marx SO. Protein kinase G phosphorylates Cav1.2 alpha1c and beta2 subunits. Circulation research. 2007;101(5):465-74.
150. Smith JA, Shah AM, Lewis MJ. Factors released from endocardium of the ferret and pig modulate myocardial contraction. The Journal of physiology. 1991;439:1-14.
151. Paulus WJ, Vantrimpont PJ, Shah AM. Acute effects of nitric oxide on left ventricular relaxation and diastolic distensibility in humans. Assessment by bicoronary sodium nitroprusside infusion. Circulation. 1994;89(5):2070-8.
152. Munzel T, Daiber A, Mulsch A. Explaining the phenomenon of nitrate tolerance. Circulation research. 2005;97(7):618-28.
153. Oelze M, Knorr M, Kroller-Schon S, Kossmann S, Gottschlich A, Rummler R, et al. Chronic therapy with isosorbide-5-mononitrate causes endothelial dysfunction, oxidative stress, and a marked increase in vascular endothelin-1 expression. European heart journal. 2013;34(41):3206-16.
154. Schwartzenberg S, Redfield MM, From AM, Sorajja P, Nishimura RA, Borlaug BA. Effects of vasodilation in heart failure with preserved or reduced ejection fraction implications of distinct pathophysiologies on response to therapy. Journal of the American College of Cardiology. 2012;59(5):442-51.
155. Takimoto E, Champion HC, Li M, Belardi D, Ren S, Rodriguez ER, et al. Chronic inhibition of cyclic GMP phosphodiesterase 5A prevents and reverses cardiac hypertrophy. Nature medicine. 2005;11(2):214-22.
156. Guazzi M, Vicenzi M, Arena R, Guazzi MD. PDE5 inhibition with sildenafil improves left ventricular diastolic function, cardiac geometry, and clinical status in patients with stable systolic heart failure: results of a 1-year, prospective, randomized, placebo-controlled study. Circulation Heart failure. 2011;4(1):8-17.

157. Lee DI, Zhu G, Sasaki T, Cho GS, Hamdani N, Holewinski R, et al. Phosphodiesterase 9A controls nitric-oxide-independent cGMP and hypertrophic heart disease. Nature. 2015;519(7544):472-6.
158. Badejo AM, Jr., Nossaman VE, Pankey EA, Bhartiya M, Kannadka CB, Murthy SN, et al. Pulmonary and systemic vasodilator responses to the soluble guanylyl cyclase stimulator, BAY 41-8543, are modulated by nitric oxide. American journal of physiology Heart and circulatory physiology. 2010;299(4):H1153-9.
159. Lasker GF, Maley JH, Pankey EA, Kadowitz PJ. Targeting soluble guanylate cyclase for the treatment of pulmonary hypertension. Expert review of respiratory medicine. 2011;5(2):153-61.
160. Pankey EA, Bhartiya M, Badejo AM, Jr., Haider U, Stasch JP, Murthy SN, et al. Pulmonary and systemic vasodilator responses to the soluble guanylyl cyclase activator, BAY 60-2770, are not dependent on endogenous nitric oxide or reduced heme. American journal of physiology Heart and circulatory physiology. 2011;300(3):H792-802.
161. Boerrigter G, Costello-Boerrigter LC, Cataliotti A, Lapp H, Stasch JP, Burnett JC, Jr. Targeting heme-oxidized soluble guanylate cyclase in experimental heart failure. Hypertension. 2007;49(5):1128-33.
162. Erdmann E, Semigran MJ, Nieminen MS, Gheorghiade M, Agrawal R, Mitrovic V, et al. Cinaciguat, a soluble guanylate cyclase activator, unloads the heart but also causes hypotension in acute decompensated heart failure. European heart journal. 2013;34(1):57-67.
163. Sharkovska Y, Kalk P, Lawrenz B, Godes M, Hoffmann LS, Wellkisch K, et al. Nitric oxide-independent stimulation of soluble guanylate cyclase reduces organ damage in experimental low-renin and high-renin models. Journal of hypertension. 2010;28(8):1666-75.
164. Bonderman D, Ghio S, Felix SB, Ghofrani HA, Michelakis E, Mitrovic V, et al. Riociguat for patients with pulmonary hypertension caused by systolic left ventricular dysfunction: a phase IIb double-blind, randomized, placebo-controlled, dose-ranging hemodynamic study. Circulation. 2013;128(5):502-11.
165. Potter LR, Abbey-Hosch S, Dickey DM. Natriuretic peptides, their receptors, and cyclic guanosine monophosphate-dependent signaling functions. Endocrine reviews. 2006;27(1):47-72.
166. Rouleau JL, Pfeffer MA, Stewart DJ, Isaac D, Sestier F, Kerut EK, et al. Comparison of vasopeptidase inhibitor, omapatrilat, and lisinopril on exercise tolerance and morbidity in patients with heart failure: IMPRESS randomised trial. Lancet. 2000;356(9230):615-20.
167. Packer M, Califf RM, Konstam MA, Krum H, McMurray JJ, Rouleau JL, et al. Comparison of omapatrilat and enalapril in patients with chronic heart failure: the Omapatrilat Versus Enalapril Randomized Trial of Utility in Reducing Events (OVERTURE). Circulation. 2002;106(8):920-6.
168. Schwarzl M, Steendijk P, Huber S, Truschnig-Wilders M, Obermayer-Pietsch B, Maechler H, et al. The induction of mild hypothermia improves systolic function of the resuscitated porcine heart at no further sympathetic activation. Acta physiologica. 2011;203(4):409-18.
169. Schwarzl M, Huber S, Maechler H, Steendijk P, Seiler S, Truschnig-Wilders M, et al. Left ventricular diastolic dysfunction during acute myocardial infarction: effect of mild hypothermia. Resuscitation. 2012;83(12):1503-10.
170. Schwarzl M, Seiler S, Wallner M, von Lewinski D, Huber S, Maechler H, et al. Mild hypothermia attenuates circulatory and pulmonary dysfunction during experimental endotoxemia. Critical care medicine. 2013;41(12):e401-10.
171. Baan J, van der Velde ET, de Bruin HG, Smeenk GJ, Koops J, van Dijk AD, et al. Continuous measurement of left ventricular volume in animals and humans by conductance catheter. Circulation. 1984;70(5):812-23.
172. Steendijk P, Staal E, Jukema JW, Baan J. Hypertonic saline method accurately determines parallel conductance for dual-field conductance catheter. American journal of physiology Heart and circulatory physiology. 2001;281(2):H755-63.
173. Aghajani E, Muller S, Kjorstad KE, Korvald C, Nordhaug D, Revhaugand A, et al. The pressure-volume loop revisited: Is the search for a cardiac contractility index a futile cycle? Shock. 2006;25(4):370-6.

174. Burkhoff D, Mirsky I, Suga H. Assessment of systolic and diastolic ventricular properties via pressure-volume analysis: a guide for clinical, translational, and basic researchers. American journal of physiology Heart and circulatory physiology. 2005;289(2):H501-12.
175. Ohte N, Cheng CP, Suzuki M, Little WC. Effects of atrial natriuretic peptide on left ventricular performance in conscious dogs before and after pacing-induced heart failure. The Journal of pharmacology and experimental therapeutics. 1999;291(2):589-95.
176. Leeuwenburgh BP, Steendijk P, Helbing WA, Baan J. Indexes of diastolic RV function: load dependence and changes after chronic RV pressure overload in lambs. American journal of physiology Heart and circulatory physiology. 2002;282(4):H1350-8.
177. Raff GL, Glantz SA. Volume loading slows left ventricular isovolumic relaxation rate. Evidence of load-dependent relaxation in the intact dog heart. Circulation research. 1981;48(6 Pt 1):813-24.
178. Fincke R, Hochman JS, Lowe AM, Menon V, Slater JN, Webb JG, et al. Cardiac power is the strongest hemodynamic correlate of mortality in cardiogenic shock: a report from the SHOCK trial registry. Journal of the American College of Cardiology. 2004;44(2):340-8.
179. Kelley KW, Curtis SE, Marzan GT, Karara HM, Anderson CR. Body surface area of female swine. Journal of animal science. 1973;36(5):927-30.
180. Schulz-Menger J, Bluemke DA, Bremerich J, Flamm SD, Fogel MA, Friedrich MG, et al. Standardized image interpretation and post processing in cardiovascular magnetic resonance: Society for Cardiovascular Magnetic Resonance (SCMR) board of trustees task force on standardized post processing. J Cardiovasc Magn Reson. 2013;15:35.
181. Dandekar VK, Bauml MA, Ertel AW, Dickens C, Gonzalez RC, Farzaneh-Far A. Assessment of global myocardial perfusion reserve using cardiovascular magnetic resonance of coronary sinus flow at 3 Tesla. J Cardiovasc Magn Reson. 2014;16:24.
182. Schwarzl M, Hamdani N, Seiler S, Alogna A, Manninger M, Reilly S, et al. A porcine model of hypertensive cardiomyopathy: implications for heart failure with preserved ejection fraction. American journal of physiology Heart and circulatory physiology. 2015:ajpheart 00542 2015.
183. Hamdani N, Krysiak J, Kreusser MM, Neef S, Dos Remedios CG, Maier LS, et al. Crucial role for Ca2(+)/calmodulin-dependent protein kinase-II in regulating diastolic stress of normal and failing hearts via titin phosphorylation. Circulation research. 2013;112(4):664-74.
184. Bernard SA, Gray TW, Buist MD, Jones BM, Silvester W, Gutteridge G, et al. Treatment of comatose survivors of out-of-hospital cardiac arrest with induced hypothermia. The New England journal of medicine. 2002;346(8):557-63.
185. Hypothermia after Cardiac Arrest Study G. Mild therapeutic hypothermia to improve the neurologic outcome after cardiac arrest. The New England journal of medicine. 2002;346(8):549-56.
186. Dae MW, Gao DW, Sessler DI, Chair K, Stillson CA. Effect of endovascular cooling on myocardial temperature, infarct size, and cardiac output in human-sized pigs. American journal of physiology Heart and circulatory physiology. 2002;282(5):H1584-91.
187. Gotberg M, Olivecrona GK, Engblom H, Ugander M, van der Pals J, Heiberg E, et al. Rapid short-duration hypothermia with cold saline and endovascular cooling before reperfusion reduces microvascular obstruction and myocardial infarct size. BMC cardiovascular disorders. 2008;8:7.
188. Gotberg M, van der Pals J, Olivecrona GK, Gotberg M, Koul S, Erlinge D. Mild hypothermia reduces acute mortality and improves hemodynamic outcome in a cardiogenic shock pig model. Resuscitation. 2010;81(9):1190-6.
189. Weiss JL, Frederiksen JW, Weisfeldt ML. Hemodynamic determinants of the time-course of fall in canine left ventricular pressure. The Journal of clinical investigation. 1976;58(3):751-60.
190. Parker JD, Landzberg JS, Bittl JA, Mirsky I, Colucci WS. Effects of beta-adrenergic stimulation with dobutamine on isovolumic relaxation in the normal and failing human left ventricle. Circulation. 1991;84(3):1040-8.

191. Karliner JS, LeWinter MM, Mahler F, Engler R, O'Rourke RA. Pharmacologic and hemodynamic influences on the rate of isovolumic left ventricular relaxation in the normal conscious dog. The Journal of clinical investigation. 1977;60(3):511-21.
192. Go AS, Mozaffarian D, Roger VL, Benjamin EJ, Berry JD, Blaha MJ, et al. Heart disease and stroke statistics--2014 update: a report from the American Heart Association. Circulation. 2014;129(3):e28-e292.
193. Cooper T, Willman VL, Hanlon CR. Cardiovascular Responses to Hyperthermia. Diseases of the chest. 1963;44:88-9.
194. Koroxenidis GT, Shepherd JT, Marshall RJ. Cardiovascular response to acute heat stress. Journal of applied physiology. 1961;16:869-72.
195. Prec O, Rosenman R, Braun K, Harris R, Rodbard S, Katz LN. The Circulatory Responses to Hyperthermia Induced by Radiant Heat. The Journal of clinical investigation. 1949;28(2):301-6.
196. Liedtke AJ, Hughes HC. Effects of hyperthermic stress on myocardial function during experimental coronary ischemia. Circulation research. 1976;39(5):647-53.
197. D'Ambra MN, Magrassi P, Lowenstein E, Kyo S, Austen WG, Buckley MJ, et al. Myocardial temperature variation: effect on regional function and coronary flow in dogs. The American journal of physiology. 1987;252(2 Pt 2):H448-55.
198. Suga H, Goto Y, Igarashi Y, Yasumura Y, Nozawa T, Futaki S, et al. Cardiac cooling increases Emax without affecting relation between O2 consumption and systolic pressure-volume area in dog left ventricle. Circulation research. 1988;63(1):61-71.
199. Little WC, Cheng CP, Mumma M, Igarashi Y, Vinten-Johansen J, Johnston WE. Comparison of measures of left ventricular contractile performance derived from pressure-volume loops in conscious dogs. Circulation. 1989;80(5):1378-87.
200. Katz AM. Cyclic adenosine monophosphate effects on the myocardium: a man who blows hot and cold with one breath. Journal of the American College of Cardiology. 1983;2(1):143-9.
201. Kusuoka H, Ikoma Y, Futaki S, Suga H, Kitabatake A, Kamada T, et al. Positive inotropism in hypothermia partially depends on an increase in maximal Ca(2+)-activated force. The American journal of physiology. 1991;261(4 Pt 2):H1005-10.
202. Langer GA, Brady AJ. The effects of temperature upon contraction and ionic exchange in rabbit ventricular myocardium. Relation to control of active state. The Journal of general physiology. 1968;52(4):682-713.
203. Mikane T, Araki J, Kohno K, Nakayama Y, Suzuki S, Shimizu J, et al. Mechanism of constant contractile efficiency under cooling inotropy of myocardium: simulation. The American journal of physiology. 1997;273(6 Pt 2):H2891-8.
204. Gillebert TC, Lew WY. Influence of systolic pressure profile on rate of left ventricular pressure fall. The American journal of physiology. 1991;261(3 Pt 2):H805-13.
205. Nelson OL, Robbins CT. Cardiovascular function in large to small hibernators: bears to ground squirrels. Journal of comparative physiology B, Biochemical, systemic, and environmental physiology. 2014.
206. Cotter G, Williams SG, Vered Z, Tan LB. Role of cardiac power in heart failure. Current opinion in cardiology. 2003;18(3):215-22.
207. Holm J, Hakanson RE, Vanky F, Svedjeholm R. Mixed venous oxygen saturation is a prognostic marker after surgery for aortic stenosis. Acta anaesthesiologica Scandinavica. 2010;54(5):589-95.
208. Holm J, Hakanson E, Vanky F, Svedjeholm R. Mixed venous oxygen saturation predicts short- and long-term outcome after coronary artery bypass grafting surgery: a retrospective cohort analysis. British journal of anaesthesia. 2011;107(3):344-50.
209. Jacobshagen C, Pelster T, Pax A, Horn W, Schmidt-Schweda S, Unsold BW, et al. Effects of mild hypothermia on hemodynamics in cardiac arrest survivors and isolated failing human myocardium. Clinical research in cardiology : official journal of the German Cardiac Society. 2010;99(5):267-76.

210. Zobel C, Adler C, Kranz A, Seck C, Pfister R, Hellmich M, et al. Mild therapeutic hypothermia in cardiogenic shock syndrome. Critical care medicine. 2012;40(6):1715-23.
211. Ikonomidis I, Tzortzis S, Triantafyllidi H, Parissis J, Papadopoulos C, Venetsanou K, et al. Association of impaired left ventricular twisting-untwisting with vascular dysfunction, neurohumoral activation and impaired exercise capacity in hypertensive heart disease. European journal of heart failure. 2015;17(12):1240-51.
212. Tschope C, Post H. Latent ischaemia as a trigger for a circulus vitiosus of inflammation, fibrosis, and stiffness in HFPEF. European journal of heart failure. 2015;17(12):1210-2.
213. Terris JM, Berecek KH, Cohen EL, Stanley JC, Whitehouse WM, Jr., Bohr DF. Deoxycorticosterone hypertension in the pig. Clin Sci Mol Med Suppl. 1976;3:303s-5s.
214. Miller AW, 2nd, Bohr DF, Schork AM, Terris JM. Hemodynamic responses to DOCA in young pigs. Hypertension. 1979;1(6):591-7.
215. Cohen DM, Grekin RJ, Mitchell J, Rice WH, Bohr DF. Hemodynamic, endocrine, and electrolyte changes during sodium restriction in DOCA hypertensive pigs. Hypertension. 1980;2(4):490-6.
216. Terris JM, Simmonds RC. The Yucatan miniature swine: an improved pig model for the study of desoxycorticosterone-acetate (DOCA) and aldosterone hypertension. Proc Soc Exp Biol Med. 1982;171(1):79-82.
217. Sweadner KJ, Herrera VL, Amato S, Moellmann A, Gibbons DK, Repke KR. Immunologic identification of Na+,K(+)-ATPase isoforms in myocardium. Isoform change in deoxycorticosterone acetate-salt hypertension. Circulation research. 1994;74(4):669-78.
218. Berecek KH, Bohr DF. Structural and functional changes in vascular resistance and reactivity in the deoxycorticosterone acetate (DOCA)-hypertensive pig. Circulation research. 1977;40(5 Suppl 1):I146-52.
219. Berecek KH, Bohr DF. Whole body vascular reactivity during the development of deoxycorticosterone acetate hypertension in the pig. Circulation research. 1978;42(6):764-71.
220. Walterhouse DO, Reinish LW, Mitchell J, Bohr DF. Aortic stiffness in the DOCA-hypertensive pig. Clin Physiol Biochem. 1984;2(4):146-53.
221. Ling WD, Brooks DP, Crofton JT, Share L, Bohr DF. Increased urinary clearance of lysine vasopressin in the deoxycorticosterone acetate-hypertensive pig. The American journal of physiology. 1989;257(6 Pt 2):R1467-73.
222. Ciccone CD, Zambraski EJ. Effects of acute renal denervation on kidney function in deoxycorticosterone acetate-hypertensive swine. Hypertension. 1986;8(10):925-31.
223. Webb RC. Potassium relaxation of vascular smooth muscle from DOCA hypertensive pigs. Hypertension. 1982;4(5):609-19.
224. Kellman P, Wilson JR, Xue H, Ugander M, Arai AE. Extracellular volume fraction mapping in the myocardium, part 1: evaluation of an automated method. J Cardiovasc Magn Reson. 2012;14:63.
225. Nadruz W. Myocardial remodeling in hypertension. J Hum Hypertens. 2015;29(1):1-6.
226. Santos M, Shah AM. Alterations in cardiac structure and function in hypertension. Curr Hypertens Rep. 2014;16(5):428.
227. Konstam MA, Kramer DG, Patel AR, Maron MS, Udelson JE. Left ventricular remodeling in heart failure: current concepts in clinical significance and assessment. JACC Cardiovascular imaging. 2011;4(1):98-108.
228. Bull S, White SK, Piechnik SK, Flett AS, Ferreira VM, Loudon M, et al. Human non-contrast T1 values and correlation with histology in diffuse fibrosis. Heart. 2013;99(13):932-7.
229. Su MY, Lin LY, Tseng YH, Chang CC, Wu CK, Lin JL, et al. CMR-verified diffuse myocardial fibrosis is associated with diastolic dysfunction in HFpEF. JACC Cardiovascular imaging. 2014;7(10):991-7.
230. Kasner M, Sinning D, Burkhoff D, Tschope C. Diastolic pressure-volume quotient (DPVQ) as a novel echocardiographic index for estimation of LV stiffness in HFpEF. Clinical research in cardiology : official journal of the German Cardiac Society. 2015;104(11):955-63.

231. Henein M, Morner S, Lindmark K, Lindqvist P. Impaired left ventricular systolic function reserve limits cardiac output and exercise capacity in HFpEF patients due to systemic hypertension. International journal of cardiology. 2013;168(2):1088-93.
232. de Simone G, Ganau A, Roman MJ, Devereux RB. Relation of left ventricular longitudinal and circumferential shortening to ejection fraction in the presence or in the absence of mild hypertension. Journal of hypertension. 1997;15(9):1011-7.
233. Wachtell K, Papademetriou V, Smith G, Gerdts E, Dahlof B, Engblom E, et al. Relation of impaired left ventricular filling to systolic midwall mechanics in hypertensive patients with normal left ventricular systolic chamber function: the Losartan Intervention for Endpoint Reduction in Hypertension (LIFE) study. American heart journal. 2004;148(3):538-44.
234. Melenovsky V, Borlaug BA, Rosen B, Hay I, Ferruci L, Morell CH, et al. Cardiovascular features of heart failure with preserved ejection fraction versus nonfailing hypertensive left ventricular hypertrophy in the urban Baltimore community: the role of atrial remodeling/dysfunction. Journal of the American College of Cardiology. 2007;49(2):198-207.
235. Masuyama T, Lee JM, Nagano R, Nariyama K, Yamamoto K, Naito J, et al. Doppler echocardiographic pulmonary venous flow-velocity pattern for assessment of the hemodynamic profile in acute congestive heart failure. American heart journal. 1995;129(1):107-13.
236. Barbier P, Solomon S, Schiller NB, Glantz SA. Determinants of forward pulmonary vein flow: an open pericardium pig model. Journal of the American College of Cardiology. 2000;35(7):1947-59.
237. Kono M, Kisanuki A, Ueya N, Kubota K, Kuwahara E, Takasaki K, et al. Left ventricular global systolic dysfunction has a significant role in the development of diastolic heart failure in patients with systemic hypertension. Hypertens Res. 2010;33(11):1167-73.
238. Young AA, Cowan BR. Evaluation of left ventricular torsion by cardiovascular magnetic resonance. J Cardiovasc Magn Reson. 2012;14:49.
239. Burns AT, La Gerche A, MacIsaac AI, Prior DL. Augmentation of left ventricular torsion with exercise is attenuated with age. Journal of the American Society of Echocardiography : official publication of the American Society of Echocardiography. 2008;21(4):315-20.
240. Notomi Y, Martin-Miklovic MG, Oryszak SJ, Shiota T, Deserranno D, Popovic ZB, et al. Enhanced ventricular untwisting during exercise: a mechanistic manifestation of elastic recoil described by Doppler tissue imaging. Circulation. 2006;113(21):2524-33.
241. Borbely A, Falcao-Pires I, van Heerebeek L, Hamdani N, Edes I, Gavina C, et al. Hypophosphorylation of the Stiff N2B titin isoform raises cardiomyocyte resting tension in failing human myocardium. Circulation research. 2009;104(6):780-6.
242. Ghofrani HA, Galie N, Grimminger F, Grunig E, Humbert M, Jing ZC, et al. Riociguat for the treatment of pulmonary arterial hypertension. The New England journal of medicine. 2013;369(4):330-40.
243. Ghofrani HA, D'Armini AM, Grimminger F, Hoeper MM, Jansa P, Kim NH, et al. Riociguat for the treatment of chronic thromboembolic pulmonary hypertension. The New England journal of medicine. 2013;369(4):319-29.
244. Degen CV, Bishu K, Zakeri R, Ogut O, Redfield MM, Brozovich FV. The emperor's new clothes: PDE5 and the heart. PLoS One. 2015;10(3):e0118664.
245. Schermuly RT, Stasch JP, Pullamsetti SS, Middendorff R, Muller D, Schluter KD, et al. Expression and function of soluble guanylate cyclase in pulmonary arterial hypertension. The European respiratory journal. 2008;32(4):881-91.
246. Zanfolin M, Faro R, Araujo EG, Guaraldo AM, Antunes E, De Nucci G. Protective effects of BAY 41-2272 (sGC stimulator) on hypertension, heart, and cardiomyocyte hypertrophy induced by chronic L-NAME treatment in rats. Journal of cardiovascular pharmacology. 2006;47(3):391-5.
247. Costell MH, Ancellin N, Bernard RE, Zhao S, Upson JJ, Morgan LA, et al. Comparison of soluble guanylate cyclase stimulators and activators in models of cardiovascular disease associated with oxidative stress. Frontiers in pharmacology. 2012;3:128.

248. Lundgren J, Kylhammar D, Hedelin P, Radegran G. sGC stimulation totally reverses hypoxia-induced pulmonary vasoconstriction alone and combined with dual endothelin-receptor blockade in a porcine model. Acta physiologica. 2012;206(3):178-94.
249. Boerrigter G, Costello-Boerrigter LC, Cataliotti A, Tsuruda T, Harty GJ, Lapp H, et al. Cardiorenal and humoral properties of a novel direct soluble guanylate cyclase stimulator BAY 41-2272 in experimental congestive heart failure. Circulation. 2003;107(5):686-9.
250. Bonderman D, Pretsch I, Steringer-Mascherbauer R, Jansa P, Rosenkranz S, Tufaro C, et al. Acute hemodynamic effects of riociguat in patients with pulmonary hypertension associated with diastolic heart failure (DILATE-1): a randomized, double-blind, placebo-controlled, single-dose study. Chest. 2014;146(5):1274-85.
251. Zhao L, Mason NA, Morrell NW, Kojonazarov B, Sadykov A, Maripov A, et al. Sildenafil inhibits hypoxia-induced pulmonary hypertension. Circulation. 2001;104(4):424-8.
252. Dumitrascu R, Weissmann N, Ghofrani HA, Dony E, Beuerlein K, Schmidt H, et al. Activation of soluble guanylate cyclase reverses experimental pulmonary hypertension and vascular remodeling. Circulation. 2006;113(2):286-95.
253. Ghofrani HA, Hoeper MM, Halank M, Meyer FJ, Staehler G, Behr J, et al. Riociguat for chronic thromboembolic pulmonary hypertension and pulmonary arterial hypertension: a phase II study. The European respiratory journal. 2010;36(4):792-9.
254. Galie N, Ghofrani HA, Torbicki A, Barst RJ, Rubin LJ, Badesch D, et al. Sildenafil citrate therapy for pulmonary arterial hypertension. The New England journal of medicine. 2005;353(20):2148-57.
255. Cawley SM, Kolodziej S, Ichinose F, Brouckaert P, Buys ES, Bloch KD. sGC{alpha}1 mediates the negative inotropic effects of NO in cardiac myocytes independent of changes in calcium handling. American journal of physiology Heart and circulatory physiology. 2011;301(1):H157-63.
256. Borlaug BA, Lewis GD, McNulty SE, Semigran MJ, LeWinter M, Chen H, et al. Effects of sildenafil on ventricular and vascular function in heart failure with preserved ejection fraction. Circulation Heart failure. 2015;8(3):533-41.
257. Paulus WJ, Vantrimpont PJ, Shah AM. Paracrine coronary endothelial control of left ventricular function in humans. Circulation. 1995;92(8):2119-26.
258. Wittstein IS, Kass DA, Pak PH, Maughan WL, Fetics B, Hare JM. Cardiac nitric oxide production due to angiotensin-converting enzyme inhibition decreases beta-adrenergic myocardial contractility in patients with dilated cardiomyopathy. Journal of the American College of Cardiology. 2001;38(2):429-35.
259. Straub A, Benet-Buckholz J, Frode R, Kern A, Kohlsdorfer C, Schmitt P, et al. Metabolites of orally active NO-independent pyrazolopyridine stimulators of soluble guanylate cyclase. Bioorg Med Chem. 2002;10(6):1711-7.
260. Takimoto E, Belardi D, Tocchetti CG, Vahebi S, Cormaci G, Ketner EA, et al. Compartmentalization of cardiac beta-adrenergic inotropy modulation by phosphodiesterase type 5. Circulation. 2007;115(16):2159-67.
261. Raskin A, Lange S, Banares K, Lyon RC, Zieseniss A, Lee LK, et al. A novel mechanism involving four-and-a-half LIM domain protein-1 and extracellular signal-regulated kinase-2 regulates titin phosphorylation and mechanics. The Journal of biological chemistry. 2012;287(35):29273-84.